# Modeling of Land Surface Temperature (LST) and Normalized Difference Vegetation Index (NDVI) in Nepal: 2000-2015

**Ira Sharma**

**A Thesis Submitted in Fulfillment of the Requirements for the Degree of**

**Doctor of Philosophy in Research Methodology**

**Prince of Songkla University**

**2018**

**Modeling of Land Surface Temperature (LST) and Normalized Difference**

**Vegetation Index (NDVI) in Nepal: 2000-2015**

**Ira Sharma**

**A Thesis Submitted in Fulfillment of the Requirements for the Degree of**

**Doctor of Philosophy in Research Methodology**

**Prince of Songkla University**

**2018**

**Thesis Title**      Modeling of Land Surface Temperature (LST) and Normalized Difference Vegetation Index (NDVI) in Nepal: 2000-2015

**Author**      Mrs. Ira Sharma

**Major Program**      Research Methodology

_____

**Major Advisor:**

…………………………....................
(Asst. Prof. Dr. Phattrawan Tongkumchum)

**Co- advisors:**

………………………………..
(Emeritus Prof. Dr. Don McNeil)

……………………………….
(Dr. Attachai Ueranantasun)

**Examining Committee:**

………………….…..…… Chairperson
(Assoc. Prof. Dr. Apiradee Lim)

…………………………….........................
(Asst. Prof. Dr. Phattrawan Tongkumchum)

………….………………….....
(Emeritus Prof. Dr. Don McNeil)

………………………………
(Dr. Attachai Ueranantasun)

…………………………………
(Prof. Dr. Nitin Kumar Tripathi)

      The Graduate School, Prince of Songkla University, has approved this thesis as fulfilment of the requirements for the Doctor of Philosophy Degree in Research Methodology.

……..……………………….……….
(Prof. Dr. Damrongsak Faroongsarng)
Dean of Graduate School

This is to certify that the work here submitted is the result of the candidate's own investigations. Due acknowledgement has been made of any assistance received.

…………………………………..Signature

(Asst. Prof. Dr. Phattrawan Tongkumchum)

Major Advisor

……………………….….Signature

(Mrs. Ira Sharma)

Candidate

I hereby certify that this work has not been accepted in substance for any degree, and is not being currently submitted in candidature for any degree.

.............................................Signature

(Mrs. Ira Sharma)

Candidate

| | |
|---|---|
| **Thesis Title** | Modeling of Land Surface Temperature (LST) and Normalized Difference Vegetation Index (NDVI) in Nepal: 2000-2015 |
| **Author** | Mrs. Ira Sharma |
| **Major Program** | Research Methodology |
| **Academic Year** | 2017 |

## ABSTRACT

The study explores the seasonal pattern and trend of LST and NDVI in Nepal from 2000 to 2015. The time series data of temperature (LST) and vegetation (NDVI) were derived from MODIS website. Natural cubic spline function, polynomial and logistic regression models were used to analyze LST while, natural cubic spline function, linear regression and GEE were used in case of NDVI. The data were seasonally adjusted in both LST and NDVI. For handling autocorrelation, autoregression of first order (AR (1)) was applied and filtered the data in LST and GEE model was used during NDVI analysis for this purpose. Here, LST and NDVI represented two parts of the study that are summarized as given below.

The first part involves the temperature change pattern in Nepal. An area of 11,902 km$^2$ within latitudes 26.92°N -28.26°N and longitudes 85.20°E-85.58°E was selected in form of 27 regions. Every region was further divided into nine sub regions. Therefore there were 243 sub regions which were analyzed one by one. Firstly, the seasonal pattern of temperature for 15 years revealed that seasonal changes were not basically different in the sub regions. Secondly, the data were fitted to polynomial regression of second order to obtain quadratic slopes of LST. The LST slopes illustrated the local pattern of temperature change during 15 years period which were categorized into five groups: 'Flat' pattern (11.5% of grid area), 'Accelerated-

increasing' pattern (25.9% of grid area), 'Decelerated-increasing' pattern (20.6% of grid area), 'Decelerated-decreasing' pattern (22.6% of grid area) and 'Accelerated-decreasing' pattern (19.3% of grid area). The patterns were regrouped into binary (accelerating and non accelerating) to model with the altitude (3 categories) and land cover (three categories) of the regions. The results showed that accelerating pattern had negative association with the altitude and no vegetated land cover. When the results were described in terms of ecozones, the area in the temperate Mountain zone dominantly showed no change or gradual increase of LST pattern. Low populated, low vegetated, snow cladded land on northern Himalaya or alpine zone had apparently decreasing LST pattern. The southern high populated, tropical Tarai zone had dominant increasing pattern.

The second part involves the vegetation change and seasonal pattern, using NDVI data, in three different regions of Nepal, east - Dhankuta (27.15°N, 87.35°E), center - Kathmandu (27.59°N, 85.39°E) and west - Surkhet (28.62°N, 81.88°E). Each region had an area of 410 km$^2$ with 6,561 grids. The analysis was done separately for systematically selected 196 grids at each region. At first, the annual seasonal pattern showed the seasonal start (greening) was earlier in east and moved gradually to the west. The case of end of season (browning) had similar results. Also, the length of season was longer in east than westward. Secondly, NDVI linear trend for 15 years showed that, except at the center, east and west suburban regions had dominant increasing trend. Lastly, to adjust for autocorrelation and applying overall 196 grids in a single model, generalized estimating equations (GEE) were used. The CI plots after this model explained, the vegetation was increasing in Nepal during these 15 years, except in Kathmandu. The recent declining trend in Kathmandu is alarming.

**Acknowledgements**

## Table of Contents

## List of Tables

## List of Figures

**Chapter 1**

**Introduction**

**1.1 Background and rationale**

The natural as well as anthropogenic activities can cause climate change. In this regard several environmental factors play key role, particularly the temperature and vegetation (Goward *et al*., 2002; Kaufmann *et al*., 2003). Globally, the temperature issues are vital to understand for controlling its negative consequences. It has been predicted that the global surface temperature, from 2009 to 2019, amidst the anthropogenic influences, has been through a continuous rise (Lean & Rind, 2009). The 5th Assessment Report (AR5) of Intergovernmental Panel on Climate Change (IPCC) has shown that average temperature on earth rose at a range of 0.65-1.06°C during a period of 1800-2012 (IPCC, 2013). Yet another important climate factor to bring about the changes in environment is the vegetation. Quantifying the type and extent of vegetation is important for resource management in the context of rapidly changing global climate and land cover issues. The worldwide study of vegetation shows its decline in many of the places (Evrendilek & Gulbeyaz, 2008; Eckert *et al*., 2015), which is being a threat to the climate and ecosystem.

The rising temperature and declining vegetation is particularly hard hitting for a low income countries like Nepal, where the alternates to cope with the changes is still not defined and the research for identifying the possible consequences are almost negligible. Nepal, extending from latitude 26.22°N to 30.27°N and longitude 80.04°E to 88.27°E covers an area of 148,181 km$^2$. It is unique for its geographical and

ecological variations. The three seasons (summer, winter and rainy) of weather and three ecozones (alpine, temperate and tropical) impart more curious about the questions, 'are the climate factors like temperature and vegetation changing their pattern and trend by time?' and 'is the change uniform by time and locations'. Hence, a need for this study was envisioned. However, in Nepal, field or station based time series data for temperature and vegetation is either much interrupted or not available for a longer period. In this situation, the satellite data are accessible and more reliable source than the field based data. Therefore, Land Surface Temperature (LST) and Normalized Difference Vegetation Index (NDVI) data derived from Moderate Resolution Imaging Spectroradiometer (MODIS) were selected for analysis in this research. MODIS is a sensor, fitted aboard the Terra and Aqua satellites by the National Aeronautics and Space Administration (NASA).

A common practice is that, the studies focus on big regions for identifying and predicting change of climate and hence the local level effects are almost overlooked. However, the changes have local level impacts on human society and environment. Therefore it is utmost to address these local level issues. In addition, the developing countries cannot afford the cost of post calamity losses. With these views and importance this study identifies change of temperature and vegetation by smaller local areas of Nepal for 15 years period.

## 1.2 Research objectives

The objectives of this study are:

1.2.1 To explore the pattern of Land Surface Temperature (LST) change in 3 different ecological zones of Nepal from 2000-2015.

1.2.2 To identify the association of LST pattern with altitude and land cover of the area

1.2.3 To explore the seasonal pattern and trend of Normalized Difference Vegetation Index (NDVI) in Nepal from 2000–2015.

## 1.3 Literature review

### 1.3.1 MODIS satellite data

Use of satellites is an advanced technique of monitoring the earth's climate. Since 1950s, NASA satellites have been observing Earth's atmosphere, oceans, land and snow from high above the earth's surface. Satellite based data, like LST and NDVI, have been widely utilized in various fields and a number of studies investigate and document their applications (Vadasz, 1994; Walther *et al*., 2002; Johannessen *et al.,* 2004; O'Donoghuea *et al*., 2010; Burke *et al.,* 2015). Data from MODIS Terra and Aqua sensors are much common for the study purpose in climate and environmental science since they efficiently detect the environmental changes due to fire, vegetation, temperature, earthquakes, droughts and flood on Earth (NASA, 2015). MODIS sensors capture a wider array of the earth's vital signs than any other sensors. For instance, the sensors measure the percent of the planet's surface that is covered by clouds almost every day, the surface temperature, in every eight day and the

vegetation cover in every 16 day (NASA, 2015). Hence, the change of the climatic factors, at a larger or smaller area, is obtained through this data which is more reliable and with less error.

### 1.3.2 LST trend and pattern

LST, MODIS sensor product for temperature, is evidenced to rise both on land and the sea. Trend of temperature throughout the world was found increasing (IPCC, 2013). The LST is commonly used to find temperature trend at local (Tran *et al*., 2006) and regional (Julian *et al*., 2006) scale. Even though it is not commonly found, there are studies that quadratic pattern of temperature change is evident (Schlenkera & Robertsb 2009; Wanishsakpong & McNeil 2016) while a lot of works have shown evidences about the linear pattern (Julian & Sobrino 2009; Karnieli *et al.,* 2009) as they focus on just the trend of change not the pattern. Most climate scientists opined that 2°C of rising temperature, than that during preindustrial time, would affect all sectors of civilization- food, water, health, land, national security, energy and economy (Mann, 2014). The change in extreme temperature cases such as heat waves, severe summer and winter storms, hot and cold days, hot and cold nights can cause negative impacts on human society and the nature. Many studies have shown temperature rise at different regions of the world such as Southeast Asia (Choprateep & McNeil, 2015), Australia (Wanishsakpong & McNeil, 2016), Arctic region (Johannesen *et al*., 2004) and China (Song *et al*., 2007).

### 1.3.3 Temperature change and altitude

Several studies have shown that the temperature and altitude are statistically associated. Their association may be either negative (Lancaster, 2012; Khandelwal *et*

*al*., 2018) or positive with the rate of temperature rise being progressively higher at higher altitudes as found around the glacial regions of Nepal (Shrestha & Aryal, 2011). The variation in temperature trend was well illustrated in a study in China (Dong, 2015), where the trend decreased with altitude below 200 m while it was weakly positive from 200 to 2,000 m, and a strongly positive temperature– altitude relation was found over 2,000 m. Hence, all these examples refer that, temperature change is seen almost everywhere with the rates being different at different places depending on other climatic and geographic factors.

### 1.3.4 Temperature and land cover

Tran *et al*. (2006) have concluded about the consequence of changing temperature, in eight megacities of Asia, that surface heat has significant association with urban growth, land cover and population density. A study on 10 megacities of the world indicates that, in most of the cities the land surface temperature is negatively associated with the vegetated and undisturbed natural areas, however, the cities show different trend, both in terms of the size and spatial distribution of urban heat island (Maria, 2012). The study of LST, NDVI and land cover (LC) in Shanghai (Yue *et at.,* 2007) and Guangzhou cities of China (Sun *et al.,* 2012) clear that the LST is positively correlated with integrated land cover index while with only NDVI it shows negative statistical relationship. Therefore, for a sustainable urban planning the knowledge of LST, LC and NDVI for every particular area is essential.

### 1.3.5 LST and different ecological zones

Ecozones or ecological zones are regions which belonged to similar natural communities, climate, topography, elevation, soil types, and other physical and

geographical characteristics. Every ecological zone has a unique pattern of response to the environmental changes. Literatures evidence that altitude and land cover have direct influence in the changing temperature change (Sun *et al.,* 2012; Khandelwal *et al.,* 2017) while some demonstrate the temperature changes as a process of desertification of arid land (Sruthi & Aslam, 2015) and glacial land (Johannessen *et al*., 2004; Clark *et al.,* 2011), while, only a few explain about the effects of changing temperature and precipitation in different terrestrial and aquatic ecological zones (Walther *et al.,* 2002). In addition, the work explaining the comparative temperature change patterns in different ecological zones is still rare.

**1.3.6 NDVI trend and pattern**

NDVI has been a data for analyzing the vegetation status in present, past and predict its future. Evrendilek & Gulbeyaz (2008) used NDVI to monitor seasonal pattern and inter annual ecosystem dynamics of different vegetation types and climate zones in Turkey. It was found that the seasonal variation was almost similar for all ecosystem dynamics. It also showed correlation with different ecosystems that is from warmer to cooler zones and from forest to barren land. Zhang *et al*. (2003) determined the intra-annual vegetation pattern in northeastern side of the USA identifying several of the phonological characteristics useful for agricultural and environmental sectors. For instance, it detected the transition dates for vegetation activities within annual time series of vegetation index. The NDVI has also been successfully used to find the vegetation change in Mongolia due to forest fire, deforestation, mining activities and urban expansion (Eckert *et al*., 2015). These studies show the trend of vegetation in different parts of the globe has been decreasing and also have negative association with the temperature (Bounoua *et al.,* 2000; Feehan *et al.,* 2009).

Another indicator of intra annual vegetation pattern (that is, seasonal pattern) is the timing of life cycle events, also known as phenology, of the plants. Wang *et al*. (2016) found that in Northern Hemisphere had been facing the early and longer greening season during 1982-2012, where rising temperature was the major determinant. Similarly, in western USA, during 1990-2002, the onset of greening varied up to eight days depending upon the land cover type (Bethany *et al*., 2007). Moreover, around Europe, Feehan *et al.,*(2009) found that species richness and biodiversity were in declining condition during the period, seasonal events were advancing at a rate of 2.5 days/ decade and it was particularly rapid in Arctic regions. This advancement of seasonal phenology was predicted to continue in future as well. Yet another study in Iberian Peninsula evidenced that water availability or rainfall was the important driver of climate change that initiated a lot of phonological changes which might hit far up to biospheric structures and the functions (Penuelas *et al*., 2004).

**1.3.7 Statistical methods**

The temperature and vegetation changes can be measured using various statistical models. There is variation of work such as computer simulation method was applied to detect the changes occuring in area of Arctic ice during a 25 years period from 1978 to 2003 (Johannessen *et al*., 2004). A piecewise logistic model was used to determine intra-annual vegetation changes in Northeastern side of USA (Zang *et al*., 2003), and an empirical ortheogonal functions (Semenov, 2007) was used to analyze the effect of climatic variability on air temperature in Northern Hemisphere altitudes during 1892 to 1999. In addition, least square linear regression method (Hansen & Schjoerring, 2003) successfully measured the reflectance of canopy biomass of vegetation in Denmark, while multiple linear regression model was used to detect

relationship of NDVI and LST (Karnieli *et al.,* 2010) showing that they were negatively associated. Yet some studies in Australia used linear regression model, factor analysis (for grouping the outcome variable) and polynomial regression model of 6th order (Wanishsakpong & McNeil, 2016) and 3rd order (Wanishsakpong *et al.*, 2015) for finding the future trend of temperature. The polynomial regression order was observed to depend on the period and characteristics of the data used. Furthermore, the natural cubic spline model was fitted to LST at Phuket Thailand by Wongsai *et al.* (2017) to identify the seasonal patterns of temperature.

In conclusion, the remote sensing data like LST and NDVI are reliable and accessible time series data which can be of significant use for the study of regions, like Nepal for example, which do not have systematic archives of long run climate data. The climatic changes in terms of temperature and vegetation still require a lot of evidences that can be of policy or the academic use. Kathmandu being a fast growing urban city needs this kind of study since it is already prone to negative climate effects due to changes in vegetation and temperature status. In addition, the studies so far show national or regional level of climate change trend and this study tries to find the local level trend of LST and NDVI using natural cubic spline function, linear regression and polynomial regression model of second order to find the time series trend and pattern in Nepal. Therefore the use of natural cubic spline function and regression model for trend analysis in a single combination would be unique in this study.

## 1.4 Conceptual framework

Figure 1.1 is the conceptual diagram to show the methodological steps of this study. To begin with, the natural cubic spline curve was fitted to the data for finding the

seasonal patterns. Then, the data were seasonally adjusted. In LST, after filtering the autocorrelation effects by first order autocorrelation (AR(1)) method, the data were fitted with polynomial second degree model to find the LST quadratic trend for 15 years. In NDVI, simple linear regression model followed by generalized estimating equations (GEE) was applied to find grid leveled as well as whole area vegetation change over 15 years period.
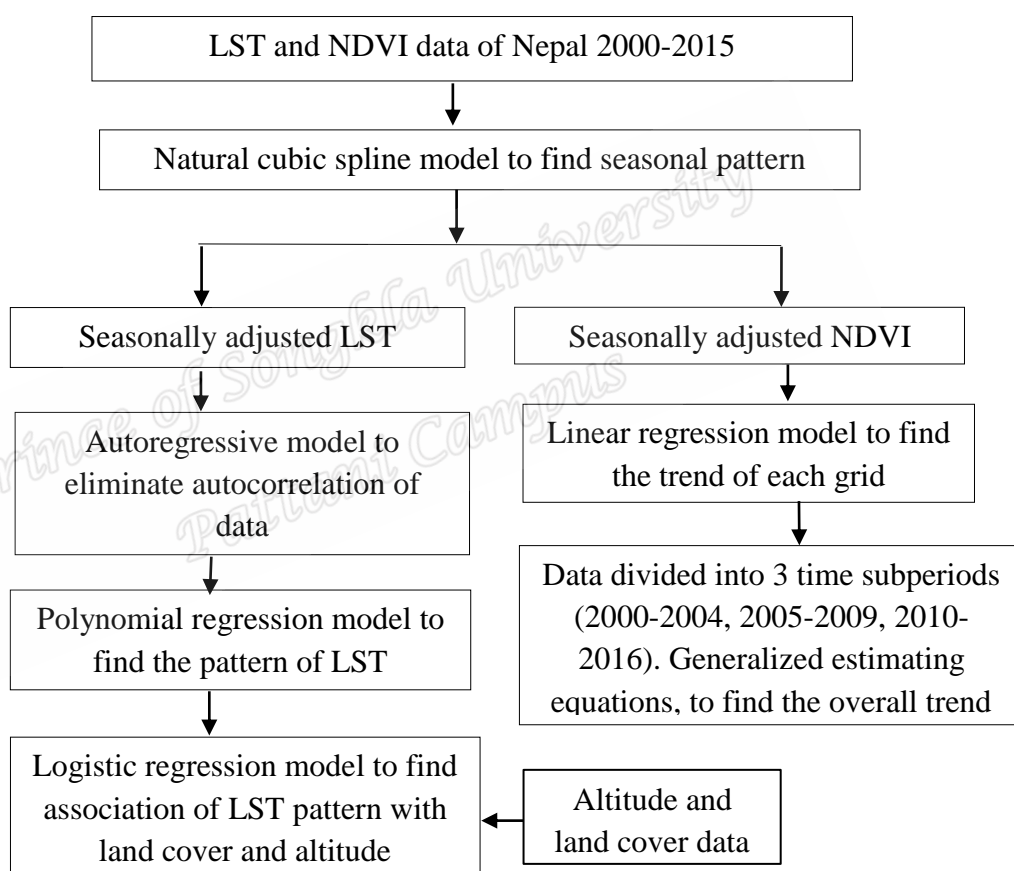


Figure 1.1 Diagram of data analysis

## 1.5 Organization of thesis

This thesis consists of the four chapters and their organization is described below:

Chapter 1 comes under the background and the objectives, literature reviews and the

conceptual framework of the study. Chapter 2 consists of the description of methodology that includes study site, data and the methods used for analysis. In chapter 3, the results showing the trend and patterns of NDVI and LST over the study area are organized where preliminary results were followed by the model results of both LST and NDVI. Finally in chapter 4 details about discussion of findings, summary of overall work and conclusion of the outcome of this research together with recommendations.

**Chapter 2**

**Methodology**

This chapter details about research methodologies used to complete this study. It describes about study area, data, data management, and statistical methods.

**2.1 Study area**

The study was done in Nepal. Nepal has three ecological zones (ecozones), alpine, temperate and tropical zones, extending from north to south of the country (Figure 2.1).
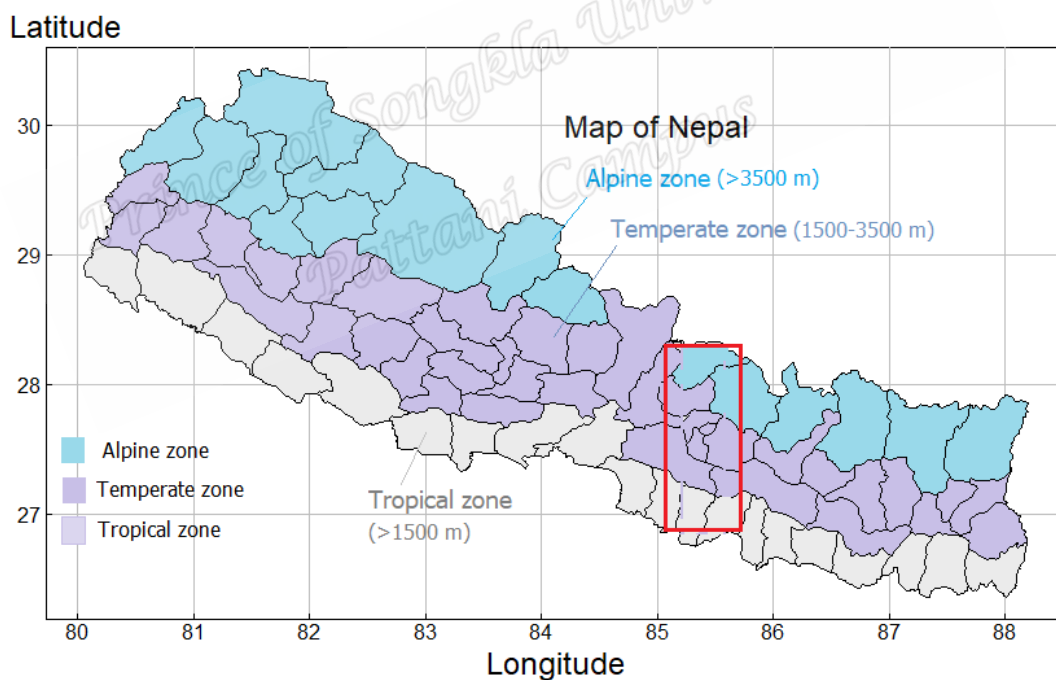


Figure 2.1 Study area for LST (in red rectangle) in Nepal

Alpine zone is snowy, dry with lower rainfall, annual mean temperature from less than – 4 to 12°C (Figure 2.2), scanty vegetation in form of coniferous forest or grasslands or alpine scrubs in higher altitudes and with snow clad Mountains on
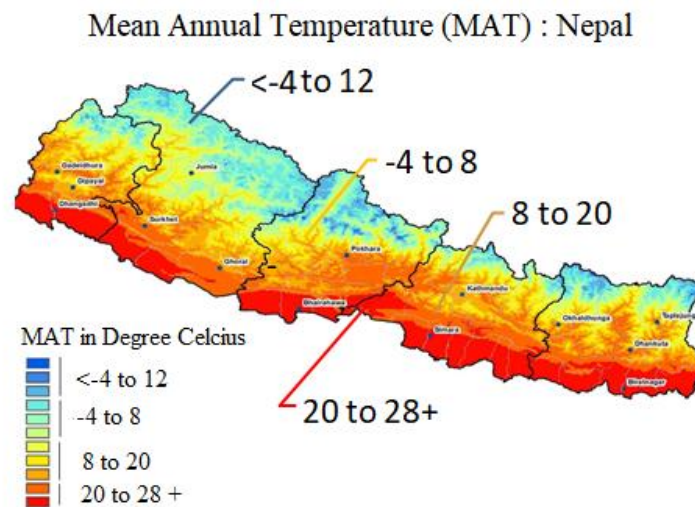
Figure 2.2 Mean annual temperature in Nepal (Source: Karki *et al.,* 2016)

northern extremes. This area has very low density of population, altitude ranging from

3500 m and above. Temperate Mountain is moderately cold and has summer

temperature with enough rainfall, annual mean temperature ranging from – 4 to 20°C,

deciduous vegetation and moderate number of population. The altitude ranges from

1,500 m to 3,500 m. While, the tropical plain land is comparatively hotter, humid with

higher temperature ranging from 20 to above 28°C, altitude from 60-1,500 m, higher

rainfall, tropical evergreen vegetation and dense population with more developmental

structures like roads, buildings, industries, vehicles etc. Basically, the country has

three different climates - summer (March to June), rainy (June to August) and winter

(November to February). The land cover on the area has basically, vegetation

including tree forests, shrub/ crop and the barren or no vegetated land. The central

Mountain belt is dominantly covered by tree forest while the shrub/ crop is located

dominantly in the southern belt. The urban builds, in urban populated areas and bare

Mountain and snow cover on northern belt represent the no vegetated land in Nepal

(Figure 2.3).
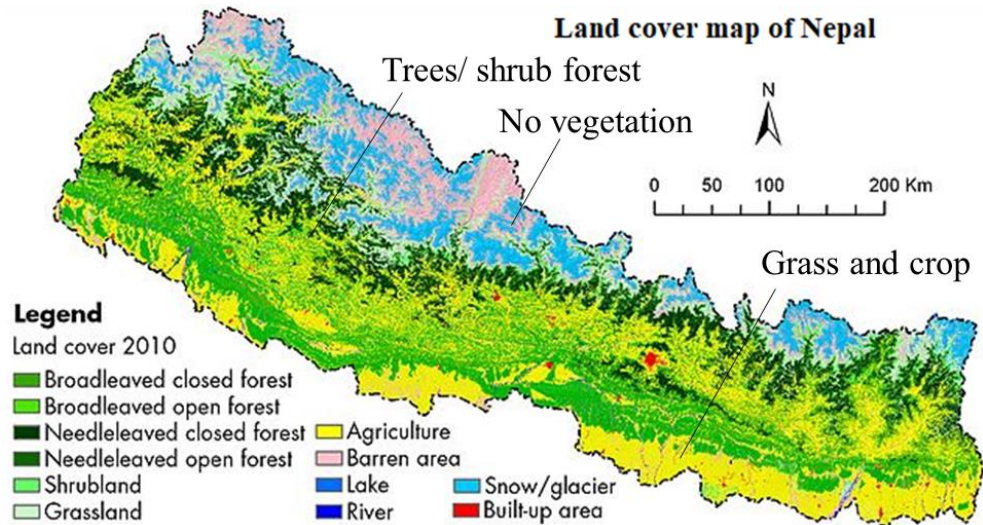
Figure 2.3 Land cover map of Nepal (Source: Wikipedia, 2018)

This study comprises two parts, they are LST and NDVI. For LST, the study area was extended within the latitudes of 26.82°N-28.35°N and longitudes 85.02°E-85.73°E of Nepal (Figure 2.1, in red box), that occupies 11,907 km$^2$. The study location is near about the center of the country in form of 27 regions, named from 1 to 27, located in three ecozones, from alpine (black polygons), temperate (red polygons) to tropical (blue polygons, Figure 2.4) zones.
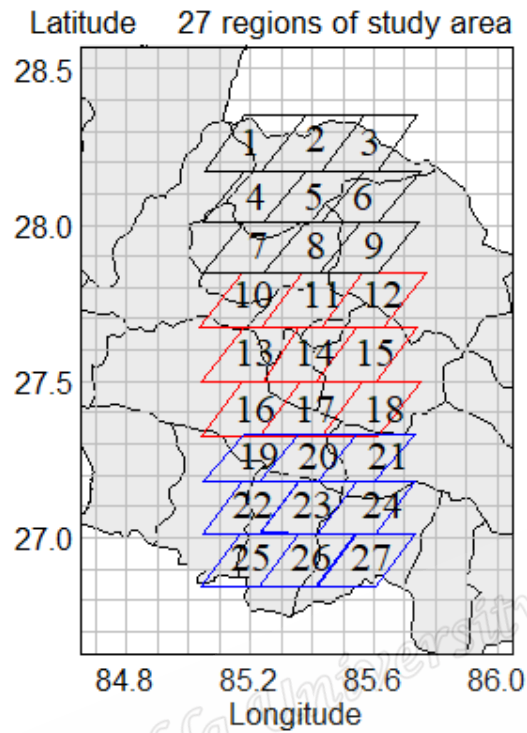
Figure 2.4 Study area for LST with 27 regions

For NDVI, the study was carried out in three regions (Figure 2.5-Figure 2.8).
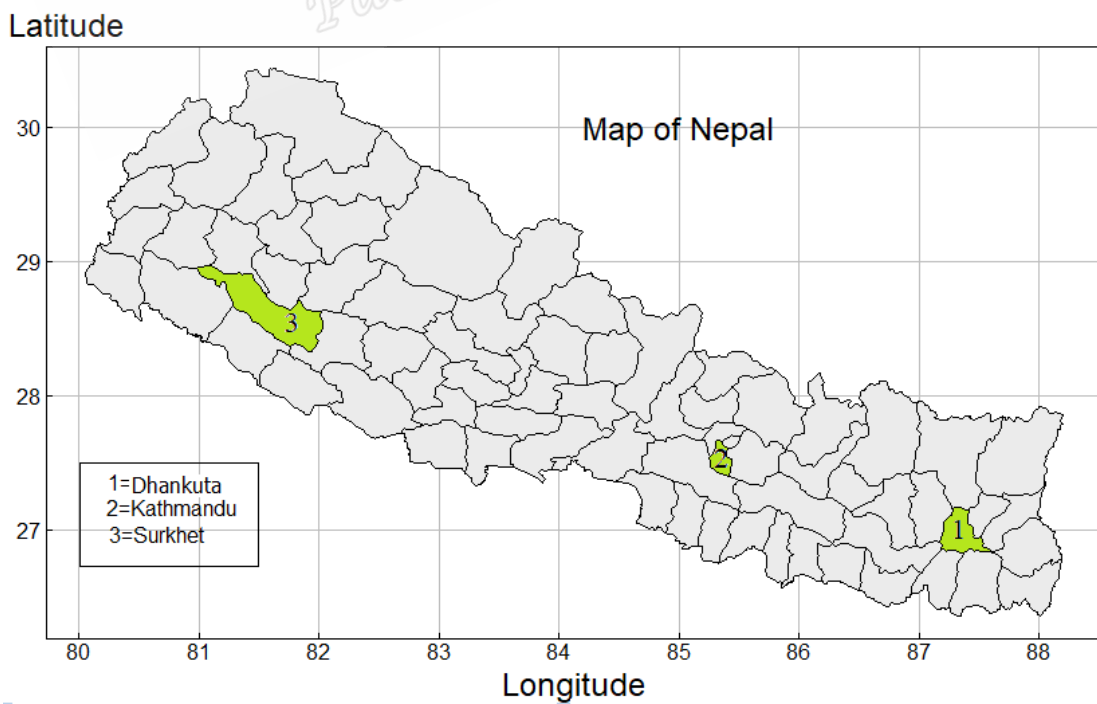


Figure 2.5 Location of three districts in Nepal
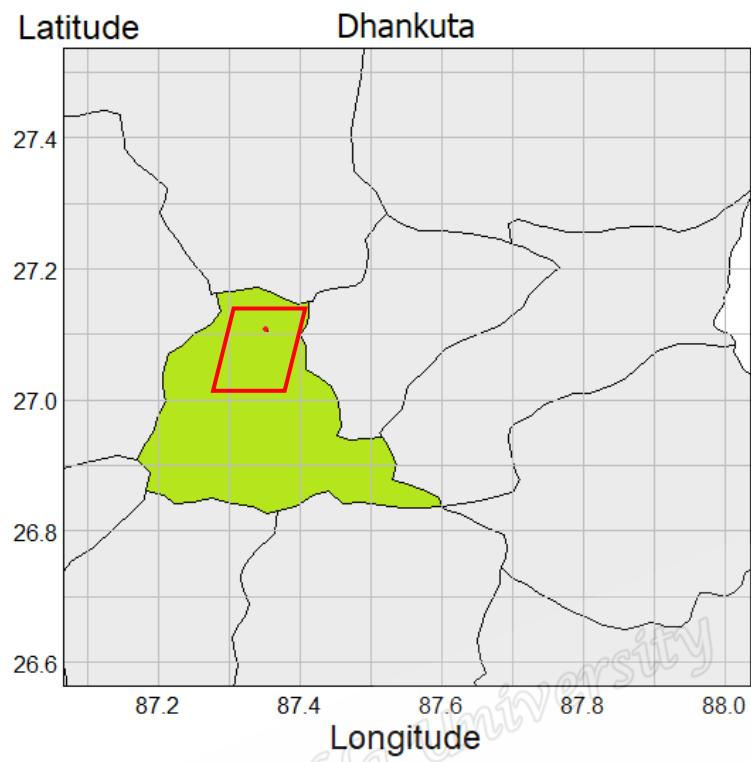
Figure 2.6 Study area in Dhankuta district
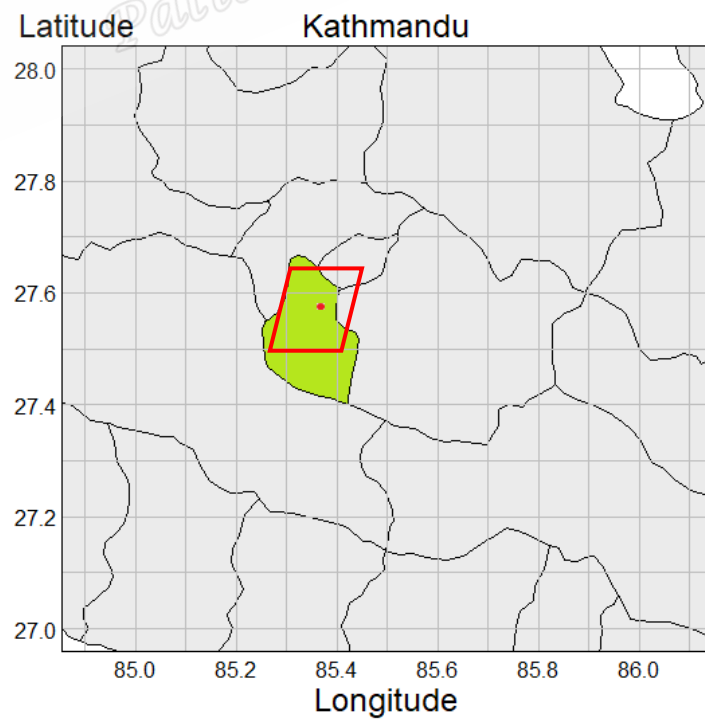


Figure 2.7 Study area in Kathmandu district
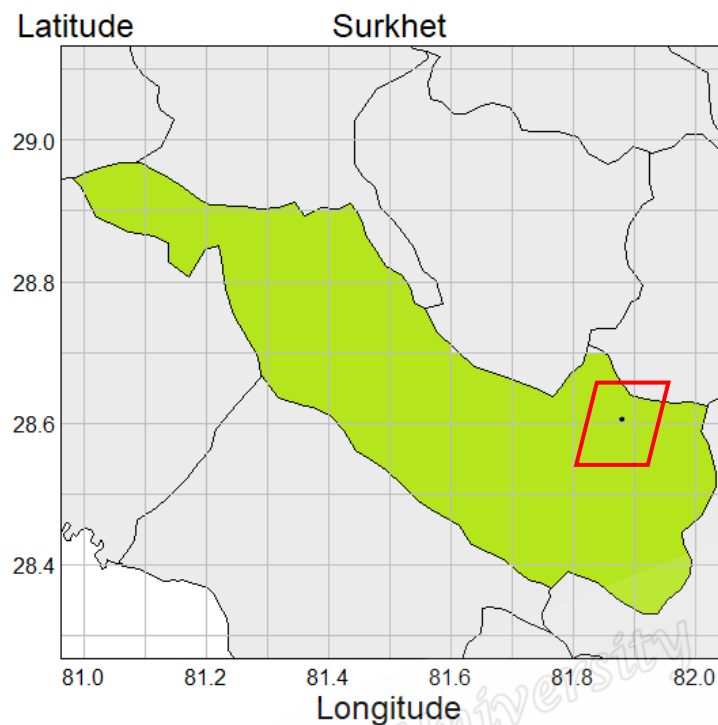
Figure 2.8 Study area in Surkhet district

All three areas are from temperate Mountain area to avoid the effect of other climate variables on different plant species from different ecozones. The area was selected randomly form east - Dhankuta (27.15°N, 87.35°E), center - Kathmandu (27.59°N, 85.39°E) and west - Surkhet (28.62°N, 81.88°E) of Nepal (Figure 2.5 to 2.8). Department of Forest Resource and Survey (DFRS, 2015), Department of Hydrology and Meteorology (DHM, 2015) and National Population and Housing Survey 2011 (NPHS 2011, 2012) of government of Nepal have reported that, Dhankuta is an eastern suburban area of 892 km$^2$ with population density of 183/km$^2$. It has an annual temperature ranging from 14.6°C (January) to 24.9°C (April), annual rainfall 1,120.8 mm and have average altitude of 1,192 m. Kathmandu is an urban area located in central region, with the area of 899 km$^2$ and the population density of 4,416/km$^2$. Its annual temperature ranges from 6.6°C (January) to 16.6°C (May), annual rainfall

1,666.6 mm and have average altitude of 1,337 m. Surkhet is a suburban area located in western region, with the area of 2,451 km$^2$ and the population density 143/km$^2$. The annual temperature of this city ranges from 15.1°C (January) to 27.0°C (April), rainfall 1,391.9 mm (July) and have average altitude of 875 m. The conventional seasons in the country were classified as summer, rainy and winter which falls in the months of March to May, June to August and December to February respectively.

## 2.2 Data

This topic includes the detail about data sources, the variables and data management processes.

### 2.2.1 Data source

LST and NDVI data are the land product subset from Terra platform. Terra is one of the sensors fitted to NASA's satellite. The data are downloaded from MODIS's website (ORNL DAAC, 2015) for a period of 15 years. These were land surface temperature and vegetation products available freely on its website and delivered along with its documents. The two predictors, land cover (LC) and altitude, used for LST analysis, were also obtained as satellite products. The LC data were obtained from the maps received during MODIS data delivery and those raster maps were converted to vectors with the help of QGIS software version 2.6.1. A satellite map of altitudes, covering whole study area of each region, was downloaded for the United States Geological Survey website (USGS, 2017). This map was dragged into the QGIS program for digitization and obtained the altitude data. The altitude was measured in meter.

**2.2.2 The variables**

**LST**

The LST, a type of temperature data from MODIS remote sensor fitted in Terra satellite by NASA, is the skin surface temperature measured by satellite on the basis of the thermal reflectance of the objects on earth. The data values are in Kelvin unit. For each region, the data had 441 km$^2$ area and 441 grids each with the size of 1×1 km$^2$. As LST is a record of 8 day frequency, there are 46 observations in one year and 690 observations in 15 years. As a data frame, for each region it has a matrix of 441 grids×690 observations. It has the first six columns (Table 2.1) detailing about data characteristics (V1 to V6) and rest all for the LST values (t1 to t441).

Table 2.1 Structure of LST data for a region as obtained from MODIS website

| Observation | Variables | | | | | |
|:---:|:---:|:---:|:---:|:---:|:---:|:---:|
| | V1 | V2 | V3 | | t440 | t441 |
| 1 | MOD11A2… | MOD 11A2 | A2000177 | … | 294.12 | 293.02 |
| 2 | MOD11A2… | MOD 11A2 | A2000185 | … | 294.84 | 293.76 |
| 3 | MOD11A2… | MOD 11A2 | A2000193 | … | 293.88 | 293.55 |
| ⋮ | ⋮ | ⋮ | ⋮ | ⋮ | ⋮ | ⋮ |
| 689 | MOD11A2… | MOD 11A2 | A2015161 | … | 291.58 | 290.86 |
| 690 | MOD11A2… | MOD 11A2 | A2015169 | … | 286.92 | 286.28 |

**NDVI**

The NDVI is a type of vegetation index from MODIS remote sensor fitted in Terra satellite by NASA and defined in terms of the red and near infra-red (NIR) reflectance values. Every green plant characteristically absorbs in the red and blue wavelengths, reflects out the green wavelength and strongly reflects in the NIR light waves. Based on this principle the data were calculated by given equation (Tucker *et al*., 2013),

$$NDVI = \frac{NIR-Red}{NIR+Red} \tag{1}$$

The data structure for NDVI is not different from that of LST, except that its area is $20.25 \times 20.25$ km$^2$. Every region has 6,561 grids each measuring $250 \times 250$ m$^2$ in area. Since the data is 16 day frequent, total observations were structured in 345 rows for 15 years' period consecutively. There are 23 observations every year. As a data frame, for each region it has a matrix of 6,561 grids$\times$345 observation. The data structure shows (Table 2.2) that the first seven columns (A1 to A7) detailing about data characteristics and rest all (v1 to v6561) for the NDVI values for all 6,561 grids. The missing data were indicated by F.

Table 2.2 Structure of NDVI data for a region as obtained from MODIS website

| Observation | Variables | | | | |
|---|---|---|---|---|---|
| | A1 | | v1 | | v6561 |
| 1 | MOD13Q1.A2000177… | ⋯ | 0.3843 | ⋯ | 0.6981 |
| 2 | MOD13Q1.A2000193… | ⋯ | 0.4144 | ⋯ | 0.6680 |
| 3 | MOD13Q1.A2000209… | ⋯ | 0.4827 | ⋯ | 0.7139 |
| ⋮ | ⋮ | | ⋮ | | ⋮ |
| 344 | MOD13Q1.A20150145… | ⋯ | F | ⋯ | 0.2781 |
| 345 | MOD13Q1.A20150161… | ⋯ | 0.5276 | ⋯ | 0.3652 |

**Land cover**

Land cover (LC) is a predictor variable for observing association with analyzed LST

quadratic curves. The data were obtained by calculating the LC codes of raster map,

obtained along LST data and digitized by using QGIS server program. It exhibits 18

different color legends with codes from 0 to 17 for land cover types in the area (Table

2.3). The data were distributed in 441 grids at each of the 27 regions. They were

further divided into three categories for the convenience of analysis and plots. They

are, highly dense vegetated land of trees and forest (LC codes 1-5, 8), scanty

vegetation with crop and grass land (LC codes 6, 7, 9, 10, 12, 14, 16) and no

vegetation on land (LC codes 0, 11, 13, 15, 17).

Table 2.3 Land cover area of 27 regions

| LC codes | LC type | Total cover (grids) |
|---|---|---|
| 0 | Water | 12 |
| 1 | Evergreen needle leaved | 60 |
| 2 | Evergreen broad leaved | 8 |
| 3 | Deciduous needle leaved | 1 |
| 4 | Deciduous broad leaved | 0 |
| 5 | Mixed forest | 5528 |
| 6 | Closed shrubland | 2 |
| 7 | Open shrubland | 46 |
| 8 | Woody savana | 1176 |
| 9 | Savanna | 10 |
| 10 | Grassland | 1235 |
| 11 | Permanent wet land | 3 |
| 12 | Cropland | 1431 |
| 13 | Urban and build up | 70 |
| 14 | Crop land and natural | 1498 |
| 15 | Snow ice | 5528 |
| 16 | Barren or sparse | 1 |
| 17 | Unclassified | 0 |

**Altitude**

Altitude is a predictor variable, similar as LC. The data had 441 rows of mean altitude for every grid in each region of study area. The altitude ranged from 71.9 m to 6,866.7 m in the study area. While analysis, the altitude for whole 27 regions were divided into three categories, >3,000 m, 1,500-3,500 m, <1,500 m based on three ecozones.

**2.2.3 Data management**

**LST**

The LST data, for 27 different regions extend from north to south of Nepal (Figure 2.3). These time series, day time temperature data were for a period of 15 years starting from 2000 (25th June) to 2015 (18th June). The missing values ranged up to 12%. First, the data for each region were divided into nine sub regions (Figure 2.9), each with $7\times7 = 49$ grids, which were named as northwest (NW), north (N), northeast (NE), west (W), center (C), east (E), southwest (SW), south (S) and southeast (SE) therefore, there were 243 sub regions in the study area. The LST data, originally given in Kelvin, was converted into degree Celsius by subtracting 273.5 from the sensor recorded raw values. Table 2.4 shows the LST data structure of a region, after eliminating the first six columns and grouping 441 grids into nine sub regions.
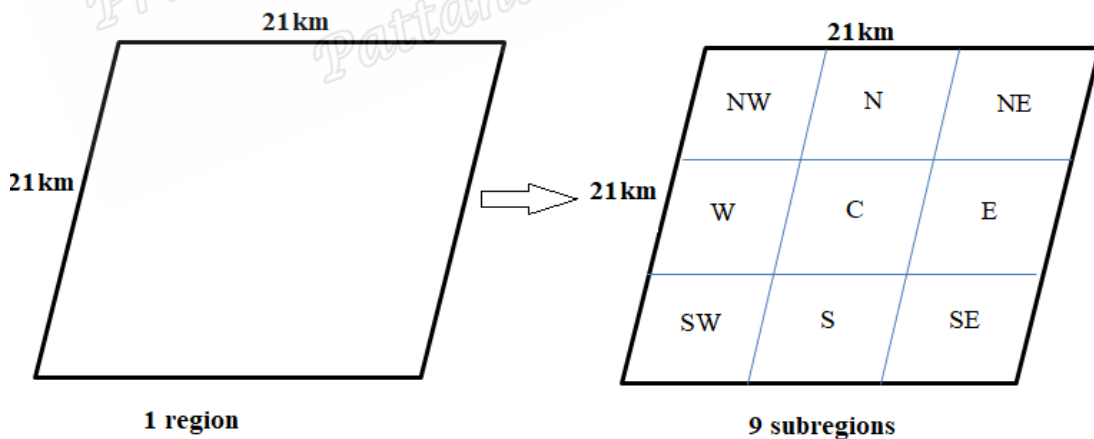


Figure 2.9 Division of one region into nine sub regions with their respective names

Table 2.4 LST data for a region after grouping into sub regions

| Observation | Variables | | | | | |
|---|---|---|---|---|---|---|
| | Year | Day | Sub-reg.1 | Sub-reg.2 | | Sub-reg.9 |
| 1 | 0 | 177 | 12.174349 | 12.14503 | ⋯ | 20.48853 |
| 2 | 0 | 185 | 22.742308 | 23.86926 | ⋯ | 25.16363 |
| ⋮ | ⋮ | ⋮ | ⋮ | ⋮ | | ⋮ |
| 690 | 15 | 169 | 22.794085 | 21.87362 | ⋯ | 23.25116 |

**NDVI**

The data for NDVI were extending from east to west of Mountain region of Nepal. The data period is the same as LST (27th June 2000 – 11th June 2015). For each grid, there were up to 10% of missing data. First of all the data for 196 grids were systematically selected from each region for the analysis. Table 2.5 shows the NDVI data structure of a region, after eliminating the first seven columns and selecting 196 grids as data variables.

Table 2.5 NDVI data for a region

| Observation | Year | Day | VI1 | | VI 196 |
|---|---|---|---|---|---|
| 1 | 0 | 177 | 0.566 | ⋯ | 0.382 |
| 2 | 0 | 193 | 0.787 | ⋯ | 0.563 |
| ⋮ | ⋮ | ⋮ | ⋮ | | ⋮ |
| 345 | 15 | 161 | 0.833 | ⋯ | 0.871 |

The data from systematically selected 196 grids were plotted separately for each grid. There was sparsity at the center of the graph, probably due to cloud or air moisture in rainy season (day 160 to 260). This problem was handled in two ways. First, highly fluctuating NDVI data in a very short period, with residual values >0.2 and $< -0.2$ (example from a grid is shown as cross marks in Figure 2.10). Second, the doubtful NDVI values for the observation days which had no LST data when compared. The NDVI could be falsified on that particular day, might happen due to weather, cloud or other technical reasons, shown as blue dots in Figure 2.10, both were eliminated. For the comparison of NDVI and LST grid to grid data values, the appropriate key grid was determined that ranged from 1-16. Our area showed grid number 10 as appropriate key grid for NDVI and LST data merging (Figure 2.11 and Figure 2.12) that is the NDVI grid, one out of 16 that corresponds to a particular LST grid, where the central coordinate of a LST grid falls on. The raw data of each NDVI grid were ranging from 1 to – 1, where, negative values up to 0 corresponds to snow and water, 0 to 0.1 meant soil, rock, concrete and barren land. Low positive values (0.2 to 0.5) represents grassland and shrubs while above 0.6 meant the forest (Weier & Herring, 2000).
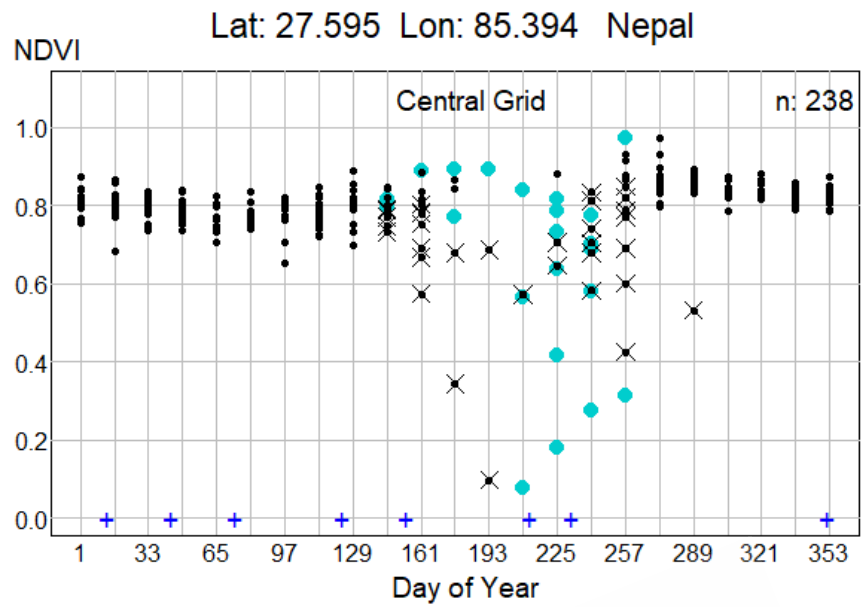
Figure 2.10 Unreliable (crossed ones) and doubtful (cyan dots) values displayed
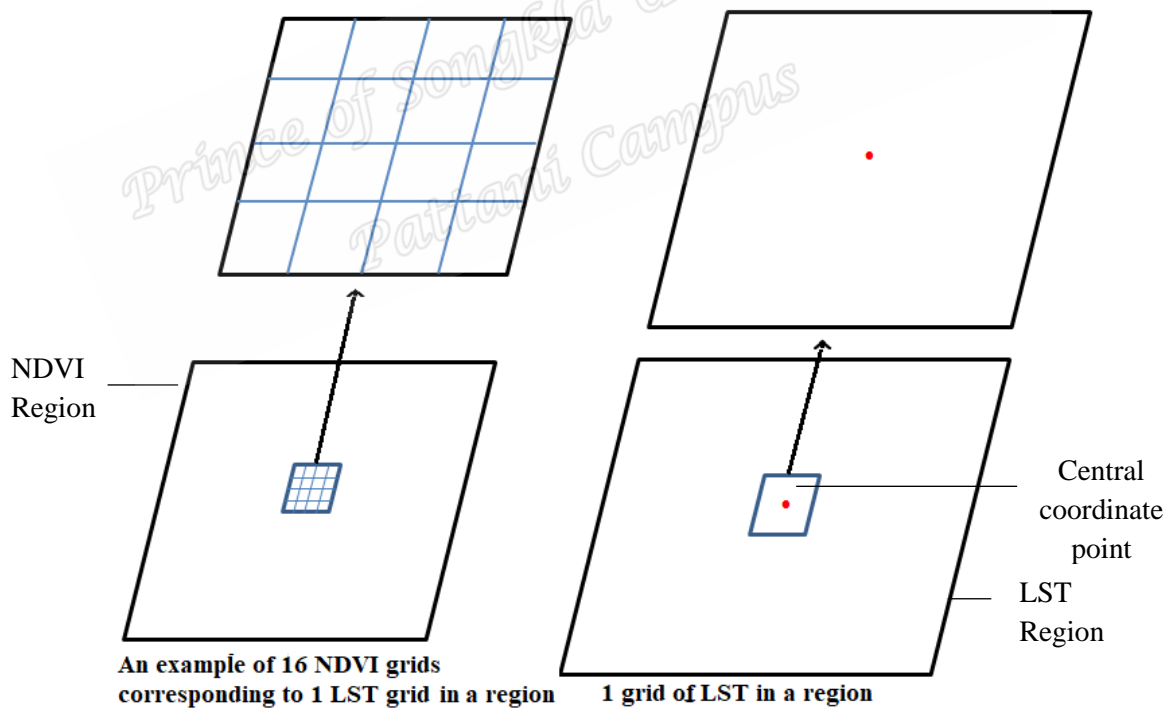


Figure 2.11 LST and NDVI grid number and size (example of central grids)
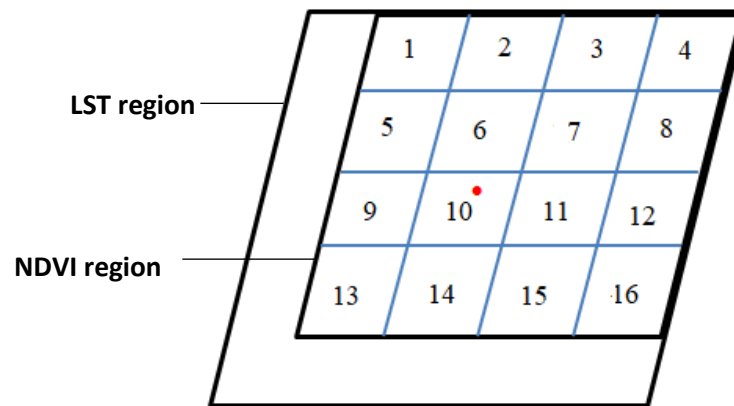
Figure 2.12 Merge of LST and NDVI showing key NDVI grid is #10 (example of

central position grid)

**Land cover and altitude**

The land cover and altitude data were obtained one by one for each of the 27 regions.

For both these data, there were 441 observations, that is for each grid of a region.

However, after the division of a region into nine sub regions, there were 243 sub

regions in whole the study area. The median value of land cover and mean value of

altitude for each sub region were calculated for analysis. Figure 2.13 and 2.14 show

the altitude and land cover data distribution in the study area respectively.
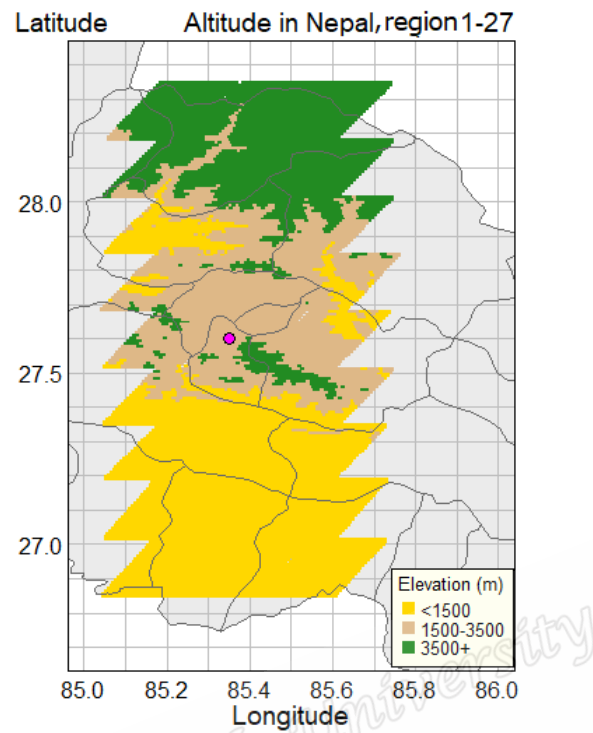
Figure 2.13 Study area showing altitude distribution
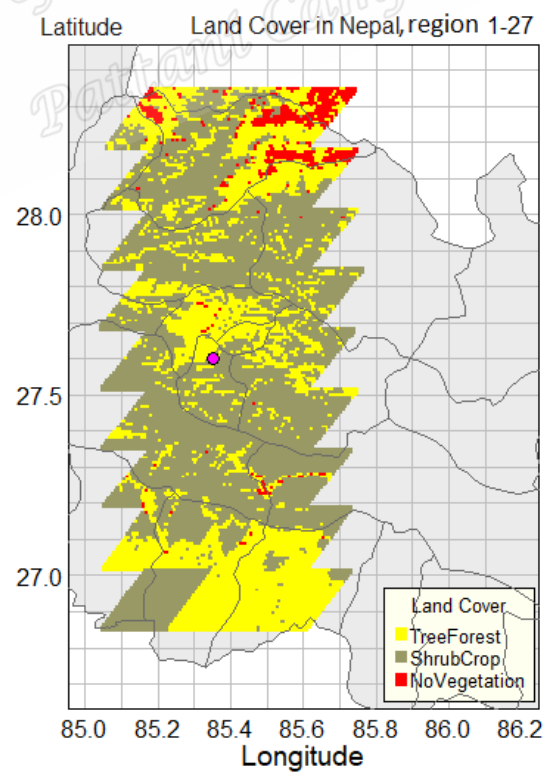


Figure 2.14 Study area showing land cover distribution

## 2.3 Statistical methods

The statistical methods used for analyzing LST and NDVI are described below.

### 2.3.1 Natural cubic spline function

A spline function is a piecewise cubic polynomial with continuous second derivatives, and is the smoothest of all functions because it has minimal integrated squared second derivative. Additionally, it can be well fitted using linear least squares regression. For fitting the model into a time series data we assume that the end of any year is followed by the beginning of the next year, the model should be a smooth periodic function with period 1 year (Wongsai *et al*., 2017). These statements clear that the most appropriate model is the natural cubic spline with boundary conditions possessing smooth periodicity. Then, by trial and error basis, adequate number of knots and their positions were fixed for fitting smooth spline curve in the plot. The formula for a cubic spline function is displayed in equation (2).

$$S_t = \alpha + bt + \sum_{k=1}^{p} c_k (t - t_k)_+^3 \tag{2}$$

where $S_t$ is the spline function, $\alpha$, $b$ and $c_k$ are the parameters in the model. $p$ is the total number of knots, $t$ denotes time in Julian day, that is, specified day of year. $t_1 < t_2 < ... < t_p$ are specified knots and $(t - t_k)_+$ means that $(t - t_k)$ is positive for $(t > t_k)$ and zero otherwise. The boundary conditions require that $S_t$ for $t < t_1$ equals $S_t$ for $t > t_p$. This method was applied in both LST and NDVI data.

### 2.3.2 Seasonal adjustment

Ideally, the model provides seasonal pattern for a year, and this suggests, it should be defined over continuous time, rather than just for 23 (NDVI) or 46 days (LST) of the

year indexing the data series. On one hand we observe the seasonal effects on data by using the models like natural cubic spline function and on the other hand this seasonal component needs to be removed for observing time series trend change. Every regression model, in a time series climate data, needs to be decomposed into its season and trend components and hence the changing trend during a period of time can be clearly explained. This minimizes the seasonal effect to the trend analysis. Therefore, for each series of data, seasonally adjusted temperatures or vegetation are computed by subtracting the seasonal pattern from the data, and then adding a constant (mean) to ensure that the resulting mean is the same as the mean of the data over the whole period. The formula took the form as,

$$y_t = x_t - \hat{x}_t + \bar{x} \tag{3}$$

where, $y_t$ is the seasonal adjusted LST or NDVI at observation $t$, $x_t$ is the observed value, $\hat{x}_t$ is the fitted value from natural cubic spline model and $\bar{x}$ is the overall mean of observed data.

### 2.3.3 First order autoregressive process

Autoregression process (AR) is used in LST data to minimize the auto correlation from its residuals (Venables & Ripley, 2002). AR(p) is an autoregressive model of the $p^{th}$ order lag and if the autocorrelations of these data were assessed by an autoregressive process of the first order lag (Cryer, 1986), the autoregression model is AR(1). The data was finally filtered to remove autoregression effects.

### 2.3.4 Second degree polynomial regression model

Finally, seasonally adjusted and autocorrelation filtered temperature values ( $y_t$ ) were fitted to polynomial regression model. It is a type of linear regression for quantitative independent variables. They are the most frequently used curvilinear response models (Neter *et al*., 1996) where there would be more than one degree of expressions ($n^{th}$ degree). The general polynomial regression model, as a second degree (n=2) of polynomial, takes the following form:

$$y_t = \alpha_0 + \alpha_1 t + \alpha_2 t^2 + \varepsilon \tag{4}$$

where $y_t$ is the seasonally adjusted, filtered temperature at time $t$, $\alpha_0$ represents the mean response of $y_t$ when $t = 0$, $\alpha_1, \alpha_2$ are coefficients and $\varepsilon$ is the error term.

### 2.3.5 Logistic regressioin model

Logistic regression is a model for fitting the data when outcome variable is dichotomous (Hosmer & Lemshow, 2000). Multiple logistic regression model is commonly used to find out the association between outcome and predictor variables, when the predictor is more than one.

$$\ln\left[\frac{p}{1-p}\right] = \mu + \beta_1 x_1 + \beta_2 x_2 \tag{5}$$

Here, $p$ is the probability of expected outcome, that is 'Accelerated' LST pattern, $\mu$ is the intercept, $\beta_1$ and $\beta_2$ are the coefficients of the independent variables $x_1$ (altitude) and $x_2$ (land cover) respectively.

### 2.3.6 Linear regression model

Linear regression is a linear approach to model the relationship between continuous outcome and the predicting variables. The association is shown by fitting straight line to the seasonally adjusted data that evidently gives the trend in time series plots. Therefore, the seasonally adjusted data were fitted to the linear regression model to find the 15 years' changing trend of NDVI.

### 2.3.7 Generalized estimating equations

To access the overall change in study area, trend for the whole study area needs to be computed. However, the data in each cell had autocorrelation within the same grid. To curb this problem, the generalized estimating equations (GEE) were applied in this work (Liang & Ziger, 1986). GEE model allows for the handling of long term pattern in the data by adjusting for autocorrelation which needs to be controlled in time series data because today's value is correlated with that of the previous and subsequent days if the unit of observation is same (Abi *et al.,* 2003). The GEE function was fitted into time series NDVI data, that were divided into three periods of five years each (2000-2004, 2005-2009 and 2010-2015) , one by one for each time section. The results were displayed as a 95% confidence intervals, calculated for each sub period. The plots easily show the NDVI changes in three time periods within three regions of Nepal.

## Chapter 3

**Results**

This chapter illustrates the analysis of LST and NDVI showing the pattern and trend of changes through 15 years' time period.

**3.1 Results of LST data**

This part of work explains about the results for seasonal pattern and time series LST pattern of its change in Nepal during 15 years' time. Each of the 27 regions (Figure 2.3) were analyzed one by one at sub region level. The results are described below.

**3.1.1 Seasonal pattern of LST**

For observing seasonal pattern of temperature between 2000 to 2015, the graph of region number 5, 14 and 23 were selected to represent alpine (Figure 3.1), temperate (Figure 3.2) and tropical (Figure 3.3) zones respectively. Each panel in Figure 3.1 to Figure 3.3 represents a sub region and eight blue positive (+) signs at the bottom of each panel show the knot positions. Each vertical gray line is an observation day and the black dots are the temperature plot, consecutively for 15 years. X-axis represents the Julian day of year and y-axis indicates the LST day temperature in °C. In each panel, a smooth spline curve (red line) is derived from natural cubic spline model. In all three zones, the temperature began to rise immediately after winter in February and the peak was seen during summer in April (day 97 to 113). By the end of May it gradually declined and reached the trough in winter during January (days 1 to 15). The $R^2$ of the models ranged from 18% to 90% and majority of them had it more than

50%. The LST was a bit sparse during rainy season, day 170 to 240. The results

showed that the seasonal pattern still did not vary much in three ecozones.
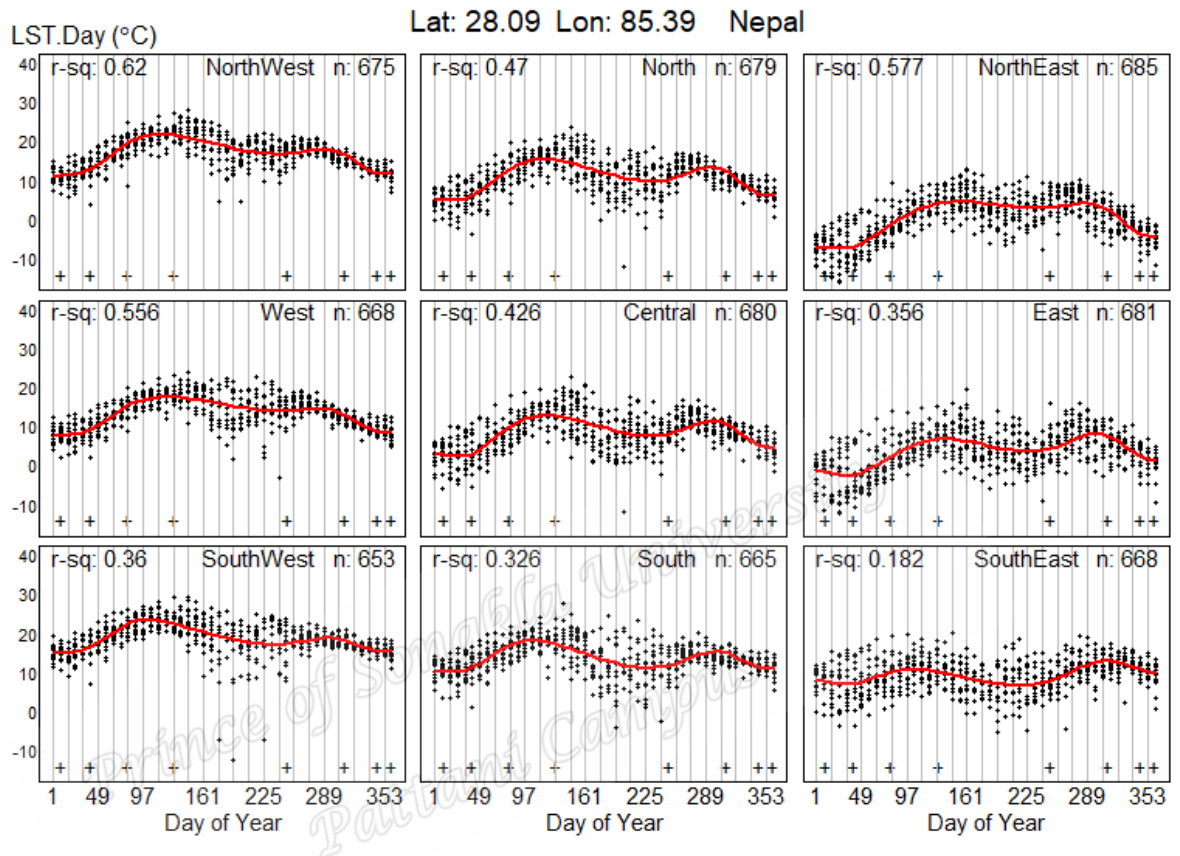


Figure 3.1 Seasonal LST pattern in alpine zone, sub region 5
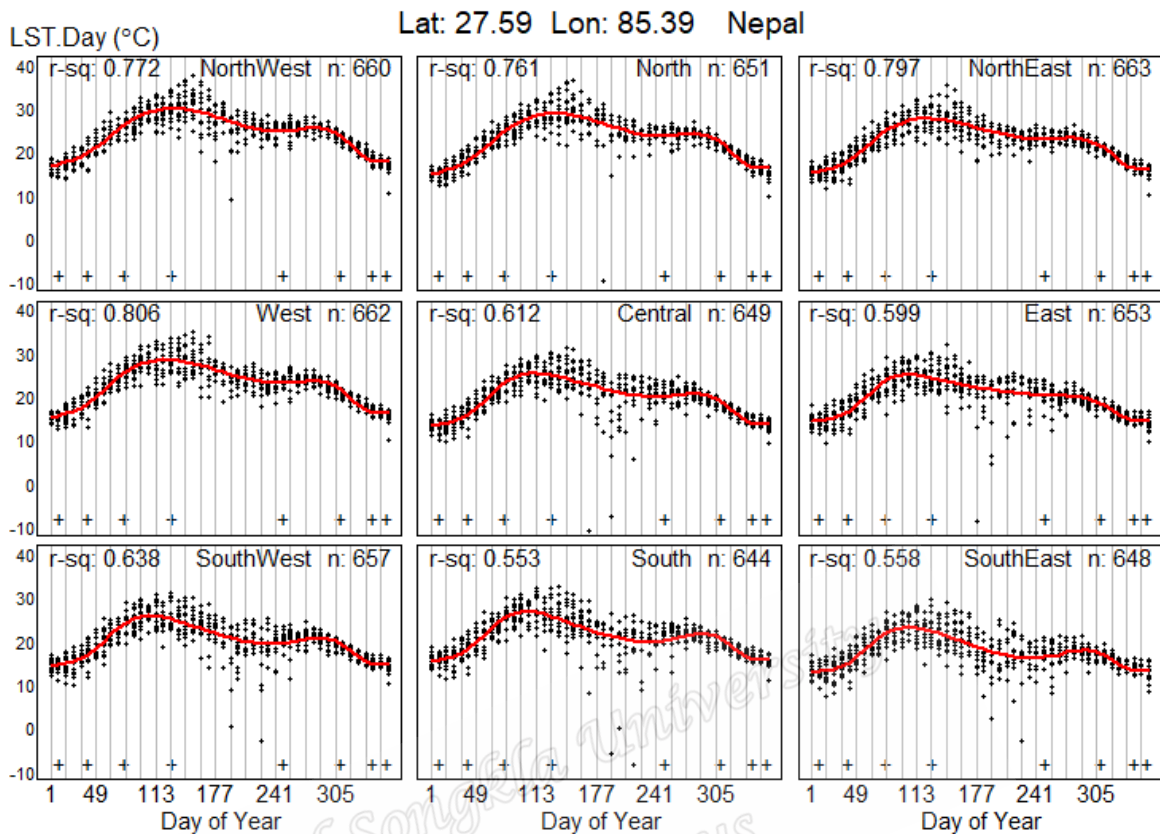
Figure 3.2 Seasonal LST pattern in temperate zone, sub region 14
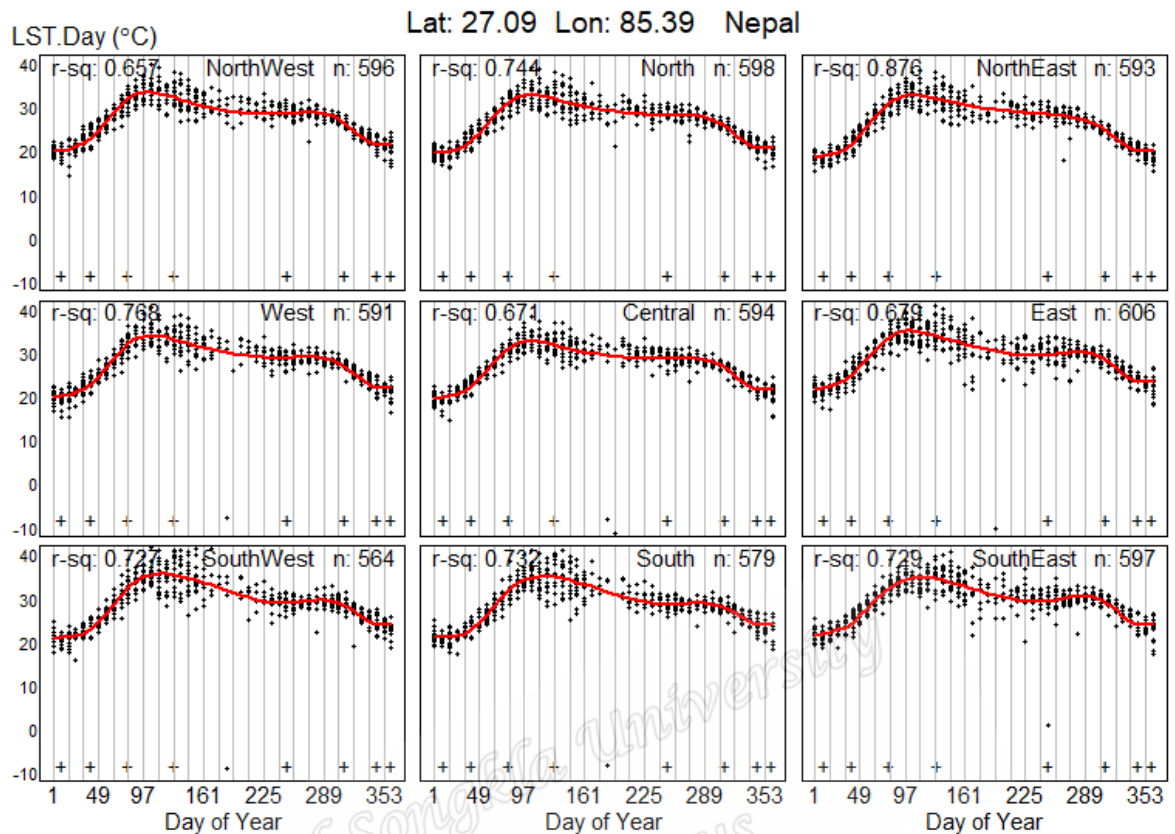
Figure 3.3 Seasonal LST pattern in tropical zone, sub region 23

Comparatively the plots of LST in alpine zone was more scattered than other two

zones and the graph shows that the peak period of summer is mostly divided into two

unlike in other two zones. The level of temperature is decreasing from tropical to

alpine zone.

### 3.1.2 LST pattern

The data were seasonally adjusted after the natural cubic spline function and the

autocorrelation effects were filtered out. Polynomial regression model was fitted to

the data to identify the LST pattern of each of 27 regions one by one.  The results of

these LST pattern were shown in Figure 3.4 to Figure 3.6 which represent region 5

(alpine zone), region 14 (temperate zone) and region 23 (tropical zone) respectively.

The panel on bottom right side of each figure shows all those curves of respective sub regions in different colors which stand for NW (black), W (blue), SW (yellow), N (red), C (cyan), S (purple), NE (green), E (pink) and SE (gray). The y-axis shows seasonally adjusted and autocorrrelation filtered temperature in degree Celsius (°C) and x-axis represents the year from 2000 to 2015, $n$ is the number of observations in each sub region, $a_i$ is the autocorrelation coefficient, Inc/dec is meant to show increase or decrease of temperature per decade and its difference between the period 2000 and 2015 gives total change of the temperature in 15 years period. The pink dots are the unreliably fluctuating LST, which are more frequent in alpine region and are eliminated during analysis.

The results of all 243 sub regions showed the rise of temperature ranging from 0.009 to 0.430°C and a fall from – 1.047 to – 0.010°C along with the autocorrelations ($a_i$) of the data below 0.35. The graphs showed, alpine region had most of the pattern facing downward and the temperature variation was highest among three ecozones. Level of temperature was much below 20°C in alpine region while in tropical and temperate zones it was distinctly above that. The patterns in alpine Himalaya were mostly downward facing or the falling type (Figure 3.4). In temperate Mountain the patterns looked almost flat with very gentle rising (Figure 3.5). While in tropical Tarai, mostly the LST patterns were upward facing or rising type (Figure 3.6). Hence, the rising pattern (the positive change during 15 years' period) was highest in Tarai (74.1% grids) than in Mountain (67.9% grids) and Himalaya (22.2% grids) regions. In overall study area, the significant rising pattern was prevalent only in 46.5% of grid area.
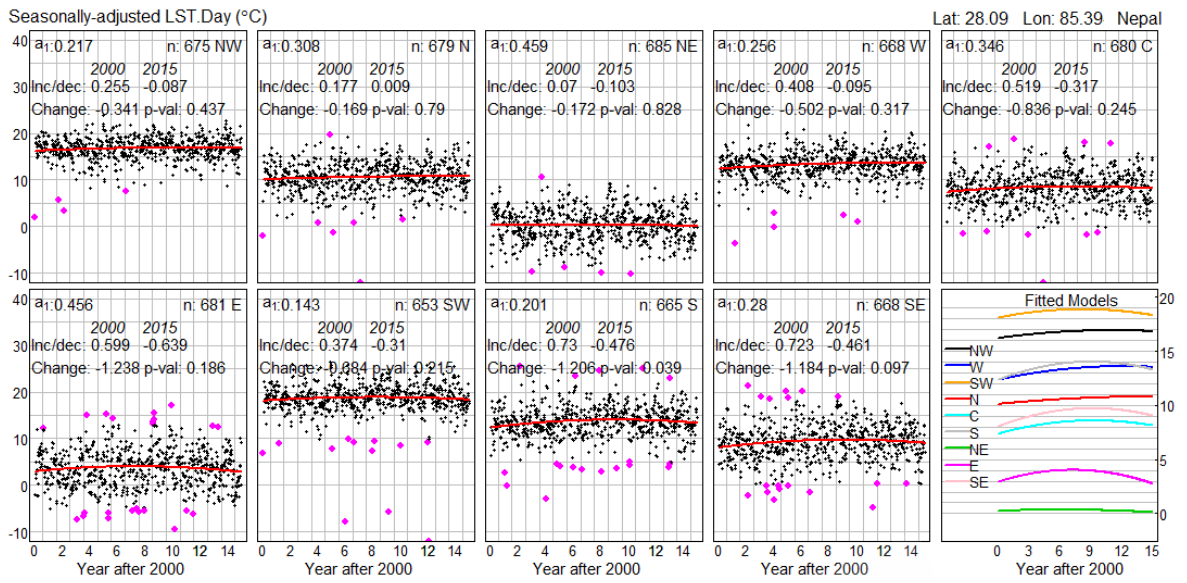
Figure 3.4 LST trend for 15 years in alpine zone, region 5
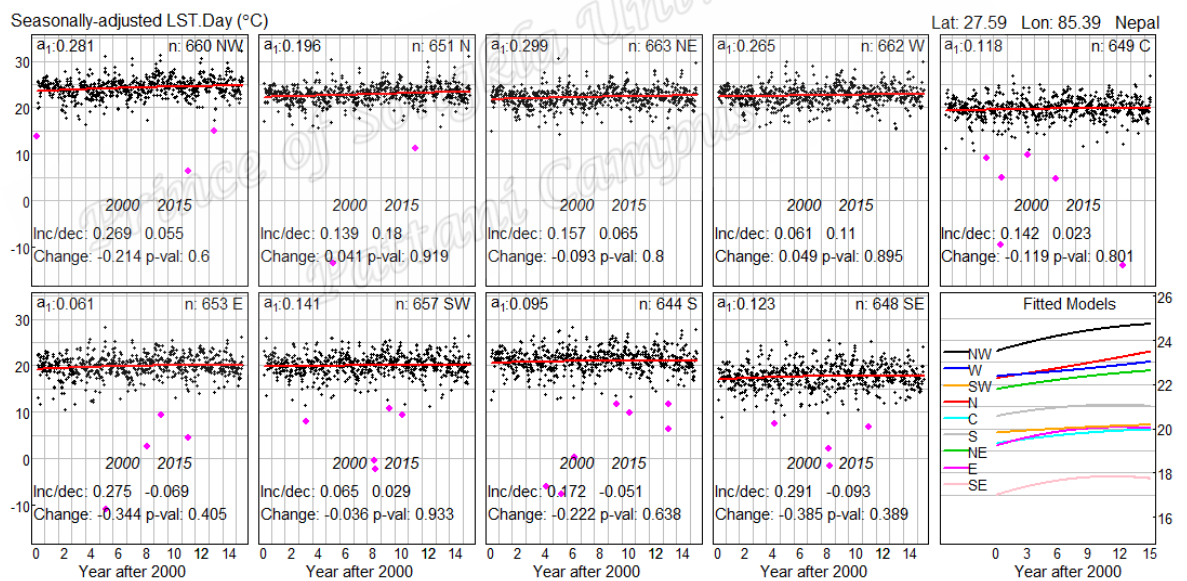


Figure 3.5 LST trend for 15 years in temperate zone, region 14
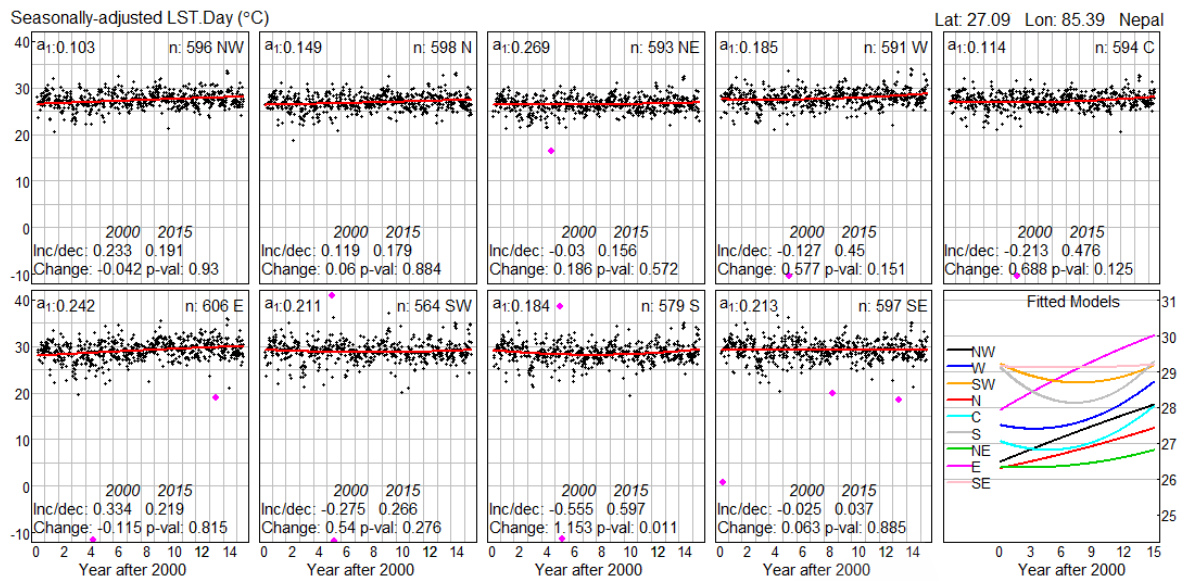
Figure 3.6 LST trend for 15 years in tropical zone, region 23

## LST pattern and altitude

The LST pattern plotted over the altitude map of study area showed that the alpine zone (Figure 3.7, in black box), with dark green color and representing >3,500 m altitude, had mostly downward facing pattern or falling type of pattern. The temperate zone (in red box), with brown color and representing 1,500-3,500 m altitude, had most of the pattern flat or gently rising. The tropical zone (in blue box), with had mostly the upward facing or rising pattern.
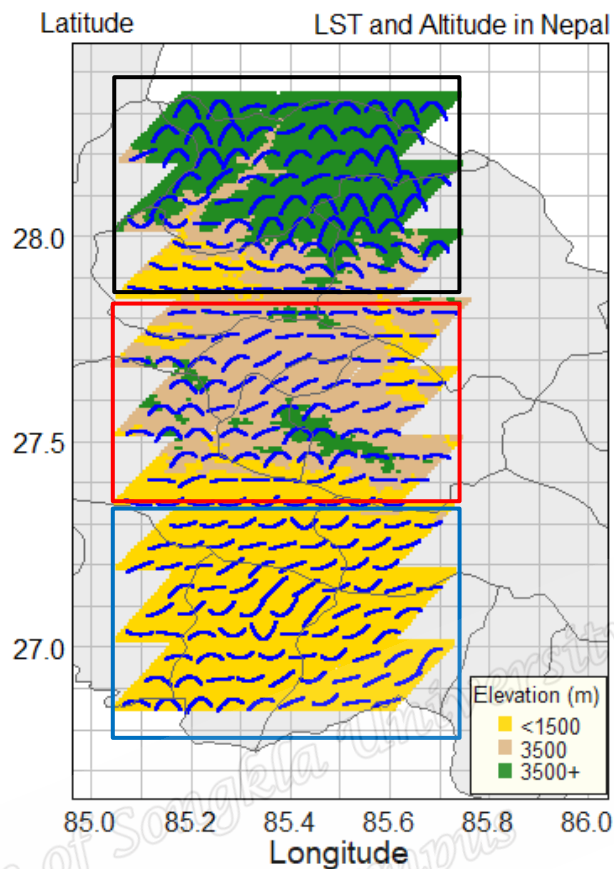
Figure 3.7 LST pattern and altitude status in the study area

**LST pattern and land cover**

The LST pattern plotted over LC map of study area showed that the alpine zone
(Figure 3.8, in black box), with red colored patches indicating the non vegetated land
had mostly downward facing pattern or falling type of pattern. The temperate zone (in
red box), with brown color indicating the tree forest, had most of the pattern flat or
gently rising. The tropical zone (in blue box), with mixed form of shrub/ crop and the
tree forest, represented by yellow color, had mostly the upward facing or rising
pattern.
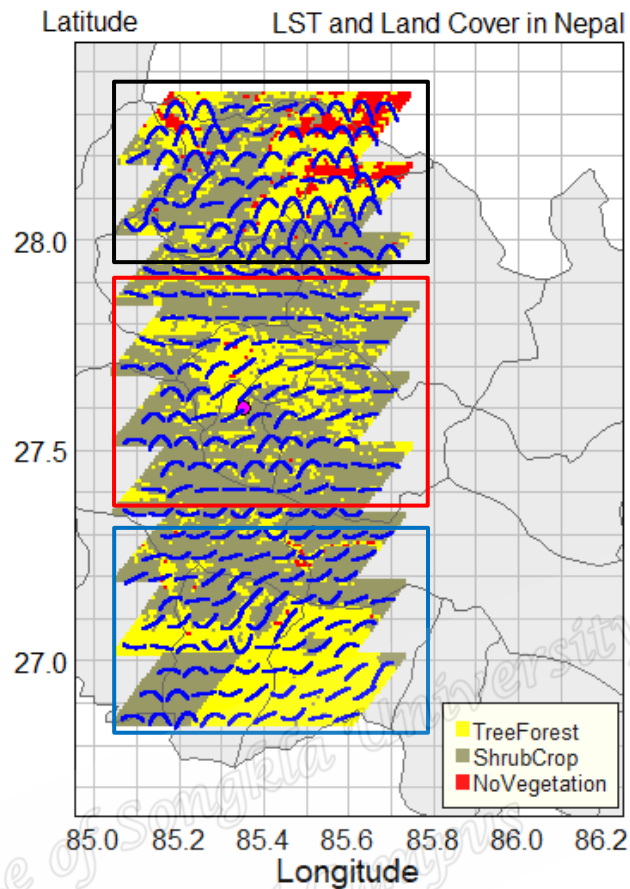
Figure 3.8 LST pattern and land cover status in the study area

### 3.1.3 Grouping of LST pattern into five categories

The various shapes of pattern when plotted on the study area map for all 243 sub regions, we can observe the various pattern distributed in the study site (Figure 3.7 and 3.8) which were grouped into five categories (Figure 3.9) based on their shape. They are, 'Flat' pattern (11.5% grid area, ⎯ , ⌢ , ⌣ ), 'Acclerated-increasing' pattern (25.9% of grid area, ╱ , ╱ ), 'Decelerated-increasing' pattern (20.6% of grid area, ╲ ), 'Decelerated-decreasing' pattern (22.6% of grid area, ⌐╲) and 'Accelerated-decreasing' pattern (19.3% of grid area, ╱ ).
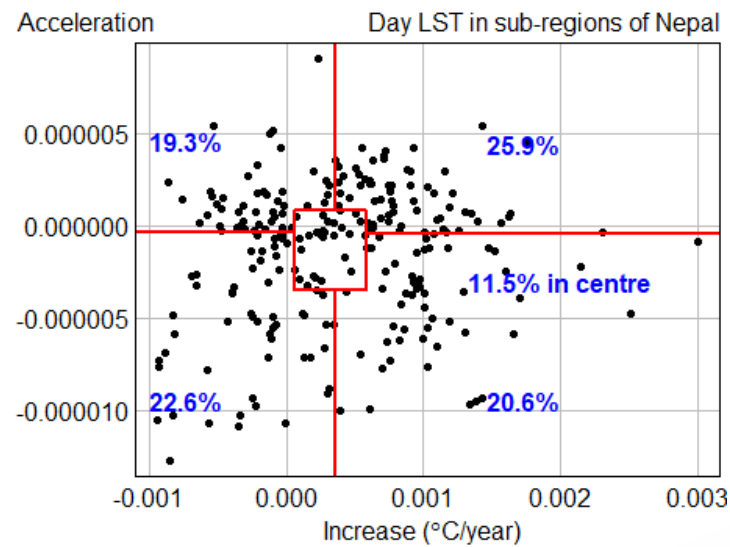
Figure 3.9 Five categories of LST curves within 27 regions

**3.1.4 Association of LST pattern with altitude and land cover**

Those five categories were regrouped into two based on whether the change of LST pattern is accelerating or not. Refering to Figure 3.9, 'Accelerating' pattern, included Accelerated-increasing pattern and Accelerated-decreasing pattern, and 'Non accelerating' pattern included rest of all LST pattern among five categories. Logistic regression model was used to find the association of LST binary pattern with altitude and LC of the area. The result showed there was negative association of LST Accelerating pattern with altitude and the non vegetated LC. The sum contrasts method was used to show 95% confidence intervals of these change. Figure 3.10 shows the CI plot of the results. Red horizontal line is the overall percentage of accelerating pattern (46.5%) and y-axis explains about the probability of accelerating pattern. On x-axis three categories of altitude and 3 of LC are observed. The green dots are crude mean of each while black dots in CI line represent the adjusted means from the whole model. The figure clears that, when the altitude is lower there is

higher probability of having accelerating pattern or vice versa. In LC, no vegetated land had less probability of having accelerating pattern of LST while the other two categories did not show significant difference from the overall acceelrating pattern.
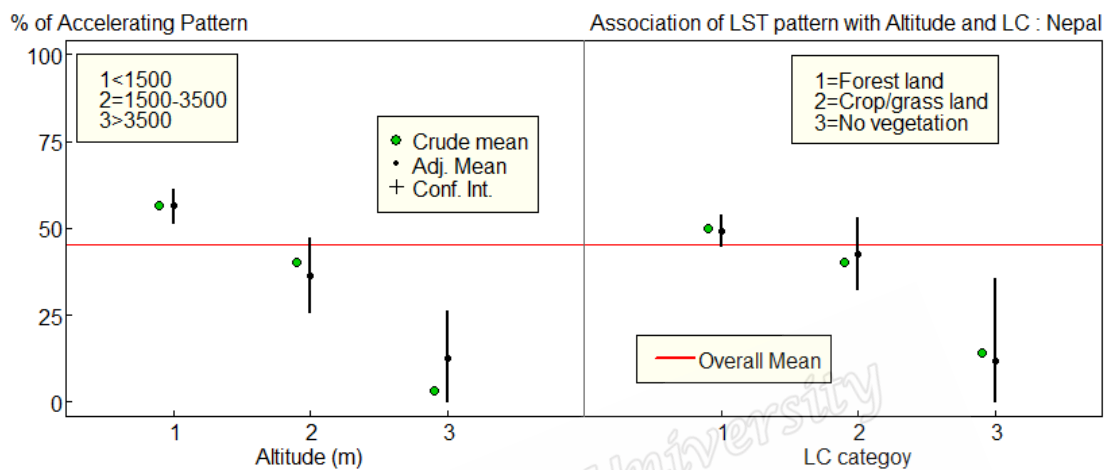


Figure 3.10 CI plots to identify the association of LST pattern with altitude and LC

## 3.2 Results of NDVI data

This part of work focusses on the results for pattern and trend of NDVI changes in Nepal during 15 years' time. Each of the three regions (refer Figure 2.5) were analyzed one by one at grid level. Since the different grids show similar ideas, out of 196 selected grids only some grids of each region were displayed for explanation below.

### 3.2.1 Seasonal pattern of NDVI

Each of the three regions were analyzed one by one for observing seasonal pattern of temperature between 2000 to 2015. Each panel in Figure 3.11 represents a grid and the symbols in figure are same as explained in seasonal LST analysis (refer section 3.1.1). X-axis represents the Julian day and y-axis indicates the NDVI values. In each panel, a smooth spline curve (red line) is derived from cubic spline model.

Out of 196, systematically selected grids for analysis of the study, only central grid was selected for display representing each of east, center and west regions (Figure 3.11). The n represents the number of observation of NDVI for each grid. The x-axis represents the observation day of year and y-axis represents the NDVI index in the selected grid. The red line is the spline fit after removal of unreliable and doubtful values and the model $R^2$ increased respectively from 11%, 15% and 58% to 86%, 50 and 82% before and after the data management process, respectively. Spline curve does not show much variation of pattern among its nearby grids since they were all from same climate zone within a distance less than 700 km. Every region showed that the vegetation grew and reached peak in rainy season and gradually declined to trough in winter. The NDVI in east region extends from 0.40-0.85 (Figure 3.11 (a)), indicating that it has a lot variation of vegetation from crops to trees, while in the center, it ranged from 0.70 to 0.90 (Figure 3.11 (b)) indicating that it lacked crops and shrubs. In the west, the range of vegetation highly fluctuated from 0.40 to 0.80 (Figure 3.11 (c)), meaning the range of vegetation is from crops to tree, similar to eastern region.

The greening observed to start in days 81, 97, 129 and browning in 257, 273, 273 in those three regions respectively. Here, both greening and browning was earlier in east than the other areas. Therefore, the start of season (greening of vegetation) had a trend to move from east to the west ward area and same was the case of browning.
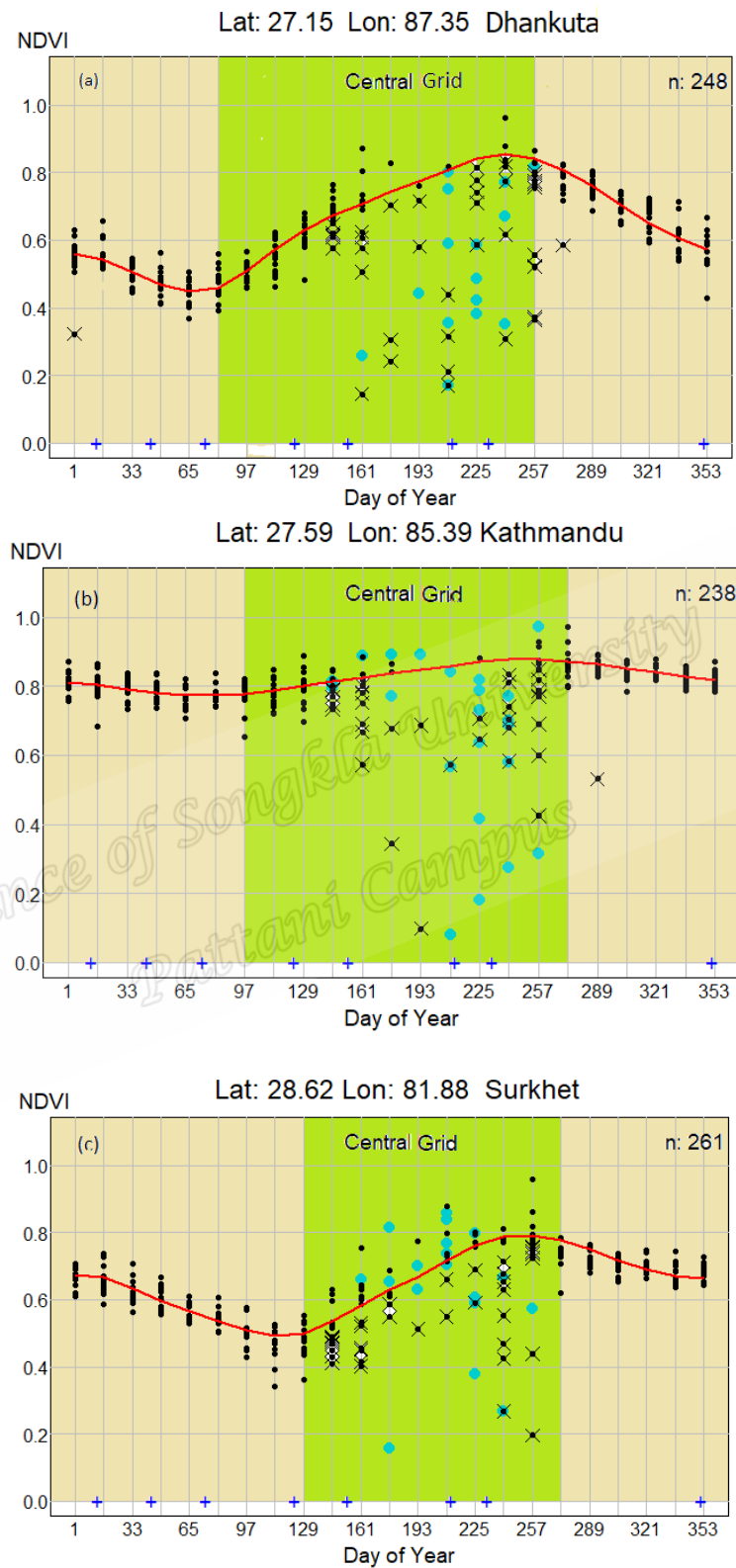
Figure 3.11 Seasonal NDV pattern in east (a), center (b) and west (c) of Nepal

This evidences that vegetation is in peak, from 160 to 290 (June to October) and lowest in winter during day 350-75 (December to March). The peak period is called greening season and trough period is called browning season. Two phenological metrices, the begining of season (start of greeening) and end of season (end of browning) were used to identify the changes in seasonal characteristics. Here, in east, center and west regions, greening started on day 81 (March 21), 97 (April 7) and 129 (May 9) while the browning starts in day 257 (September 17), 273 (October 3) and 273 (October 3) respectively every year. Therefore the greening was earlier and longer in east than west region of Nepal.

**3.2.2 NDVI trend**

**Linear trend**

Linear regression model was used to observe the trend of NDVI, for 196 grids in each of the three regions which were modeled one by one. The data were plotted and the annual seasonal fluctuation of NDVI, derived from the natural cubic spline function was added back to the plot and shown in red line along with green that explained the NDVI trend for 15 years period. In Figure 3.12 to Figure 3.14, black dots are data plotted year wise. The increasing or decreasing trend (Inc/dec) per decade and respective p-values from linear regression show how much vegetation has been changed from 2000 to 2015. Here, n represents the number of observation in each plot. In eastern region (Figure 3.12), the statistically significant increase and decrease occurred in 59.2% and 6.9% of the area that cleared about the dominant increasing trend of vegetation. The central region (Figure 3.13) has mixed form of result. Total significant rise was seen in 22.9%  area while 24.5% had significant decline. Finally

the western part showed 61.2% grids had the significant increase and 14.8% had

decreasing (Figure 3.14) trend.
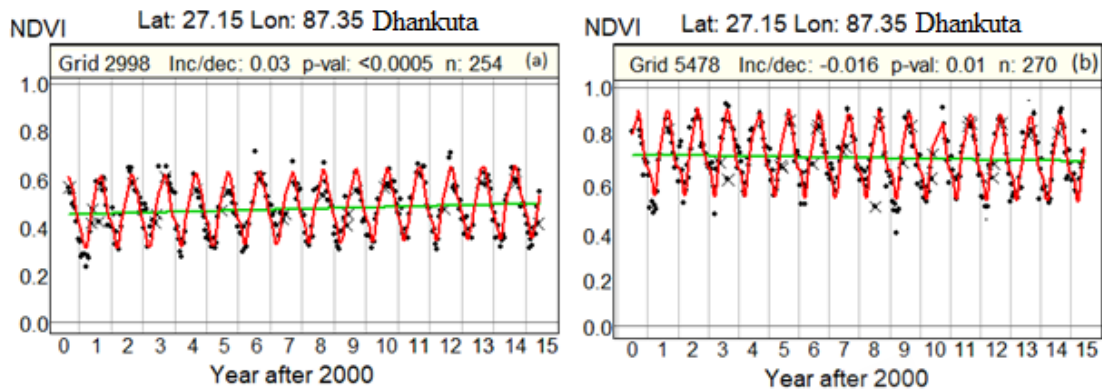


Figure 3.12 Linear trend of NDVI show ing an increase (a) and a decrease (b) in east
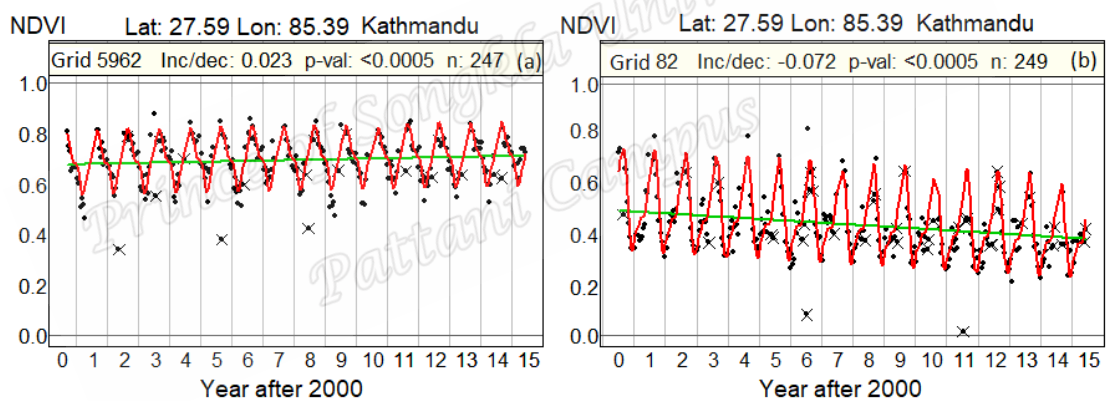


Figure 3.13 Linear trend of NDVI showing an increase (a) and a decrease (b) in center
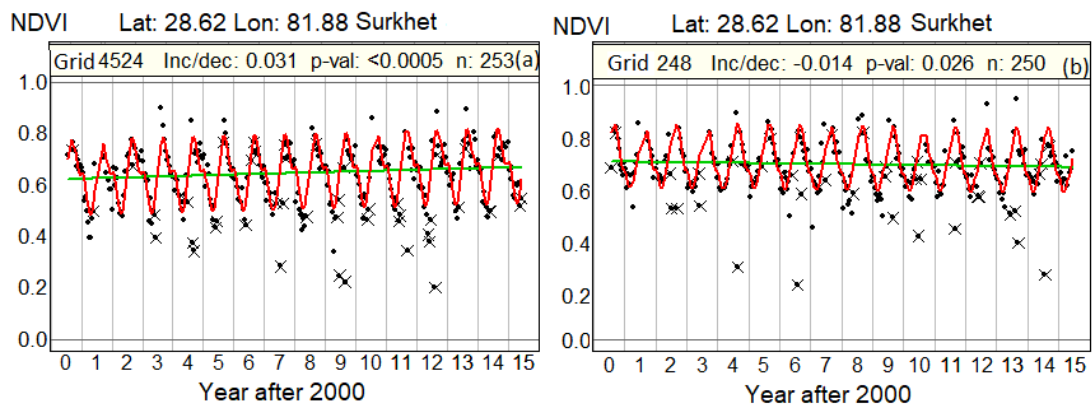


Figure 3.14 Linear trend of NDVI showing an increase (a) and a decrease (b) in west

**GEE and confidence interval plots**

To derive further conclusion about the overall change of NDVI in each region GEE was fitted to 196 grids in combined form but divided the time frame into three sections, 2000-2004, 2005-2009 and 2010-2015, due to reason, GEE can fit well in the data having correlations in outcome varaible within the cluster. A 95% CI plots were drawn from the coefficient values of the model to show vegetation trend in three time sections (Figure 3.15). The red horizontal line is the the level of no change of NDVI. Vertical lines are the confidence intervals (CI) of each of the five year period data. X-axis indicates three sections of time for each region and y-axis represents the change of NDVI per decade. The results showed that the NDVI trend was overall increasing in east and west regions while it was decreasing in the center.
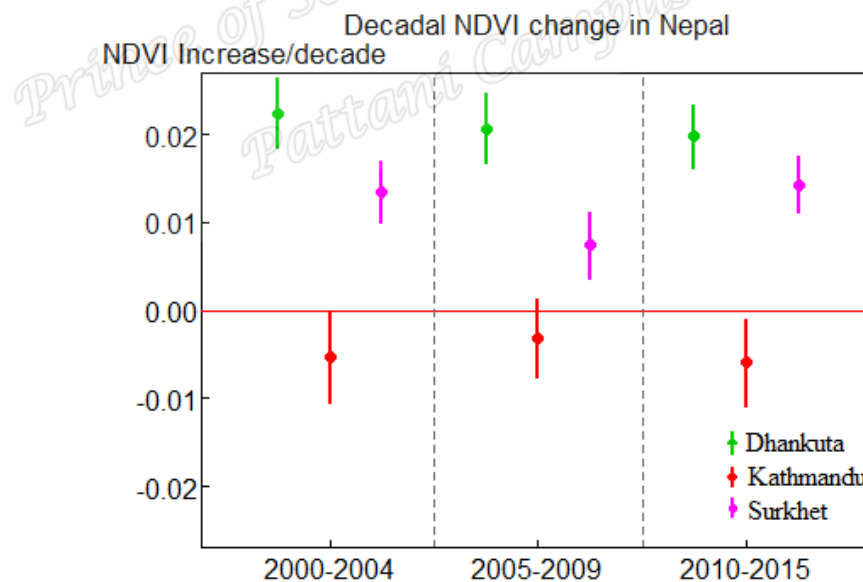


Figure 3.15 Confidence interval plots of NDVI change in three time sections during 2000-2015 in east (Dhankuta), center (Kathmandu) and west (Surkhet) of Nepal

## Chapter 4

## Discussion, summary and conclusion

### 4.1 Discussion

### 4.1.1 Study of LST

The altitude, in Nepal, ranges from 60 m from the sea level to 8,848 m, the highest summit of the world the Mount Everest, while moving from north-south width. Therefore, within this altitudinal variation a huge diversity in nature can be obtained. The variation of soil type and rainfall are much different even from east to west or north to south of Nepal. Moreover, the climate variables are quite sensitive to respond the geographical or ecological variations. The previous studies have shown that, at the expense of macro-level spatial analysis, the local level climate changes have often been overlook. Therefore, this study identified the changing temperature and vegetation pattern in Nepal at local levels.

The study applied a combination of natural cubic spline function and polynomial regression model for LST pattern analysis. MODIS LST time series data had uncertain and missing values due to cloud cover. Even in that situation, it has been suggested that the cubic spline function can be used to detect the seasonality in MODIS LST time series (Wongsai *et al*., 2017). The seasonal temperature pattern showed almost similar peaks (in summer) and troughs (in winter) in all sub regions suggesting that they do not vary in these locations. In contrast, the study by Portmann *et al.* (2009) in USA showed that annual maximum and minimum temperature trend can significantly vary but at a larger distance areas. The local variation in annual

temperature pattern might have happened due to the effect of different natural (vegetation, altitude and topography) and human factors (land use and urban activities). The tropical zone had mostly 'Accelerating' pattern and the temperate zone dominantly had Flat pattern. Both of these regions had lower altitude and dense population. The alpine zone had mostly 'Non accelerating' pattern, might be due to lower human activities and higher altitude. Hence, this study has revealed a strong negative association between temperature pattern and altitude. A work in Malawi Africa with the altitude (900-2,400 m) had investigated a coherent result of negative association between temperature and altitude (Lancaster, 2012). The temperature trend and altitude relationship studied in China by Dong (2014), explored some differing results. The temperature was decreasing below altitude 200 m and increasing from 200-2,000 m and weakly positive above 2,000 m. Even though the altitude and temperature change has a very strong statistical relationship, all these studies revealed that it can be either positive or negative, depending on the altitude level, topography and land use pattern of the location. Moreover, the association of LST pattern with LC showed that significant association of non accelerating pattern was prevalent in the non vegetated area. The study of three ecozones show completely distinct results and that give a clear picture about how the temperature pattern locally look like and it assures that they differ in different ecozones as well. The binary category of LST pattern shows that accelerating and 'Non accelerating' pattern were in almost 4.5:5.5 ratio, indicating that more than fifty percent area has non accelerating pattern. The interesting part of this result is that most of the accelerating pattern were observed in tropical Tarai while in temperate Mountain and alpine Himalaya zones the pattern are mostly flat or non accelerating. Hence, accelerating pattern of temperature is seen

progressive from north to south of Nepal. The previous studies have shown that the accelerating pattern is due to more urban builds and higher population (Sun & Kafatos, 2007; Maria 2012; Sun *et al*., 2012) or the altitude (Aigang, 2009; Khandelwal *et al.,* 2017) and both factors are in reversed condition from south to north. Additionally, in alpine zone snow clad land is seen as a unique feature. The previous studies show a contrasting result that (Johanssen *et al.,* 2004; Chen *et al.,* 2013; Shrestha *et al.,* 2016) the rate of ice melt in snow clad lands is much higher due to the effect of anthropogenic activities and a consequent rising temperature. That has alarmed the whole world about the global warming scenario from melting of snow caps to rising of sea levels. However, Westergaard-Nielsen *et al.* (2018) studied that the thick snow clad surfaces in Greenland do not show rising LST pattern and that the result is coherent with ours. Therefore, all snow clad lands do not have same rising pattern of temperature and that might depend on population density, the thickness of snow over the ground surface or else.

All those previous studies differ from ours in that, they show the association of temperature itself with the other variables while ours explain the relationship with the type of temperature change pattern. Those studies mostly explain gross picture of temperature change in a big region that does not give the idea of local pattern. In this study it is clear that the local variation of the changing pattern of temperature do exist at any particular area. The ecozones were identified as a part that can contribute for an important information of pattern of local temperature change in this single study. Even though the absolute causes of this kind of differences in temperature pattern in three ecozones is out of the scope of this study the associations of these pattern with altitude and land cover in the selected area have been observed. However, the detail of

the causes of these pattern can be further explained in future work. Also, the trend of future pattern can be explored in longer period data by using other appropriate tools such as spline curves or polynomial regression with higher degrees.

### 4.1.2 Study of NDVI

Regarding vegetation, the seasonal pattern showed the vegetation increased to highest level at the end of rainy season that is during September and eventually declined to the minimum level in the winter season during January to March. This result is consistent with other studies in tropical or temperate climate zones where seasonal fluctuation is commonly exhibited in vegetation (Zhang *et al.,* 2016; Chen *et al.*, 2014; Suepa *et al.,* 2016; Evrendilek & Gulbeyaz, 2008; Yin *et al.,* 2016). High humidity, temperature and rainfall favours, the plant growth and refoliation during rainy season. Also, the science has proved that, the growth of plants including its metabolic rates is much reduced in cooler air temperature (Fitter & Hay, 2002). The grid level regression analysis showed that NDVI was dominantly increasing in east and west sub urban areas while it was slightly decreasing in central urban Kathmandu. Additionally, the significance of the trend in vegetation changes for overall study area was identified by using GEE. The 95% confidence interval plots of vegetation showed significant rise in east and west regions while there was overall decline in the central regions. The global NDVI trend, including India and Southeast China, was found increasing during 1982-2012 (Liu *et al*., 2015). A coherent result was seen in Tibetan plateau during 2000 to 2009 (Zhang *et al*., 2013). Nepal is located between these two countries and can expect a similar pattern in the country. Even though the result was consistent in east and west regions, Kathmandu showed declining vegetation, might be due to dense population and fast urbanizing city area. In addition, Uddin *et al*.

(2015) have shown a contrasting result that the vegetation is continuously declining over the past few years in Nepal. But it was limited to only alpine region which represents very small fragment of vegetation in Nepal. However, this is pointing to our results with declining tendency of vegetation found in center.

Further investigation is still required to understand the potential reasons behind this seasonal pattern and the trend of vegetation and temperature pattern. Probable climate factors that can bring variations in temperature and vegetation change patterns will be more relevant to analyze in future.

**4.2 Summary**

This study is about the modeling of LST and NDVI pattern and trend in Nepal during 2000-2015 by using appropriate statistical methods. Therefore the analysis has two parts, LST and NDVI.

**4.2.1 Analysis of LST**

MODIS is a sensor, fitted into the Terra satellite by NASA, that measures environmental variables like LST in the whole world at a fixed interval of time. LST is measured in every eight day. The LST data were ordered for 27 regions that covered ecozones from North to South of Nepal. Each region was $21 \times 21$ km$^2$ and the data are framed into the grids of size $1 \times 1$ km$^2$ for every region. Hence there were 441 grids per region. To reduce spatial correlation, every region is divided into nine sub regions each covering a total of $7 \times 7$ grids. Hence in 27 regions there are 243 sub regions altogether. Using natural cubic spline function, polynomial regression and logistic regression models as a new combination of method, this study tries to explore the changing pattern at local level.

The data were accounted for seasonal adjustment and autocorrelation effects so that they could be noise and error free and can successfully be applied to find the temperature pattern. The natural cubic spline function helped to find the seasonal pattern of LST and the polynomial model was used for observing seasonal pattern and time series trend at every sub region. The observed patterns of temperature were binomially categorized and explored its association with altitude and land cover of the area.

Although the seasonal pattern of LST were comparatively consistent with respect to the nearby locations, the temperature trend varied a lot. They were more effective in explaining how the actual path (pattern) of temperature change looked like during a period of time. The various patterns were first categorized into 5 groups, Accelerated-increasing (25.9%), Decelerated-increasing (20.6%), Accelerated-decreasing (19.3%), Decelerated-decreasing (22.6%) and others showing Flat pattern (11.5%). These pattern were further recategorized into two, 'Accelerating' or 'Not accelerating' type. In 27 regions, 46.5% area had 'Accelerating' pattern of LST. Ecozone wise, alpine region had lowest 'Accelerating' pattern (22.2%) than temperate (67.9%) and tropical (74.1%). The sum contrast method was used to obtain confidence intervals for comparing adjusted mean within each category of both the predictor variables with the overall mean. The altitude below 1,500 m (tropical zone) had higher probability of 'Accelerating' LST pattern while altitude 1,500-3,500 m (tropical zone) had no significant difference from overall acceleration. However, above 3,500 m altitude (alpine zone), there was lower probability of having 'Accelerating' LST pattern. Moreover, the 'Accelerating' pattern was significantly negative with non vegetated land cover. The overall results gave an idea of local variation of temperature changing

pattern, its relation with altitude and land cover as well as a comparative picture of LST in three ecozones.

### 4.2.2 Analysis of NDVI

The NDVI data were measured in every 16 days interval. Data are obtained in form of grids of size $250 \times 250$ m$^2$ for NDVI. The NDVI was ordered for three different regions of Nepal covering east, center and west of Nepal, all belonging to temperate Mountain zone. The NDVI data were managed for both unreliable (highly fluctuating in a short time frame and sparse) and doubtful (when LST for the particular day was doubtful) values. The analyses were done at grid level. The studies about NDVI, so far had analyzed the data for wider regions while this study attempts to obtain results from each grid of the study area.

Natural cubic spline function with linear regression and GEE models could successfully show the seasonal pattern and changing trend of NDVI in three ways, at three study sites from east to west of Nepal. Initially, the seasonal pattern in every grid was analysed, secondly, the trend of individual grid cells and finally, the trend of whole study area in three time sub periods were investigated. In addition comparison of rate of changes in those time segments as well as among the study sites were done.

The results cleared that greening and browning of vegetation were earlier and longer in east side than west by more than 15 days, might be due to positive association with rainfall towards the eastern area that gets more rainfall by the virtue of its location. Finally, GEE model was used to explore the trend of NDVI change in 15 years period from 2000 to 2015. It identified that east and west regions, which were sub urban

areas, had apparently increasing trend of NDVI in all three periods during 2000 to 2015, while at central Kathmandu, a growing urban city showed a decreasing trend.

## 4.3 Conclusion

These studies illustrate the simple and effective approaches to time series data for assessing spatial and temporal changes of climate variables like LST and NDVI at a local scale. The LST showed similar seasonal pattern, a peak around April and trough around January every year for each ecozone in the study area. Also, LST pattern is found accelerating in southward area which is more populated. Five different types of LST pattern were identified: Flat, Accelerated-increasing, Accelerated-decreasing, Decelerated-decreasing and Decelerated-increasing. The binomial forms of those LST pattern showed that Accelerating pattern had negative association with altitude and no vegetated land cover. Regarding NDVI, the seasonal pattern did not show much variation among three districts from east to west of Nepal and the phenology (time for seasonal greening and browning of vegetation) was found to shift from east to west every year.  However the time series change in overall region showed a significant rise of vegetation in east and west sub urban areas, while, a serious decline was observed in central urban area. The methods can be generalized and also provide a basis for climate change information at a local level that can help local stakeholders in their long or short run development affairs.

## 4.4 Limitations

Some limitations do exist in the study. The cause of change and pattern is not adequately studied here and therefore the association with NDVI and LST with different climate variables is required to answer why a particular pattern of NDVI or

LST do occur at specific regions in Nepal. This question would guide us for the further continuation of the research.

## 4.5 Implication and Recommendation

The local level temperature or vegetation change in Nepal is essential to monitor for a proper control of negative consequences. The idea of seasonal as well as time series variation of temperature and vegetation at a local scale is of importance to local government and stakeholders to get idea for successful formulation of plans before starting any developmental, social and economic activities. Furthermore, the study can extend to a wider area, covering whole of the country and apply much simpler method for instance, only the spline function for both seasonal pattern and trend.

# References

Abi, K.L., Mearns, L.O. and Nyenzi, B. 2003. Weather and climate as health exposures. Edited by McMichael, A.J., Campbell-Lindrum, D.H., Corvalan, C.F., Abi, K.L., Githeko, A., Scheraga, J.D. and Woodward, A. In, Climate change and human Health: risks and responses. Chapter 2. Pp:18-40. WHO, Geneva, Swetzerland.

Bethany, A.B., Robert, W.J., John, F.,H. and John, M.F. 2007. A curve fitting procedure to derive inter-annual phenologies from time series of noisy satellite NDVI data. Remote Sensing of Environment. 106 (2007), 137-145.

Bounoua, L., Collatz, G.J., Los, S.O., Sellers, P.J., Dazlich, D.A. and Tucker, C.J. 2000. Sensitivity of climate to changes in NDVI. American Meteorological Society. 13, 2277-2292.

Bradley, B.A., Jacob, R.W., Hermance, J.F. and Mustard, J.F. 2007. A curve fitting procedure to derive inter-annual phenologies from time series of noisy satellite NDVI data. Remote Sensing of Environment. 106, 137-145.

Burke, M., Hsiang, S.M. and Miguel, E. 2015. Global non-linear effect of temperature on economic productivity. Research Letters. Doi: http://dx.doi.org/10.1038/nature 15725.

Chooprateep, S. and McNeil, N. 2015. Surface air temperature changes from 1909 to 2008 in Southeast Asia assessed by factor analysis. Theoretical and Applied Climatology. 123(1), 361-368.

Clark, P.U., Shakun, J.D., Baker, P.A., Bartlein, P.J., Brewer, S., Brook, E. *et al*. 2012. Global climate evolution during the last deglaciation. PANAS PLUS. Doi: www.pnas.org/cgi/doi/10.1073/pnas.1116619109.

Cryer, J.D. 1986. Time series analysis, United . R.R., Donnelley and Sons Company, USA

DFRS (Department of Forest Research and Survey). 2015. State of Nepal's Forest. Ministry of Forest and Soil Conservation (MFSC), Government of Nepal. Kathmandu.

DHM (Department of Hydrology and Meteorology) . 2015. Study of climate and climatic variables in Nepal. Ministry of Science, Technology and Environment. Government of Nepal. Available online: www.dhm.gov.np.

Dong, D., Huang, G., Qu, X., Tao, W. and Fan, G. 2015. Temperature trend–altitude relationship in China during 1963–2012. Theoretical and Applied Climatology. 122(1), 285-294.

Dormann, C.F., McPherson, J.M., Arau jo, M.B., Bivand, R., Bolliger, J., Carl, G. *et al.* 2007. Methods to account for spatial autocorrelation in the analysis of species distribution data: a review. Ecography 30. 609-628.

Eckert, S., Husler, F., Liniger, H. and Hodel, E. 2015. Trend analysis of MODIS NDVI time series for detecting land degradation and regeneration in Mongolia. Journal of Arid Environments. 113, 16-28.

Evrendilek, F. and Gulbeyaz, O. 2008. Deriving vegetation dynamics of natural terrestrial ecosystems from MODIS NDVI/EVI data over Turkey. Sensors. 8, 5270-5302.

Feehan, J., Harley, M. and Minnen, J. V. 2009. Climate change in Europe. 1. Impact on terrestrial ecosystem and biodioversity: A review. Agron. Sustain. Dev, 29, 409-421.

Fitter, H. and Hay, R.K.M.. 2002. Environmental physiology of plants, 3rd edn., Academic Press, New York (NY).

Goward, S.N., Xue, Y. and Czajkowski, K.P. 2002. Evaluating land surface moisture conditions from the remotely sensed temperature/ vegetation index measurements: An exploration with the simplified simple biosphere model. Remote Sensing of Environment. 79, 225-242.

Hansen, P.M. and Schjoerring, J.K. 2003. Reflectance measurement of canopy biomass and nitrogen status in wheat crops using normalized difference vegetation indices and partial least squares regression. Remote Sensing of Environment. 86, 542-553.

Hosmer, D.W. and Lemeshow, S. 2000. Applied Logistic Regression, Second edition, Wiley, Inc., New York.

IPCC (Intergovernmental Panel on Climate Change), 2013. Summary for policymakers. Climate change 2013: The Physical Science Basis. Contribution of Working Group I to the Fifth Assessment Report of the Intergovernmental Panel on Climate Change. Cambridge University Press.United Kingdom and New York (NY).

Johannessen, O.M., Bengtsson, L., Miles, M.W., Kuzmina, S.I., Semenov, V.A., Alekseev, G.V. *et al*., 2004. Arctic climate change: observe and modeled temperature and sea-ice variability. Tellus. 56, 328-341.

Julian, Y. and Sobrino, J.A. 2009. The yearly land cover dynamics (YLCD) method: an analysis of global vegetation from NDVI and LST parameters. Remote Sensing of Environment. 113, 329-334.

Karki, R., Talchabhadel, R., Aalto, J. and Baidya, S.K. 2016. New climatic classification of Nepal. Theoretical and Applied Climatology. Volume 125 (3-4), 799-808.

Karnieli, A., Agam, N., Pinker, R.T., Anderson, M., Imhoff, M.L., Gutman, G.G. *et al.* 2010. Use of NDVI and Land Surface Temperature for Drought Assessment: Merits and Limitations. Journal of Climate. 23, 618-633.

Kaufmann, R.K., Zhou, L., Myneni, R.B., Tucker, C.J., Slayback, D., Shabanov, N.V. *et al.* 2003. The effect of vegetation on surface temperature: a statistical analysis of NDVI and climate data. Geophysical Research Letters. 30 (22), (3)1-(3)4.

Khandelwal, S., Goyal, R., Kaul, N. and Mathew, A. 2018. Assessment of land surface temperature variation due to change in elevation of area surrounding Jaipur, India. The Egyptian Journal of Remote Sensing and Space Science. 21(2018), 87-94.

Lancaster, I.N. 2012. Relationships between altitude and temperature in Malawi. South African Geographical Journal. 62(1), 89-97.

Lean, J.L. and Rind, D.H. 2009. How will Earth's surface temperature change in future decades? Geophysical Research Letters. 36, L15708. Doi: http://dx.doi.org/10.1029 /2009GL038932.

Liang, K. and Zeger, S.L. 1986. Longitudinal data analysis using generalized linear models. Biometrika. 73, 13-22.

Liu, Y., Li, Y., Li, S. and Motesharrei, S. 2015. Spatial and temporal pattern of global NDVI trends: correlations with climate and human factors. Remote Sensing. 7, 13233-13250.

Mann, E.M. 2014. Earth Will Cross the Climate Danger Threshold by 2036. Scientific American, Available online: http://www.scientificamerican.com /article/earth-will-cross-the-climate-danger-threshold-by-2036/, 14th July 2016.

Maria, B. 2012. Thesis: Remote sensing for analysis of Rrelationships between land cover and land surface temperature in ten megacities. School of Architecture and the Built Environment Royal Institute of Technology (KTH), Stockholm, Sweden.

NASA (National Aeronautics and Space Administration). 2015. The Earth's Observatory. Available online: http://earthobservatory.nasa.gov/Features/GlobalWarming/page5.php., 14th July 2016.

NPHS 2011 (National Population and Housing Survey 2011). 2012. National Planning Commission. Central bureau of statistics, Government of Nepal.

Neter, J., Kuther, M.H., Nachtsheim, C.J. and Wasserman, W. 1996. Applied Linear Statistical Models. Times Mirror Higher Education Group, U.S.A.

O'Donoghuea, S.H., Drapean, L. and Peddemors, V.M. 2010. Broad scale distribution pattern of sardine and their predators in relation to remotely sensed environmental condition during the KwaZulu-Natal sardine run. African Journal of Marine Science. 32(2), 279-291.

ORNL DAAC. 2015. MODIS subset of NASA earth data. Available online: http://daacmodis.ornl.gov/cgi-bin/MODIS/GLBVIZ_1_Glb/modis_subset _order _global_col5.pl., 30th April 2016.

Penuelas, J., Filella, I., Zhang, X., Llorens, L., Ogaya, R., Lloret, F. *et al*. 2004. Complex spatiotemporal phonological shifts as a response to rainfall changes. New Phytologist.161, 837-846.

QGIS (Quantum Geographical Information System). 2017. Version 2.6.1. Brighton. Available online: http://www.gisblog.com/qgis-2-6-brighton-released/.

R Core Team. 2015. R: A language and environment for statistical computing. R Foundation for Statistical Computing, Vienna, Austria. Available online: http://www.R-project.org/.

Schlenkera, W. and Roberts, M.J. 2009. Nonlinear temperature effects indicate severe damage to U.S. crop yields under climate change. PNAS. 106(37), 15594-15598.

Semenov, V.A. 2007. Structure of temperature variability in the high latitudes of the Northern Hemisphere. Atmospheric and Oceanic Physics. 43( 6), 687-695.

Shrestha, A.B. and Aryal, R. 2011. Climate change in Nepal and its impact on Himalayan glaciers. Regional Environmental Change. 11, 55-77.

Song, L., Cannon, A.J. and Whitfeld, P.H., 2007. Changes in seasonal patterns of temperature and precipitation in China During 1971-2000. Advances in Atmospheric Sciences. 24(3), 459-473.

Sruthi, S. and Aslam, M.A.M. 2015. Agricultural drought analysis using the NDVI and LST data; a case study of Raichur district. Aquatic Procedia of International Conference on Water Resources, Coastal and Ocean Engineering (ICWRCOE 2015). Doi: http://dx.doi.org/10.1016/j.aqpro.2015.02.164.

Sun, Q., Wu, Z. and Tan J. 2012. The relationship between land surface temperature and land use/land cover in Guangzhou, China. Environmental Earth Science. 65, 1687-1694.

Tran, H., Uchihama, D., Ochi, S. and Yasuoka, Y. 2006. Assessment with satellite data of the urban heat island effects in Asian mega cities. International Journal of Applied Earth Observation and Geoinformation. 8(1), 34-48.

Tucker, C.J., Pinton, J.E., Brown, M.E., Slayback, D.A., Pak, E.W., Mahoney, R. *et al.* 2013. An extended AVHRR 8-km NDVI dataset compatible with MODIS and SPOT vegetation NDVI data. International Journal of Remote Sensing. 26(20), 44485-4498.

Uddin, K., Chaudhary, S., Chettri, N., Kotru, R., Murthy, M., Chaudhary, R.P. *et al.* 2015. The changing land cover and fragmenting forest on the Roof of the World: A case study in Nepal's Kailash Sacred Landscape. Landscape and Urban Planing. 141, 1-10.

USGS (United States Geological Survey). 2017. NASA EOSDIS Land Processes DAAC, USGS Earth Resources Observation and Science (EROS) Center, Sioux Falls, South Dakota . Available online: lpdaac.usgs.gov/data_access/gdex.

Vadasz, V. 1994. On the relationship between surface temperature, air temperature and vegetation index. Advances in Space Research, 14(3), (3)41-(3)44.

Venables, W.N., and Ripley, B.D., Modern Applied Statistics with S, Springer, Queensland, 2002.

Walther, G-R, Post, E., Convey, P., Menzel, A., Parmesank, C., Beebee, T.J.C. *et al*. 2002. Ecological responses to recent climate change. Nature. 416, 389-395.

Wang, S., Yang, B., Yang, Q., Lu, L., Wang, X. and Peng, Y. 2016. Temporal trends and spatial variability of vegetation phenology over the northern hemisphere during 1982-2012. PLoS ONE, 11(6), e0157134. Doi: https://dx.doi.org/10.1371/journal.pone.0157134.

Wanishsakpong, W. and McNeil, N. 2016. Modeling of daily maximum temperature over Australia from 1970 to 2012. Meteorological Applications. 23, 115-122.

Wanishsakpong, W., Khairil, A.N. and McNeil, N. 2015. Clustering and forecasting maximum temperature of Australia. Chiang Mai Journal of Science, 42(X), 1-11.

Weier, J. and Herring, D. 2000. Measuring vegetation (NDVI and EVI). NASA Earth Observatoy. Available online: https://earthobservatory.nasa.gov/Features/MeasuringVegetation/measuring_vegetation_1.php.

Wikipedia, 2018. Geography of Nepal. Available online: https://en.wikipedia.org/wiki/Geography_of_Nepal.

Wongsai, N., Wongsai, S. and Huete, A.R. 2017. Annual seasonality extraction using the cubic spline function and decadal trend in temporal daytime MODIS LST data. Remote Sensing. 9, 1254. Doi: http://dx.doi.org/10.3390/rs9121254.

Yue, W., Xu, J., Tan, W. and Xu, L. 2007. The relationship between land surface temperature and NDVI with remote sensing: application to Shanghai Landsat 7 ETM+ data. International Journal of Remote Sensing. 28 (15), 3205-3226.

Zhang, Y, Gao, J., Liu, l., Wang, Z., Ding, M. and Yang, X. 2013. NDVI-based vegetation changes and their responses to climate change from 1982 to 2011: A case study in the Koshi River Basin in the middle Himalayas. Global and Planetary Change. 108, 139-148.

Zhang, X., Fried, M.A., Schaaf, C.B., Strahler, A.H., Hodges, J.C.F., Gao, F., Reed, B.C. and Huete, A. 2003. Monitoring vegetation phenology using MODIS. Remote Sensing of Environment. 84(3), 471–475.

# Jurnal
## Teknologi

# Modeling of satellite data to identify the Seasonal patterns and trends of vegetation index in Kathmandu Valley, Nepal from 2000 to 2015

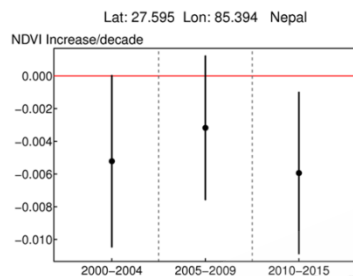Ira Sharma, Attachai Ueranantasun*, Phattrawan Tongkumchum

Faculty of Science and Technology, Prince of Songkla University, Pattani Campus. 181 Charoenpradit Rd., Rusamilae, Muang Pattani, Pattani 94000

*Corresponding author
attachai.u@psu.ac.th

## Graphical abstract



Lat: 27.595  Lon: 85.394  Nepal

## Abstract

Normalised difference vegetation index (NDVI) data were analysed to identify the seasonal patterns and the time series trends of vegetation in Kathmandu. The data were managed in three steps: reordering, removal of unreliable values and validating. A cubic spline function was used to examine annual seasonal patterns that revealed regular seasonal peaks (day 225 to 280) and troughs (day 50 to 81) of vegetation and start of greening from April and of browning from November. Linear regression models were fitted to seasonally adjusted NDVI, which statistically showed 40.70% of the grid cells had a significant increase and 24.71% of it had decreasing trends. To adjust for autocorrelation, generalized estimating equations (GEE) were fitted to the data for whole area that showed, the overall vegetation has been significantly declining at a rate of -0.005 ℃ and -0.006 ℃ per decade for 2000-2004 and 2010-2015 respectively. The recent period of decline is alarming for a growing city like Kathmandu.

*Keywords*: Satellite data, normalised difference vegetation index, cubic spline function, linear model, generalized estimating equations

## 1.0 INTRODUCTION

Vegetation is a general term for plant life, referring to the ground cover, and is the most abundant biotic element on Earth. It is essential for sustaining the ecological system of the Earth and serves critical functions at all possible spatial scales [1]. Therefore, quantifying the time trends of types, extents and characteristics of vegetation is of utmost importance for resource management, addressing the climatic issues among others. The worldwide studies of vegetation show that it has been changing in location dependent manners [2, 3]. The changes in vegetation on the land surface affect climates at both regional and global regions from short to extended periods of time [4]. Most of the factors that cause climate change are correlated with

vegetation [3, 5, 6]. Therefore, a study of quantitative changes of vegetation is important for assessing climate change related issues. However, reliable and complete data are challenging to obtain, especially in low-income countries where the field data inventory system is not yet properly in place. In this situation, the remote sensing or satellite data provide the best alternative, and one of the most common types of satellite based data is the Normalised Difference Vegetation Index (NDVI) from Moderate Resolution Imaging Spectro-radiometer (MODIS) [2, 7, 8, 9, 10].

MODIS is a sensor, fitted aboard the Terra and Aqua satellites by the National Aeronautics and Space Administration (NASA), and it monitors environmental changes due to fire, vegetation, temperature, earthquakes, droughts and floods ot

Earth [10]. Normalised Difference Vegetation Index (NDVI) is created based on MODIS remote sensors capturing the spectral behaviour of vegetation. The theory behind these sensing data is that vegetation reacts differently to different parts of the electromagnetic spectrum (including visible light). The electromagnetic waves are typically absorbed in the red and blue wavelengths, so reflected light retains the green wavelengths, with strong reflection also in the near infrared (NIR) wavelengths [11]. Based on this, the NDVI is calculated as a normalised ratio of the NIR and red bands. In every grid, each observation time is 16-day period. Therefore, in every year, the number of observation times is 23 and, consequently, a total of 345 times for 15 years period. NDVI for each observation time can be computed as follows,

$$NDVI_i = (NIR_i - RED_i)/(NIR_i + RED_i) \qquad (1)$$

where $i$ denotes an observation time (1, 2, 3, ..., 345). $NDVI_i$ is the NDVI value of the observation $i$, while $NIR_i$ is the NIR reflectance and $RED_i$ is the RED reflectance of the observation $i$, respectively.

NDVI has been found more reliable [12] than other data types and equally useful for study purposes in either local [13] regional [7] or global scales [3]. The analysis of large areas is common in prior research studies [2, 6, 9, 13] in which NDVI has been applied for detecting changes. The local changes need to be analysed in a relatively small area for benefit of the local government or the local people. In a macro-level spatial variation analysis, often the local level changes have been overlooked. Additionally, an analysis of remote sensing data over a smaller area for understanding the seasonal patterns and trends in detail is still seldom pursued.

A country where the vegetation data are considered fairly significant for environmental issues is Nepal, as the Department of Forest Research and Survey has reported that 40.36% of its total land areas is still covered by forests [14]. Regarding the vegetation in Nepal, most studies have been regional [15, 16] or on the national level [17, 18]. Studies have been carried out using remote sensing data to investigate the changes in land covers [16, 18, 19] and farming or grazing areas [15, 17] and the associated factors. However, assessment of changes in vegetation as a natural resource, in particular for Nepal, is still lacking. Moreover, the current and accurate data on vegetation index, especially including historic time series has not been widely available. It is also difficult to survey the vegetation in Nepal because of complications in its geography. This lack of vegetation studies and relevant data is also evident for Kathmandu valley, a part of the mountain range in middle Nepal. Because Kathmandu valley is the fastest growing urban region, the vegetation changes are necessary to assess for urban planning and environmental

concerns. Therefore, a preliminary step is to understand the interactions of vegetation and other factors, and to identify the patterns and trends through temporal and spatial analysis techniques. This study was aimed to identify the inter-annual temporal trends and intra-annual seasonal patterns using NDVI as remote sensing data for Kathmandu valley from 2000 to 2015 by using appropriate statistical methods.

## 2.0  METHODOLOGY

### 2.1  The Data

The Kathmandu valley, covering an area of 900 km$^2$, consists of the three major districts, Kathmandu, Bhaktapur and Lalitpur, with the highest population density (>4000/ km$^2$) in Nepal. Kathmandu valley has a warm temperate climate with dry and cold winters [14]. The temperature is highest (>30°C) in April and May, and the lowest (<1°C) in December and January. There is a heavy monsoon period in middle of the year. It has three main annual seasons, summer, rainy fall and winter. Regarding vegetation, the valley consists of mostly the temperate varieties. The plants shed off their leaves during winter, give sprout from March, and become fully canopy loaded in June [20].



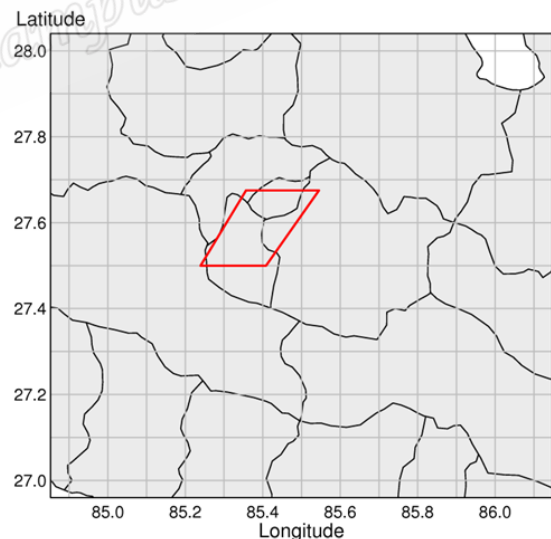**Figure 1** Study area in Kathmandu (demarked as parallelogram at the center)

The NDVI data were downloaded from MODIS's website for data subset [21] for the study area around Kathmandu valley as shown in Figure 1. The coordinates of the central point of the study area are 27.595°N and 85.394°E. Regarding the format of NDVI data from MODIS, the area around the central point was obtained with 250×250 m$^2$ grid as spatial

resolution. The covered area extended on all four sides 10 km away from the center (East, West, North and South). As a result, the study area was automatically generated to cover 20.25×20.25 or 410.0625 km², with 6561 grid cells (81×81) of 250×250 m² each. The downloaded data were specified for a period from 2000, the starting point of MODIS service, to 2015. The NDVI data were recorded once every 16 days. For each grid cell, there were around 23 observations per year, accumulating to maximally 345 observations over the 15 years. Some observations were missing due to the sensor's technical problems, and the actual total count of observations for each grid cell was typically below this maximum.

The raw data for each selected NDVI grid cell were divided by 10000 to adjust the values to the range from −1 to 1. The negative values up to 0 correspond to water. The values from 0 to 0.1 indicate soil, rocks or concrete, snow land and barren land. The low positive values (0.2 to 0.4) mean shrubs and grass land. Values close to 1 (0.6 and above) are detected for forests [22]. Therefore, the greater the NDVI value is, the denser the vegetation is in the area.
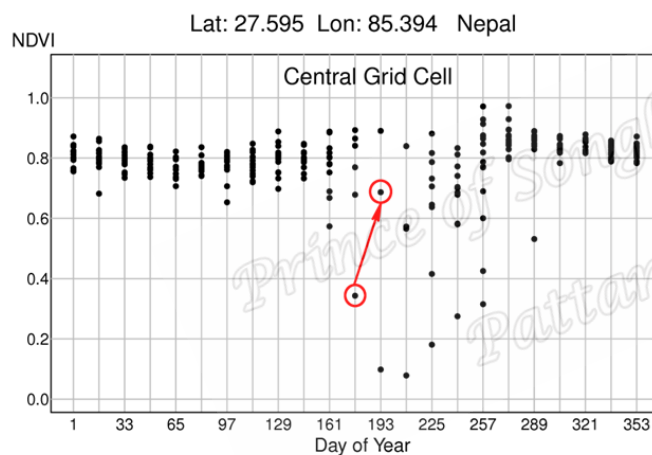


**Figure 2** The plot of NDVI from the central grid cell showing unreliable low indices

As an example, the total scatter plot of NDVI data across the central grid is displayed in Figure 2. Here, n represents the total number of observations and every dot on each vertical grid line represents one observation value on the same recording period (23 periods). Therefore, every vertical line on the x-axis displays 15 NDVI values corresponding to a particular day in each of the 15 years, in a consecutive manner. This plot starts from Julian day 1 and ends on day 365. However, the data needed to be further organized before going to analysis due to three problems. Firstly, during the raining season or between days 160 and 260, sparse NDVI values could be seen. This scarcity could affect the analysis for determining seasonal patterns, which needs uncensored data. The second problem was rapid increases in NDVI within a short time periods (within a

few weeks or months), which was virtually impossible. This was attributed to growth of plants and these NDVI observations were considered unreliable (an example is illustrated by an arrow between two encircled dots in Figure 2). The final problem for these data was that, on a heavily clouded or wet day, NDVI might be perturbed by obstruction of the sensor by clouds or water vapour, and the data would need to be validated. The NDVI data then needed to be cross compared with another MODIS signal at the same location and time, to confirm it.
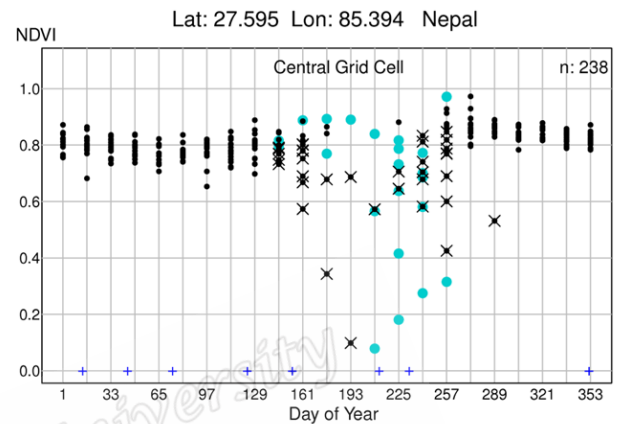


**Figure 3** The plot showing unreliable (cross marks) and doubtful (blue dots) data for the central grid cell

To solve the aforementioned problems, the data were cleaned in the following steps. First, the data were reordered to start from day 190 and end on day 189 as shown in Figure 4 to move scarcity to beginning and end of the period. This made the data more continuous for further analysis. Second, the data points were deemed unreliable if they were greater than 0.02 or lower than −0.02, and consequently were removed to reduce the level of fluctuation, while still maintaining the normality assumption of residuals in data. Those data points are shown with cross marks in Figure 3. Finally, to check NDVI's validity, Land Surface Temperature (LST) was selected to confirm that all the signals were valid. For the same location and the same observation day, if LST was not realistic, for example the LST went missing or the temperature could not be detected, it confirmed the MODIS did not work properly. Thus, other measured signals of that day, including NDVI, were doubtful. On these grounds, 23 NDVI values were identified as doubtful and were duly removed. These doubtful data are depicted as bigger dots in Figure 3. In total 59 unreliable and doubtful NDVI values were detected and removed. The remaining 238 NDVI observations for this grid after removal of doubtful and unreliable values were used for the analysis. The same procedure was carried out for each grid cell of the study area. R Statistical Programming version 3.2.1 [23] was implemented for data management and graphical displays.

## 2.2 The Statistical Methods

There were three main steps of data analysis in this study. First, the NDVI data, at individual grid cell level, were used for analysing the intra-annual seasonal patterns. The second step was trend analysis for each grid cell, for which, the data were seasonally adjusted and linear models were fitted to identify trends of individual grid cells. Finally, the data for the whole area were divided into three 5-year periods (2000 to 2004, 2005 to 2009 and 2010 to 2015) for analysis and comparison of the overall NDVI changes in a smaller time frame. To clarify the data structure in this study, the three main notations of the data are defined. Firstly, $j$ denotes an observation time after omitting the observations of unreliable and doubtful data for each grid cell. Therefore, it varies among different grid cells and takes the maximum of 345, but usually has the value below the maximum ($j =$ 1, 2, 3, ...., n, where n =< 345). Secondly, $q$ denotes an observation time after omitting unreliable and doubtful data for 5-year period for each grid cell with the maximum of 115 observations, so $q =$ 1, 2, 3, ..., m, where m =< 115. Lastly, $r$ denotes a grid cell, considered a cluster for the analysis. In this study, then, $r =$ 1, 2, 3, ..., N, where N = 49.

This study used the cubic spline function to find the seasonal pattern of NDVI. This pattern is calculated by fitting a cubic spline function to the 15-year data combined and plotted in one-year format. This enables the extraction of the seasonal pattern in a year without concerning the long-term trend. Furthermore, the function satisfies a special boundary condition where the functions beyond the first and last knot points are linear with the same slope. Thus, the cubic spline function is a combination of cubic and linear terms. In this study, the cubic spline took the form,

$$S = \alpha + bt + \sum_{k=1}^{p} c_k (t - t_k)_+^3 \qquad (2)$$

where, $S$ is the spline function, $t$ is time in Julian day, and $\alpha$, $b$ and $c_k$ are the coefficients of the model. $t_k$ is the location of a knot, while $t_1 < t_2 < ... < t_p$ are the specified knots and $(t - t_k)_+$ is the positive part of $(t - t_k)$ or max $\{0, (t - t_k)\}$.

The data were, then, seasonally adjusted to stabilize the mean. Because of the additive form of the seasonal component retrieved from the cubic spline function, the seasonal adjustment can be realized by subtracting the original values from seasonal component and then adding the difference between the means of seasonal component and seasonally adjusted NDVI [24], which is presented as,

$$y_j = (x_j - S_j) - \overline{(x_j - S_j)} + \bar{x} \qquad (3)$$

here, $y_j$ is the seasonally adjusted NDVI at observation $j$, while $x_j$ is NDVI and $S_j$ is the seasonal component value extracted from cubic spline function at observation $j$, respectively. $\overline{(x_j - S_j)}$ and $\bar{x}$ are the means of $(x_j - S_j)$ and $x_j$, respectively.

The seasonally adjusted NDVI data were further used for detecting the time series trend over the 15 year period. Therefore, linear models were fitted separately to the seasonally adjusted data at every grid cell, to extract the trends. The form of a linear model is,

$$y_j = \beta_0 + \beta_1 t_j + \varepsilon_j \qquad (4)$$

here, $y_j$ is the seasonally adjusted NDVI, $t_j$ is the time at each observation and $\varepsilon_j$ is the error term of the data, for each observation $j$, respectively. $\beta_0$ is the intercept of the linear equation and $\beta_1$ is the coefficient of the time $t_j$.

To account for the overall change in the study area, trends for the whole study area were computed. However, the data for a linear trend in each grid cell had spatial correlation within the cell. To tackle this problem, the Generalized Estimation Equations (GEE) were applied in this study. GEE is an extension of linear model that is specially designed for correlated data [25]. Furthermore, from the fitted models explaining the NDVI changes for all 15 years, it was difficult to distinguish the details of trends within this period. Therefore, the data were divided into three periods of 5 years each (2000-2004, 2005-2009 and 2010-2015) and fitted with GEE models separately. To display the results, 95% confidence intervals were calculated for each sub-period and plots were produced to show the changes in three time frames for NDVI in Kathmandu valley. The equations for GEE and related equations [25, 26] can be explained as follows. The generalized linear model can take the form of,

$$E(Y_{qr}) = \mu_{qr}, \mu_{qr} = g^{-1}(T_{qr}B) \qquad (5)$$

where $Y_{qr}$ is a vector of seasonally adjusted NDVI at observation time $q$ in a grid cell $r$. $E(Y_{qr})$ or $\mu_{qr}$ is an expected value of $Y_{qr}$, $g^{-1}$ is an inverse link function of $T_{qr}$, a matrix of observation days and $B$, a vector of regression coefficients.

Taking into account of all 49 grid cells together for the data of 5-year period, the GEE or quasi-score equation to estimate $B$ is as follows,

$$\sum_{r=1}^{N}\left(\frac{\partial \mu_r}{\partial B}\right)_r^T V_r^{-1}(y_r - \mu_r) = 0 \qquad (6)$$

here, $\left(\frac{\partial \mu_r}{\partial B}\right)_r^T$ is a transposed matrix of partial derivatives, where $\mu_r$ is a vector of expected values of NDVI at a grid cell $r$. $y_r$ is a vector of NDVI data at a grid cell a grid cell $r$ and $V_m^{-1}$ is the inverse of the variance-covariance matrix of NDVI.

All data analysis and graphical displays were in R Statistical Programming version 3.2.1 [23].

## 3.0  RESULT AND DISCUSSION

### 3.1  Result

#### 3.1.1  Seasonal Pattern from Cubic Spline Function

Eight knots were selected to fit the cubic spline function, shown as plus signs at the bottom of Figure 4, at the position of 15, 40, 70, 120, 150, 200, 230 and 350 days. The model gave the coefficient of determination ($R^2$) equal to 50%. The thin line in Figure 4 is the spline fitted before removal of unreliable and doubtful values, while thick line is the spline fit after rearrangement of data and removal of unreliable and doubtful values.

#### 3.1.2  Trends for Individual Grid Cells from Linear Model

For each grid cell, a linear regression model was fitted for the whole 15-year seasonally adjusted data. To illustrate the result, 12 grid cells were selected as representatives of three types of changes- an increase (e.g. grid cells, 242, 2086, 2574, 2580, 4942, 4948 and 5430), a decrease (e.g. grid cells, 248, 730, 736 and 2092) and a no-change (e.g. grid cell 5436), which are shown in Figure 5(a) to 5(l). The annual seasonal fluctuation cycle of NDVI, obtained from the spline function was added back for plotting and is shown as a wavy red line, along with a straight green line depicting the NDVI patterns and trends over 15 years. The dots in the figure are year-wise

data points. The crosses are unreliable and doubtful data, removed before the cubic spline fit. The increasing or decreasing trend (Inc/dec) per decade and respective p-values from linear regression are shown in each picture. Here, n represents the number of observations in each plot.
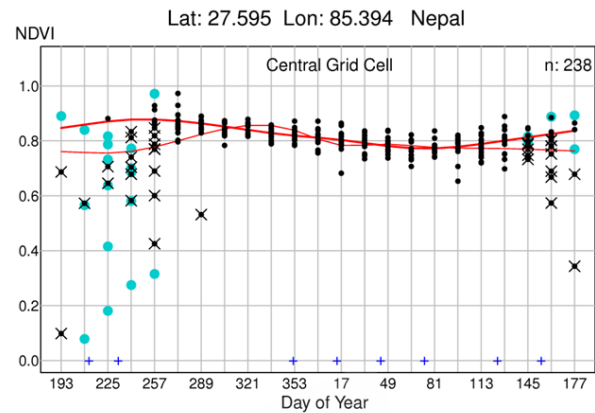


**Figure 4** Spline curves before (thin line) and after (thick line) removing unreliable and doubtful values

The results from all grid cells showed NDVI ranging from 0.3 to 0.9. The seasonal pattern was roughly unchanged for every year as shown in Figure 5. The linear trends illustrated a distinct variation between different years and locations among the grid cells. Moreover, 40.7% of the cells had statistically significant rise, while significantly declining trends were seen in 24.7% of the cells. Out of all grid cells, only 1.2% of the cells did not show any change in NDVI while rest 33.4% grid cells had changes but were not significant at all. Hence, the results showed a mixed picture of increasing and decreasing trends in NDVI, by grid cell location in the study area.

#### 3.1.3  Trend for the Whole Area and Confidence Interval Plots from GEE

Finally, the GEE were fitted to the data divided into three time periods. The time series plots were drawn to illustrate the trend from GEE in each period. The rates per decade change are -0.005, -0.003 and -0.006 during 2000-2004, 2005-2009 and 2010-2015, respectively. The rate of change showed statistically significant association in only the first and the last periods (p values 0.050 and 0.018 respectively) and the overall decline throughout 15 years period is evident in the graph (Figure 6 (a), (b) and (c)).

As the results from GEE models, 95% CI plots of NDVI for all 49 grids were drawn to observe the confidence levels of the change. In Figure 7, the CI for the period of 2005-2009 is crossing a zero value. Therefore, NDVI can be considered statistically unchanged, coinciding with the p value. However, in other two periods of 2000-2004 and 2010-2015, NDVI showed a statistically declining trend with negative CIs. As shown in Figure 7, the rate of change for the years 2000 to 2004 is ranging from -0.010 to 0 per decade, while that for the years 2010 to 2015 is ranging from -0.011 to -0.001 per decade.

Regarding the distribution of the data, NDVI is found slightly left skewed. However, this distribution is acceptable in this study because GEE can be used with the condition of the distribution assumption being relaxed [27].
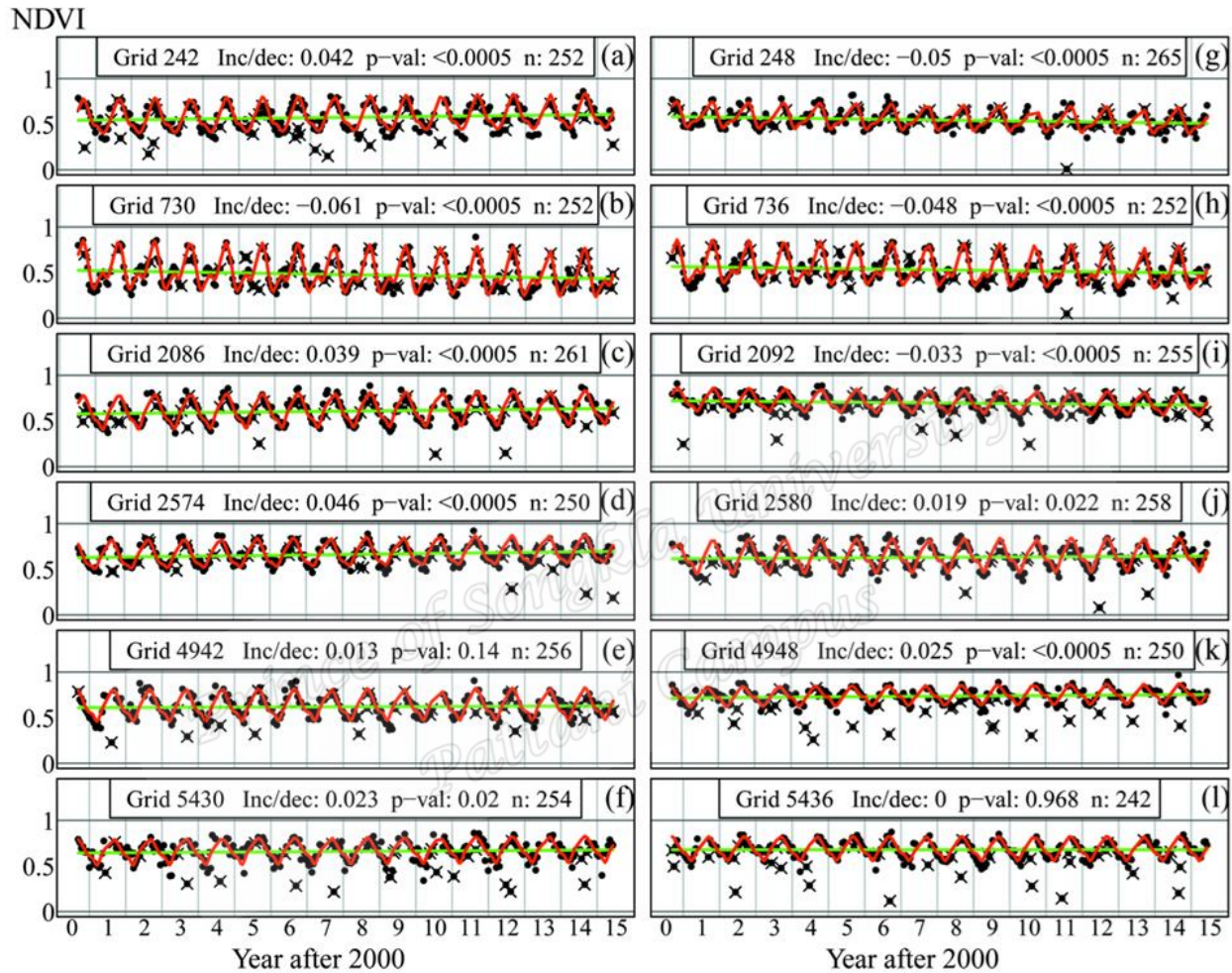


**Figure 5** Time series plot of vegetation showing increasing, decreasing and no-change trends in 12 *different grids*

## 3.2 Discussion

In this study, the seasonal pattern of vegetation showed the highest level in the rainy season during days 241 to 257 (September) and gradually declined to the lowest level in the winter season during days 50 to 97 (February to April). Actually the winter begins from December, but the vegetation declines from the end of the rainy season to the end of January. This time variation of NDVI (decline) by season might be due to the time taken for plant defoliation till the minimum temperature day. The greening of vegetation started from day 97 (April) to the time when the atmospheric temperature adequately warmed up in the summer, while the rising of temperature began from mid of February (after day 45). The seasonal pattern of NDVI growth, however, presented a slight gap between seasons and the vegetation growth, can be another inherent topic for further study.

During the rainy season, the plant growth and refoliation is much favoured by high humidity, temperature and rainfall. Later the growth ceases with heavy defoliation and physiological dormancy after the onset of dry and cold winter season. Therefore, the seasonal pattern of NDVI, as seen in the results, fluctuated driven by these phenomena. This result is particularly helpful in agricultural sector to understand the annual climate response of vegetation or crops, especially to understand the

existing phenological characteristics of the area. This summer-winter vegetation character is well supported by the previous studies where there is higher growth of vegetation in warmer seasons than in winter [8, 12]. Also, it is scientifically proved that, a relatively cooler air temperature reduces the plant metabolic rates including its growth [27]. These prior reports corroborate the results in this study.
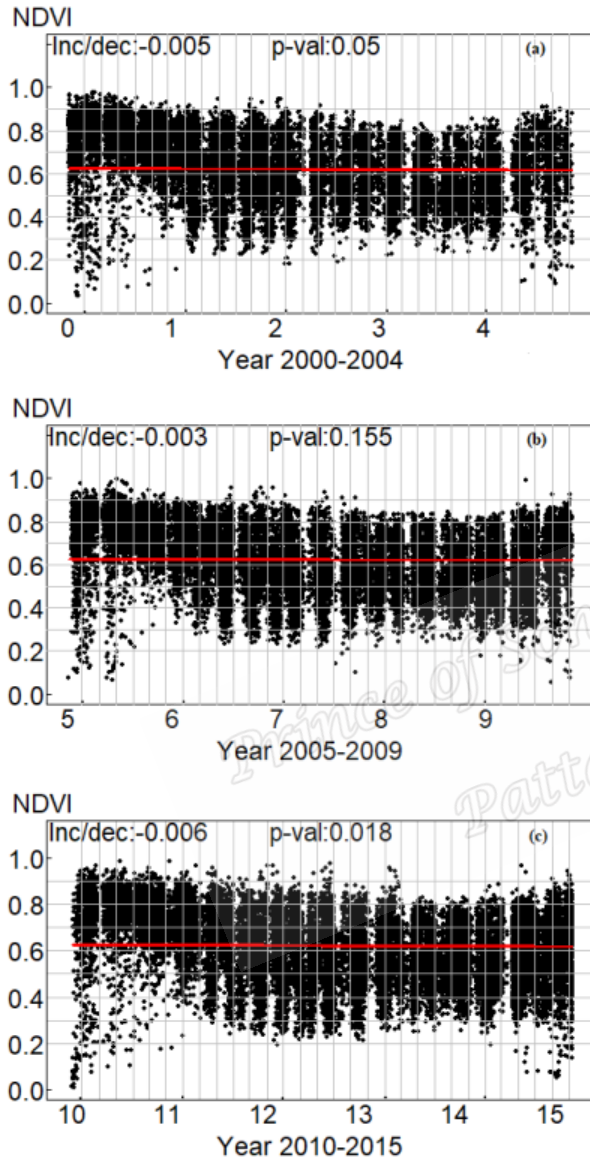


**Figure 6** The trend of overall NDVI (from GEE model) during 2000-2004 (a), 2005-2009 (b) and 2010-2015 (c)

In the trend analysis, the statistical results showed that significantly increasing or decreasing grid cells were numerically close to each other and the rest were insignificant on the level of individual grid cells. After GEE, the trends in vegetation changes for the whole study area could be assessed. The 95% confidence interval plots of vegetation showed significant declines in the periods 2000-2004 and

2010-2015, while the mid period showed no change and the rate of decline was the highest in recent years. The Global NDVI trend studied during 1982-2012 showed an increasing trend in many parts of the world including India and Southeast China [3]. The similar result was seen in Tibetan plateau of China during 2000 to 2009 [13]. Nepal lies in between these land blocks and may have similar pattern overall. However, as Kathmandu is a growing densely populated city, it may have been locally affected by several other factors, such as high density of population, resource exploitation, pollution and unplanned urbanization causing the decline of vegetation. In addition, Uddin *et al.* [28] have explained that the overall vegetation in Nepal is in a state of decline over the past few years. This is consistent with the declining pattern of vegetation found in this current study. Additionally, the method of data rearrangement and cleaning significantly contributed to obtaining much improved results from cubic spline fitting, to get the seasonal patterns. Otherwise, the same spline fitting technique before data management showed a lower NDVI scale even in the rainy season. This method of managing data can also be applicable to other types of noisy data with periodic censoring.

Hence it was found that the overall vegetation around Kathmandu valley is declining in recent years, at different rates by time period, while the seasonal patterns show no remarkable changes. Further investigation is still required to understand the potential reasons behind this seasonal pattern and the trend.

The limitation of this study is that it covers only a part of Nepal. With extended study areas, a complete picture of the vegetation changes for the country could be revealed. Also, this study includes only one indicator from a variety of remote sensing data. Therefore, the inclusion of more indices of satellite data can provide more information regarding changes in vegetation and other related factors in the region.
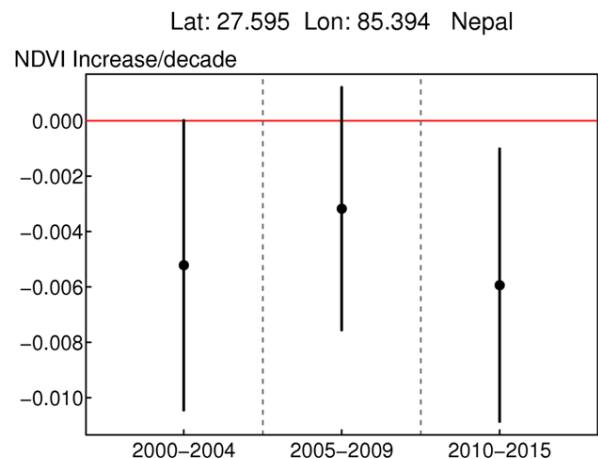


**Figure 7** Confidence Interval plots of the overall NDVI trends in three time frames

## 4.0  CONCLUSION

This study showed the changing pattern and trend of NDVI in three ways. Firstly, the seasonal pattern at grid cell level showed the local level annual changes, and secondly, the trend of individual grid cells indicated the changes in small, grid level areas and the proportions of each change. Finally, the detail of trends for the whole study area in three time periods were investigated. In addition, a comparison of rates of changes in those time segments was carried out. Hence, it was clear that the vegetation in this study site had different rates of decline in different time frames, since 2000.

The spatio-temporal changes of vegetation are a serious threat to ecosystems today. Therefore, this is an alarming signal for the policy makers around Kathmandu valley and measures to prevent a further vegetation decline should be taken. Technically, the study concludes that applying spline function fit and linear models along with GEE help successfully analyse the seasonal patterns and time profiles of changes in NDVI. Some other environmental factors could be added to predict probable causes of vegetation decline. This study indicates that simple yet effective approaches to time series data for assessing spatial and temporal changes in urban vegetation at a local scale can provide basic information for urban planners and anthropogenic studies.

## Acknowledgement

## References

[1]    Archibold, W. O. 1995. *Ecology of World Vegetation*. Springer Science and Business Media. Dordrecht.

[2]    Eckert, S., F. Husler, H. Liniger, and E. Hodel. 2015 Trend Analysis of MODIS NDVI Time Series for Detecting Land Degradation and Regeneration in Mongolia. *Journal of Arid Environment*. 113: 16-28.
DOI: http://dx.doi.org/10.1016/j.jaridenv.2014.09.001.

[3].   Liu, Y., Y. Li, S. Li, and S. Motesharrei. 2015. Spatial and temporal patterns of global NDVI trends: correlations with climate and human factors. *Remote Sensing*. 7: 13233-13250.
DOI : http://dx.doi.org/10.3390/rs71013233

[4]    Bounoua, L., G. J. Collatz, S. O. Los, P. J. Sellers, D. A. Dazlich, C. J. Tucker, and D. A. Randall. 2000. Sensitivity of Climate to Changes in NDVI. *Journal of Climate*.13: 2277-229.

[5]    Goward, S. N., Y. Xue, and K. P. Czajkowski. 2002. Evaluating Land Surface Moisture Conditions from the Remotely Sensed Temperature/Vegetation Index Measurements: An Exploration with the Simplified Simple Biosphere Model. *Remote Sensing Environment*. 79: 225-242.

[6]    Kaufmann, R. K., L. Zhou, R. B. Myneni, C. J. Tucker, D. Slayback, N. V. Shabanov, and J. Pinzon. 2003. The Effect of Vegetation on Surface Temperature: A Statistical Analysis of NDVI and Climate Data. *Geophysical Research Letters*. 30 (22): (3)1-(3)4.
DOI: http://dx.doi.org/10.1029/2003GL018251.

[7]    Piao, S., J. Fang, L. Zhou, Q. Guo, M. Henderson, W. Ji, Y. Li, and S. Tao. 2003. Interannual Variations of Monthly and Seasonal Normalised Difference Vegetation Index (NDVI) in China from 1982 to 1999. *Journal of Geophysical Research*. 108.
DOI: http://dx.doi.org/10.1029/2002JD002848.

[8]    Evrendilek, F., and O. Gulbeyaz. 2008. Deriving Vegetation Dynamics of Natural Terrestrial Ecosystems from MODIS NDVI/EVI data over Turkey. *Sensors*. 8: 5270-5302.
DOI: http://dx.doi.org/10.3390/s8095270.

[9]    Karnieli, N., R. T. Agam, M. Pinker, M. L. Anderson, G. G. Imhoff, N. Gutman, N. Panov, and A. Goldberg. 2010. Use of NDVI and Land Surface Temperature for Drought Assessment: Merits and Limitations. *Journal of Climate*. 23: 618-633.
DOI: http://dx.doi.org/ 10.1175/2009JCLI2900.1.

[10]   [NASA] National Aeronautics and Space Administration. 2015. *Global Climate Change: Vital Signs of the Planet*. NASA. URL: http://climate.nasa.gov/effects.

[11]   Kumar, L., K. Schmidt, S. Dury, and A. Skidmore. 2002. Imaging Spectrometry. *Imaging Spectrometry and Vegetation Science*. Chapter 5. Springer, Netherlands. 111-155.

[12]   Yin, G., Z. Hu, and X. Chen. 2016. Vegetation Dynamics and Its Response to Climate Change in Central Asia. *Journal of Arid Land*. 8(3): 375-388.
DOI: http://dx.doi.org/10.1007/s40333-016-0043-6.

[13]   Zhang, Y., J. Gao, L. Liu, Z.Wang, M. Ding, and Yang X. 2013. NDVI-based Vegetation Changes and Their Responses to Climate Change from 1982 to 2011: A Case Study in the Koshi River Basin in the Middle Himalayas. *Global and Planetary Change*. 108: 139-148.
DOI: https://doi.org/10.1016/j.gloplacha.2013.06.012.

[14]   DFRS] Department of Forest Research and Survey. 2015. *State of Nepal's Forest*. Ministry of Forest and Soil Conservation (MFSC), Government of Nepal. Kathmandu.

[15]   Haack, B. N., and G. Khatiwada. 2007. Rice and Bricks: Environmental Issues and Mapping of the Unusual Crop Rotation Pattern in the Kathmandu Valley, Nepal. *Environmental Management*. 39: 774-782.
DOI: http://dx.doi.org/10.1007/s00267-006-0167-0.

[16]   Thapa, R. B., and Y. Murayama. 2011. Urban Growth Modeling of Kathmandu Metropolitan Region, Nepal. *Computers, Environment and Urban Systems*. 35: 25-34.
DOI:http://dx.doi.org/10.1016/j.compenvurbsys.2010.07.005

[17]   Gumma, M. K., D. Gauchan, A. Nelson, S. Pandey, and A. Rala. 2011 Temporal Changes in Rice-Growing Area and Their Impact on Livelihood Over a Decade: A Case Study of Nepal. *Agriculture Ecosystems and Environment*. 142: 382-392.
DOI: http://dx.doi.org/10.1016/j.agee.2011.06.010.

[18]   Poudel, B., Z. Yi-Li, L. Shi-Cheng, L. Lin-Shan, W. Xue, and N. R. Khanal. 2016. Review of Studies on Land Use and Land Cover Change in Nepal. *Journal of Mountain Science*. 13(4): 643-660.

[19]   Poudel, K. P., and P. Anderson. 2010. Assessing Rangeland Degradation Using Multi Temporal Satellite Images and Grazing Pressure Surface Model in Upper Mustang, Trans Himalaya, Nepal. *Remote Sens Environ*. 114: 1845-1855.
DOI: http://dx.doi.org/10.1016/j.rse.2010.03.011.

[20] Maharjan, S. R., D. R. Bhuju, and C. Khadka. 2006. Plant Community Structure and Species Diversity in Ranibari Forest, Kathmandu. *Nepal Journal of Science and Technology*. 7: 35-43.

[21] [ORNL DAAC] Oak Ridge National Laboratory Distributed Active Achieve Center. 2015. MODIS subset of NASA Earth Data.
URL: http://daacmodis.ornl.gov/cgi-bin/MODIS/GLBVIZ_1_ Glb/modis_subset_order _global_col5.pl.

[22] Weier, J., and D. Herring. 2000. *Measuring Vegetation (NDVI and EVI)*. NASA Earth Observatory.
URL:http://earthobservatory.nasa.gov/Features/Measuring Vegetation/.

[23] R Core Team. 2015. R: A Language and Environment for Statistical Computing, R Foundation for Statistical Computing, Vienna, Austria, 2015. URL: http://www.R-project.org/.

[24] Wongsai, N., S. Wongsai and A. R. Huete. 2017. Annual Seasonality Extraction Using the Cubic Spline Function and Decadal Trend in Temporal Daytime Modis Ist Data. *Remote Sensing*. 9: 1254. DOI: http://dx.doi.org/10.3390/rs9121254

[25] Liang, K., and S. L. Zeger. 1986. Longitudinal Data Analysis Using Generalized Linear Models. *Biometrika*. 73: 13-22.

[26] Dormann, C. F., J. M. McPherson, M. B. Arau´jo, R. Bivand, J. Bolliger, G. Carl, R. G. Davies, A. Hirzel, W. Jetz, W. D. Kissling, I. Ku¨hn, R. Ohlemu¨ller, P. R. Peres-Neto, B. Reineking, B. Schro¨der, F. M. Schurr, and R. Wilson. 2007. Methods to Account for Spatial Autocorrelation in the Analysis of Species Distributional Data: A Review. *Ecography*. 30: 609-628.
DOI: http://dx.doi.org/10.1111/j.2007.0906-7590.05171.x.

[27] Fitter, H., and R. K. M. Hay. 2002. *Environmental Physiology of Plants*. 3rd ed. New York (NY), Academic Press.

[28] Uddin, K., S. Chaudhary, N. Chettri, R. Kotru, M. Murthy, R. P. Chaudhary, W. Ning, M. S. Sahash, and S. K. Gautam. 2015. The Changing Land Cover and Fragmenting Forest on the Roof of the World: A Case Study in Nepal's Kailash Sacred Landscape. *Landscape and Urban Planing*. 141: 1-10.
DOI: http://dx.doi.org/10.1016/j.landurbplan.2015.04.003.

Ref: No. 6592(11).3 / 074

April 24th, 2018

Ira Sharma
Mathematics and Computer Science
Faculty of Science and Technology
Prince of Songkla University
Pattani Campus, Pattani 94000

Dear Ira Sharma:

Thank you for the manuscript entitled *"Modeling of LST to Determine Temperature Patterns and Detect their Association with Altitude in Kathmandu Valley of Nepal"*, which you submitted for possible publication in the Chiang Mai University Journal of Natural Sciences.

I am pleased to inform you that the Editorial Committee has now agreed to accept your revised manuscript for publication.

Please be advised that you will be expected to assist the Journal with any editorial questions that may arise as part of the final editing and publication process, without which assistance your manuscript may potentially not be printed.

Thank you for choosing the CMU Journal of Natural Sciences as your preferred medium for publication.

Yours sincerely,

Associate Professor Komgrit Leksakul, D.Eng.
Editor-in-Chief
Tel: 053 94 3603
Fax: 053 94 3600
E-mail: cmupress.th@gmail.com
http://cmuj.cmu.ac.th

**Remark**: The above article will be published in Chiang Mai University Journal of Natural Sciences Volume 17 Number 4 October – December, 2018.

**Appendix II**

**Paper II**

**Modeling of LST to Determine Temperature Patterns and Detect their Association with Altitude in Kathmandu Valley of Nepal**

**ABSTRACT**

Land Surface Temperature (LST) data, around Kathmandu Valley of Nepal from 2000 to 2015, were analyzed to determine the temperature patterns. The cubic spline function was used to show seasonal patterns which were similar for all sub regions, with a single summer peak and a winter trough. The data were then seasonally adjusted to remove seasonal effects and then filtered with the first order autocorrelation. The second degree polynomial regression model identified fifteen different patterns revealing that 65.43% of the area had 'accelerating' pattern while 'non accelerating' pattern was seen in 34.57% of the area. The logistic regression confirmed that the patterns have significant association with the altitude (p-value= 0.006). Hence a varying pattern of temperature by location and time was identified in this study and the methods can be generalized to larger areas.

**Keywords:** Land Surface Temperature, cubic spline function, polynomial regression model and temperature patterns.

**Introduction**

The temperature change, a crucial environmental problem, is particularly hard-hitting for low income countries which rely on natural resources for the economy and livelihood. The most important problem is the warming of land surface that imparts a direct influence on the surrounding ecosystem. The land surface temperature is related to both the natural and human activities, such as agriculture (Schlenker and Roberts, 2009; Smith et al., 2009), health-care and life (Dhimal et al., 2015; Xu et al., 2015), environment (Jones et al., 1999; Johannssen et al., 2004) and energy (Paniagua-Tineo et al., 2011; Jaglom et al., 2014) and hence affects every sphere of human life.

Amidst the anthropogenic influences, global surface air temperature, from 2009 to 2019, was predicted to show a continuous rise (Lean and Rind, 2009). The average temperature of the earth had been increasing at a range of 0.65-1.06°C over a period of 1880-2012 and it was getting more serious and steeper on land surface due to combined effect of natural and human forces (Intergovernmental Panel on Climate Change [IPCC], 2013). Despite its wide scope and importance, many questions regarding the trend and pattern of temperature change mechanisms are yet to be properly addressed. The literatures so far have identified temperature change through annual seasonal patterns (Portmann et al., 2009) and the trends (Hughes et al., 2006; Devkota, 2014) but the analysis of annual temperature patterns that explain about the characteristics of the change is rare. This is also needful for local government and the people to imply an effective strategy for mitigating its negative consequences in situ. However, a reliable and complete data is challenging to obtain, especially in low-income countries where the field data inventory system is not yet properly in place. In this situation, the remote sensing or satellite data provide the best alternative, and one of the common satellite based data is the Land Surface Temperature (LST) from Moderate Resolution Imaging Spectro-radiometer (MODIS) (Wan et al., 2004).

Many studies have used several ways of analysis of temperature data including simulation model (Johannessen et al., 2003), remote sensing algorithm (Li et al., 2013), and various statistical techniques (Hughes et al., 2006; Dong et al., 2014; Me-ead and McNeil 2016). Wanishsakpong and McNeil (2016) used a polynomial regression model to investigate trend and pattern of Australian temperature. More recently, Wongsai et al. (2017) used cubic spline to investigate annual seasonal pattern and decadal trend of LST data.

Nepal is more vulnerable to climate change impacts because the country has ecologically, biologically, and geographically diverse regions (KC and Ghimire, 2015). It was facing a maximum temperature increase of 0.03°C in summer and 0.05°C in winter, every year during 1978 and 2008 (Joshi et al., 2011). The growing urban region around Kathmandu Valley is suffering from unmanaged human encroachment and excessive pollution (United Nations [UN]-Habitat, 2015), which has consequent impact on the environmental temperature. Although, temperature variations and trends were studied in Nepal (Sano et al., 2005; Shrestha and Aryal, 2011; Devkota, 2014), the study to find the annual temperature patterns around the valley probably, is a different attempt. In fact, the global or regional climate change analyses usually average away the local variability and hence cannot represent the local variations of temperature (IPCC, 2013). Therefore, this study aims to identify comprehensive patterns of temperature change and analyze their association with altitude at local regions in Kathmandu over 15 year period. It is assumed that altitude has some relationship with the temperature change pattern in general (Stroppiana et al., 2014; Shrestha and Aryal, 2011; Lancaster, 2012).

## 2. Materials and Methods

The study area extends around the central coordinate of 27.595°N and 85.394°E, covering a total of 3969 km$^2$ area around the Kathmandu Valley of Nepal (Figure 1). It is a hilly region with temperate climate and has three distinct annual seasons- winter, summer and rainy fall. Nepal Population and Housing Census 2011 (NPHC 2011, 2012) reveals that Kathmandu valley is the fastest growing and most populated city of Nepal having a population density of 2731/km$^2$ while around the valley the density is below 275/km$^2$. The physiography of Nepal shows that there is hot plain land on southern belt and as we move towards north the altitude gradually increases while the temperature declines with land elevation (United Nations Environment Program [UNEP], 2001).
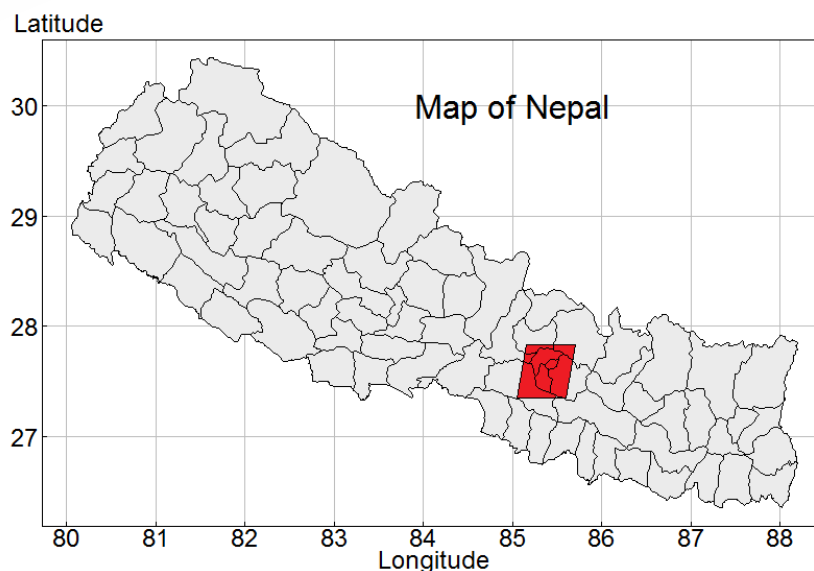
Figure 1. Map of Nepal showing study area (shaded box)

*The Land Surface Temperature data*

The Land Surface Temperature (LST) data, for nine regions representing the total study area, were retrieved from MODIS website (Oak Ridge National Laboratory Distributed Active Archive Center [ORNL DAAC], 2015). MODIS is a sensor, fitted aboard the Terra and Aqua satellites by the National Aeronautics and Space Administration (NASA). It monitors environmental changes due to fire, vegetation, temperature, earthquake, drought and flood on the earth (NASA, 2015). LST, one of the products of MODIS, has dynamic ranges, high radiometric resolutions and accurate calibrations (Wan et al., 2004). Regarding the format of LST data from MODIS, for each region, the area around the central point was obtained with $1\times1$ $km^2$ grid as a spatial resolution. The covered area extended from all four sides 10 km away from the center (i.e., East, West, North and South). As a result, the study area was automatically generated to cover $21\times21$ $km^2$ with 441 grids of 1 $km^2$ each. The data were retrieved one by one for each of the nine regions for a period from May 2000 to June 2015.

The data were recorded in every eight days interval, that resulted into 46 observations per year approximately and accumulating to maximally 690 over 15 years. Some observations were missing (average 9.68% in nine regions) due to the sensor's technical problem, and the actual total count of observations for each grid cell was typically below the maximum. Figure 2 shows the area for nine regions, each region was divided further into nine sub regions to ensure more details of changing patterns in a smaller area, of approximately $7\times7$ $km^2$ that is equal to 49 grids in every sub region. The LST data for each sub region were taken as an average of 49 grids for every observation so as to reduce spatial correlation and to represent temperature for each sub region. The average LST were analyzed for each of the 81 sub regions. The central region is served as an example for sub regions (Figure 2) which were named as North-East (NE), North (N), North-West (NW), West (W), Central (C), East (E), South-West (SW), South (S) and South-East (SE) based on their locations.
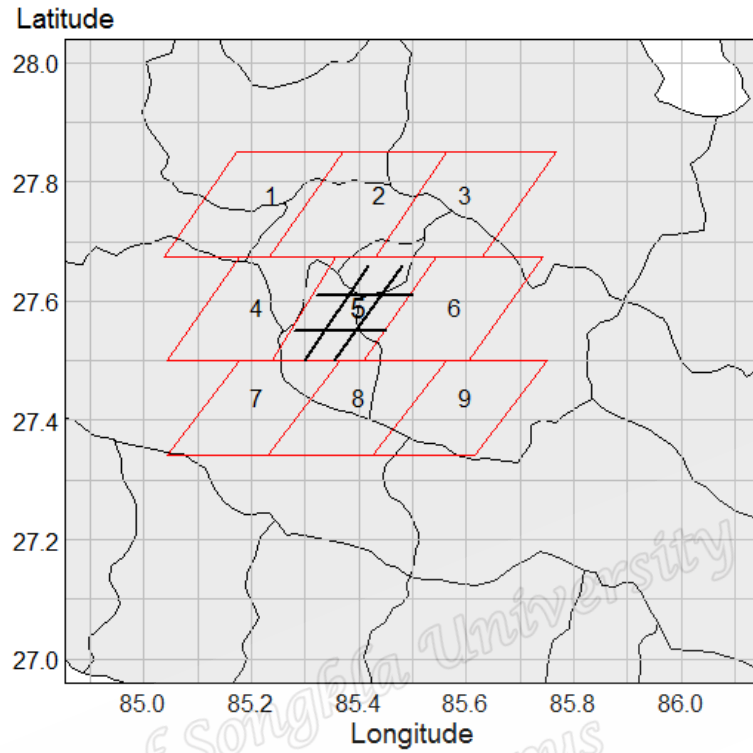
Figure 2. Study area of nine regions and the sub regional division in center

*Altitude Data*

The altitude data for 81 sub regions were obtained from Google Earth. First, nine different location points or their coordinates were calculated systematically, as a three by three matrix in each sub region. The altitudes of all these points were retrieved from Google Earth Images. These nine altitudes from each sub region were averaged to get a single altitude to represent a particular sub region. The altitudes ranged from 435 m to 2245 m., which were grouped into two categories - the altitudes below 1500 m and higher than that and hence the variable of altitude became binary.

*Statistical methods*

Cubic spline function was fitted with selected number of knots to find the seasonal temperature patterns. The function took the form:

$$s_t = \alpha + bt + \sum_{k=1}^{p} c_k (t - t_k)_+^3 \qquad (1)$$

Where, $\alpha$, $b$ and $c_k$ are the parameters in the model. $t$ denotes time in Julian days, that is, specified day of year. $t_1 < t_2 < ... < t_p$ are specified knots and $(t - t_k)_+$ is $t - t_k$ for $t > t_k$ and 0 otherwise.

The temperature data were seasonally adjusted by subtracting the spline fitted values ($y_{sp}$) from the temperature ($y$) and then adding back the mean of the temperature ($\bar{y}$) of each sub region. The formula took the form:

$$y_{sa} = y - y_{sp} + \bar{y} \tag{2}$$

The dependencies among the seasonally adjusted temperature data were reduced by removing the auto-correlations at lag 1 term (equivalent to 8 day period). The auto-correlation at lag 1 term ($a_1$) was shown in Figure 5. The data were then filtered (Wanishsakpong and McNeil, 2016; Me-ead & McNeil, 2016). The filtered temperature data were finally fitted with polynomial regression model of second degree (quadratic model). The model took the form:

$$y_{fsa} = b_0 + b_1 t + b_2 t^2 + \varepsilon \tag{3}$$

Here, $b_0$ is the constant and $b_1$, $b_2$ are the coefficients. The time of observation was represented by $t$ and $\varepsilon$ is the error term. The estimated temperature increase or decrease was calculated based on the first derivative of the quadratic function.

All the temperature patterns obtained from equation 4 are then categorized into a binary form (accelerating or nonaccelerating pattern). The association between the temperature patterns and altitude of the study area was identified using logistic regression model which took the form:

$$\ln\left(\frac{p}{1-p}\right) = \alpha + \beta x \tag{4}$$

where $p$ denotes the expected probabilities of the accelerating temperature pattern, α is intercept, $x$ is the determinant variable that is altitude and $\beta$ is regression coefficient. The data used to construct the model comprised of 81 observations.

R Statistical Programming (R Core Team, 2015) was used for overall data analysis and graphical displays.

## 3. Results

The LST data for all the sub regions were plotted. The annual seasonal patterns of LST are quite similar and the cubic spine does not show much variation across the nine regions. As an example, the central region was shown in Figure 3 that explains seasonal temperature pattern of every sub region. Nine panels represent the sub regions and eight positive (+) signs at the bottom of each panel show the knot positions. Each vertical gray line represents an observation day and the black dots are the temperature plotted consecutively for 15 years. In each panel, a smooth spline curve (gray line) is derived from cubic spline model with $r^2$ ranging from 0.50 to 0.81. The temperature began to rise immediately after winter in February and the peak was seen during summer in March, April and May (day 80 to 140). By the end of

May it gradually declined and reached the trough in winter during December, January and February (days 350 to 40).
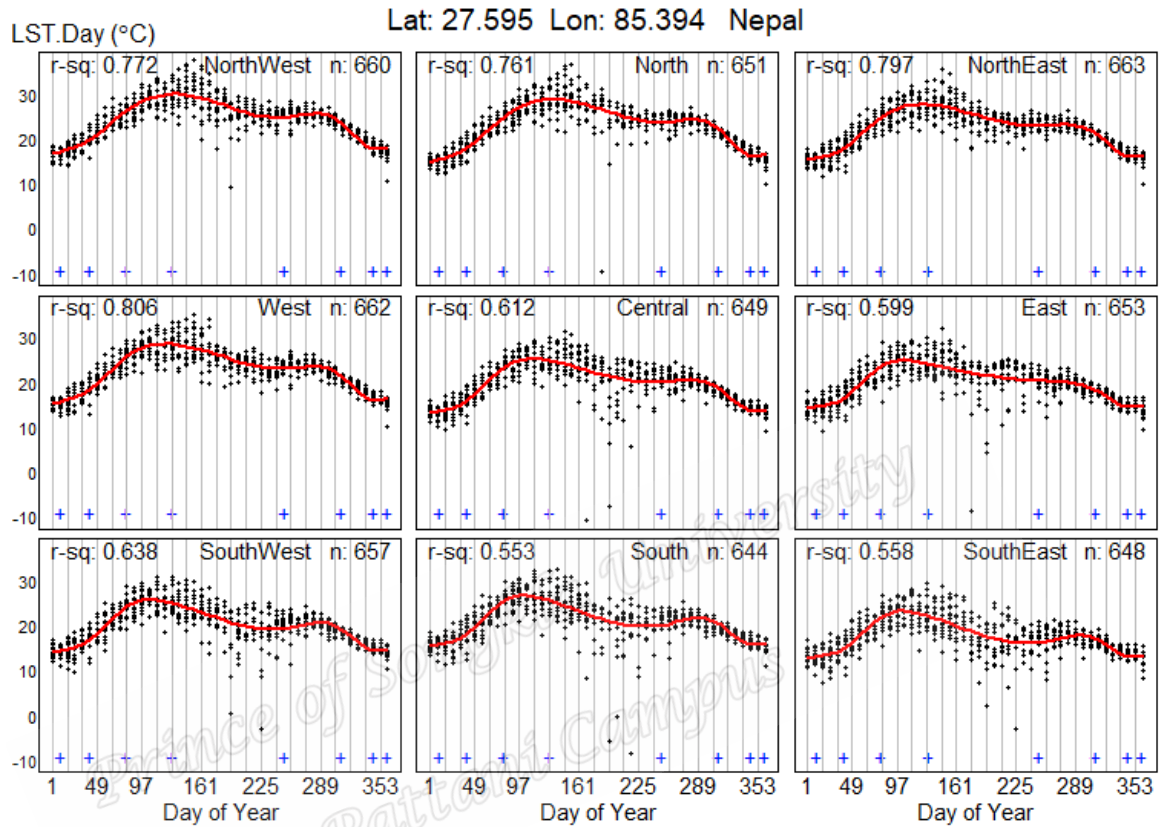


Figure 3. Cubic spline function showing seasonal patterns of temperature changes in nine sub regions of central region during days 1 to 365

Figure 4 is the illustration of 81 seasonal temperature patterns. Each panel represents nine sub regions of the respective region represented by different types of lines. Each line type stands for a particular location of the sub region, that is, black solid for NW, black dashed for N, black dotted for NE, black dotdash for W, gray solid for C, gray dashed for E, gray dotted for SW, gray dotdash for S and light gray for SE sub regions. The figure shows that the seasonal patterns do not have remarkable difference by location except slight variations in temperature levels in regions two, eight and nine.
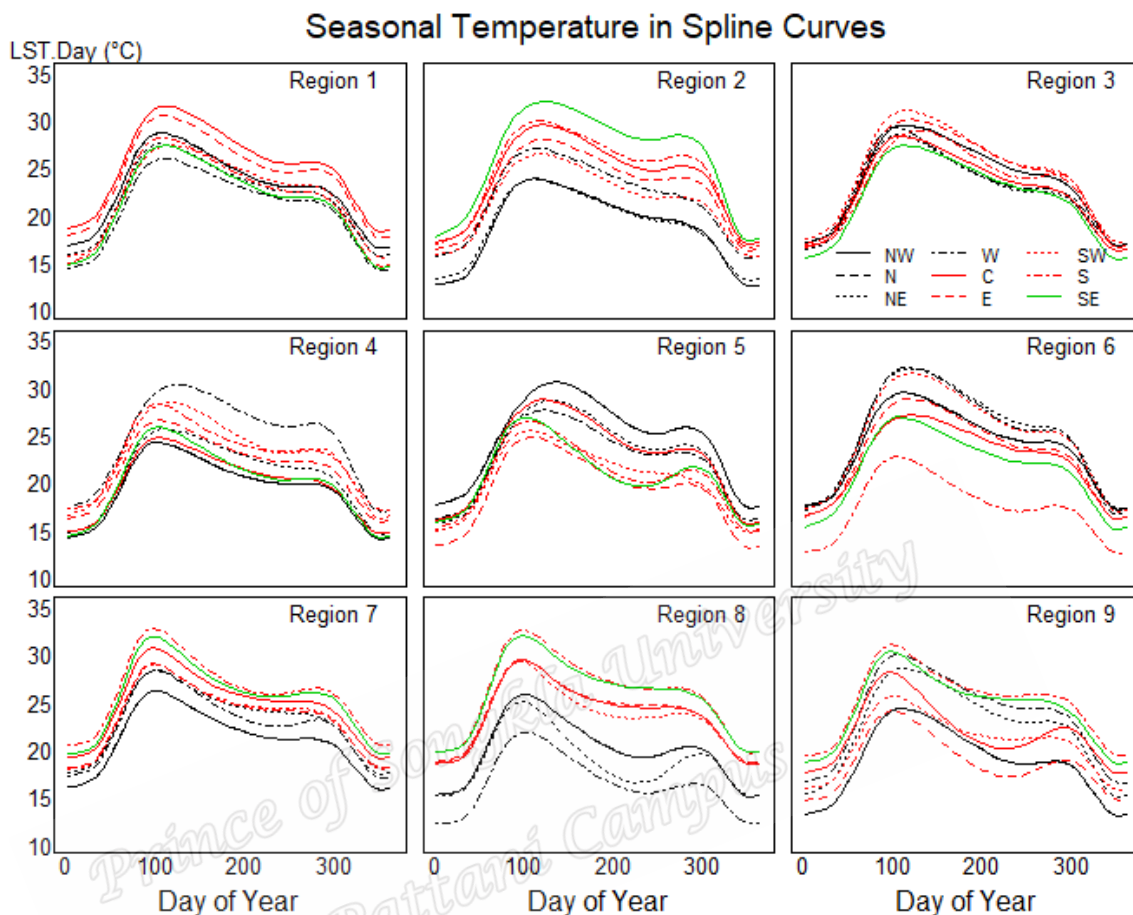
Figure 4. Seasonal temperature patterns of 81sub regions within respective nine regions

Seasonally adjusted, filtered temperature data, for every sub region, were subjected to the quadratic model and an example was shown in Figure 5, for central region. It illustrates the quadratic curves of nine sub regions in nine different panels. The tenth panel, on bottom right side, shows all those curves in 9 different types of lines, one for each sub region. The y-axis shows seasonally adjusted temperature in degree Celsius (°C) and x-axis represents the year from 2000 to 2015, $n$ is the number of observations in each sub region, $a_1$ is the autocorrelation of sub region level data, Inc/dec is meant to show increase or decrease of temperature per decade and its difference between the period 2000 and 2015 gives total linear change of the temperature in 15 years period. The p-values of the quadratic model in each sub region are also shown. During 15 years period the study area showed net rise of temperature ranging from 0.009 to 0.430 °C and the fall from -1.047 to -0.010 °C along with the auto-correlations ($a_1$) of the data below 0.35.
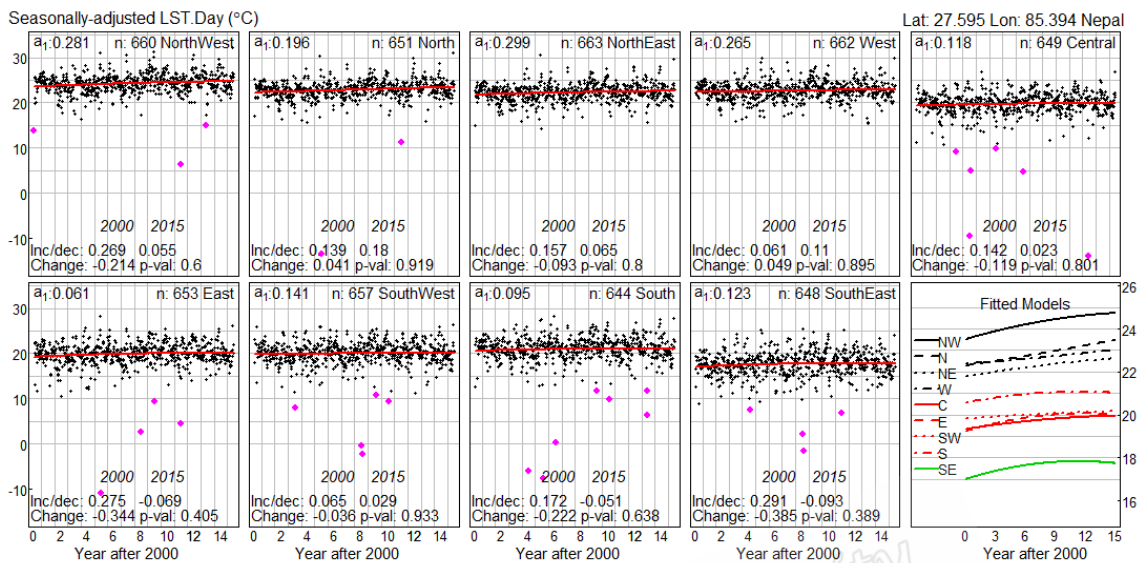
Figure 5. Temperature patterns of nine sub regions of central region

The quadratic curves of the temperatures in 81 sub regions, plotted altogether in the map of study area (Figure 6), showed 15 different patterns which were categorized into two groups based on their shape. The first one is 'accelerating' pattern with 65.43% of the area coverage, the other one is 'non accelerating' with 34.57% coverage. The accelerating pattern included all the patterns that were in rising tendency ( ⟋ , ⌣ ) while the next one included rest of all, like, thorough declining ( ⌢ ), recently declining ( ⌢ ) or the one showing no changes ( ⎯ ). All of them were supposed to impart no risk effects to environment.
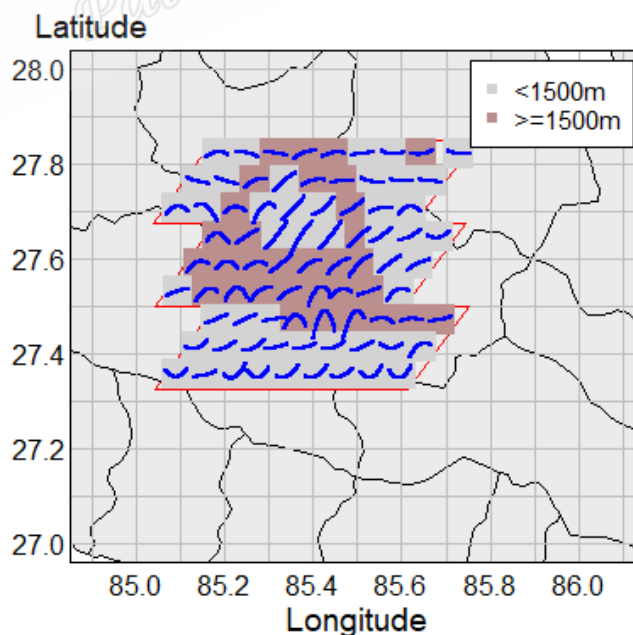


Figure 6. Temperature patterns of 81 sub regions with altitude levels

Along with the temperature patterns, Figure 6 also shows the altitudes (shaded area) in the region. Here, 60.49% of sub regions had the altitudes lower than 1500 m and the rest of the area has higher altitudes. The core center, that is Kathmandu valley, was surrounded by high altitude while rest of the part has lower altitude. The logistic model applied to these variables showed that the temperature patterns was negatively associated (regression coefficient= -1.36, p-value=0.006) with the altitude of the site. It means, the accelerating temperature slopes were found to associate mostly with the lower altitudes and vice versa (Figure 6). Figure 7 illustrates the 95% confidence interval plot after the logistic model and it reveals that the accelerating temperature pattern is more likely to associate with lower altitude area.
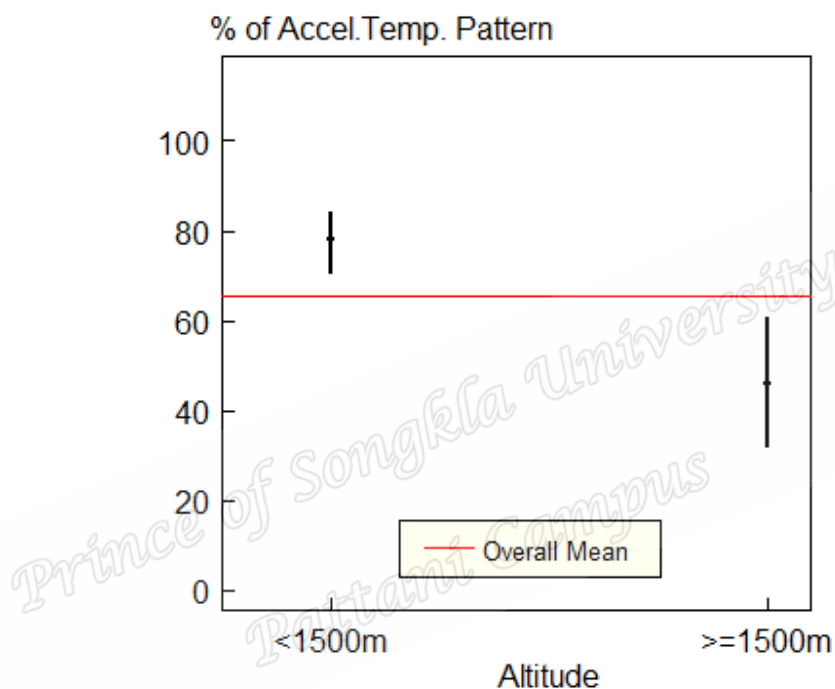


Figure 7 Confidence intervals plot showing association between temperature pattern and altitude

## 4. Discussion

This study applied a combination of cubic spline function and polynomial regression model for temperature pattern analysis. The data were MODIS LST time series for Kathmandu Valley of Nepal. Cloud cover and rainy seasons cause uncertain and missing values in LST time series. It has been suggested that the cubic spline function can be used to detect the seasonality in MODIS LST time series. The cubic spline function helped in annual seasonality extraction, even when there were missing values in time series (Wongsai et al., 2017). Since MODIS provides LST time series data for each grid ($1 \times 1$ km$^2$) the cubic spline can be applied to each LST time series (of every grid). In this study, the LST data for each sub region were aggregated and analyzed. Moreover, the sub region level results can be obtained for any extent of area coverage (each region can be bigger than 21x21 km$^2$) and any length of time we need.

The seasonal temperature patterns showed almost similar peaks (in summer) and troughs (in winter) in all sub regions suggesting that they did not vary in those locations. A contrasting result was observed by Portmann et al. (2009) who studied the distribution of temperature pattern in USA and showed

that annual maximum and minimum temperature trends could significantly vary at different sites but at a larger distance areas. They also pointed out that this variation was associated with the rainfall. The temperature can be higher or lower depending on topography (Fu and Rich, 2002) or land cover (Yue et al., 2007) as well. However, the seasonal patterns in our study detected only the variation of temperature level for the panels 2 and 8. Here, the difference seen in the level of temperature might have caused due to the climate factors like topography, rainfall, altitude or land cover.

Previous study had shown that the trend of LST could be explained by a simple linear regression model (Stroppiana et al., 2014). Nonetheless, the linear model might not be the appropriate way to estimate trends for shorter periods. A polynomial pattern of temperature was identified in Australia from 1970 to 2012 (Wanishsakpong and McNeil 2016) where the 6th degree polynomial regression model had been used because the data were for more than 40 years. It could be seen that, within 40 years, a 15 year periodic temperature pattern were well explained and hence in our study, having shorter time frame data, a polynomial with lower degree (2nd) was used. Hence, the annual temperature patterns illustrated in 15 groups are more interesting in this study. The patterns suggested the local variation of temperature change in the study area, that might be due to the effect of different natural (vegetation, altitude and topography) and human factors (land use and urban activities). The southern and the central sub regions have accelerating pattern. Both of these regions had lower altitude and dense population. The north and west area, both having higher altitude, had 'non accelerating' pattern. The literatures had showed that the analysis of regional or global scale data is very common to determine trends (Hughes et al., 2006; Devkota, 2014) and patterns (Zhou et al., 2009; Wanishasakpong and McNeil, 2016) of temperature but the results do not illustrate the pattern at a particular locality in a huge study area. At the expense of macro-level spatial analysis, often, the local level changes have been overlooked. However, this study not only improves the understanding of temperature patterns in Kathmandu but also provides a basis for urban planning and environmental management at local level.

Some authors have pointed out that there is association between temperature and elevation (Fu and Rich, 2002; Pouteau et al., 2011; Stroppiana et al., 2014). The correlation is greater in winter and lower in summer and also known not to be consistent throughout the year as well as the study period while in our study, the logistic model aimed to explain the higher probability of having accelerating temperature pattern with respect to the lower altitude. The results were found consistent with the study by Stroppiana et al. (2014) that temperature change and patterns have negative association with altitude. Shrestha and Aryal (2011) showed that the rising temperature change was progressive towards the higher altitudes in Himalayan glacial region of Nepal where the area had mostly the altitude more than 4000 m and that might be the cause of the contrast with our results. However, in Malawi Africa with the altitude (900m -2400m) of similar range showed a coherent result of negative association between temperature and altitude (Lancaster, 2012). The temperature trend and altitude relationship studied in China by Dong (2014), explored some differing results that, the temperature was decreasing below altitude 200m and increasing from 200-2000m and weakly positive above 2000m. Even though the altitude and temperature change has a very strong statistical relationship, all these studies revealed that it can be either positive or negative depending on the altitude level, topography and land use pattern of the location.

This research helps understanding the distribution of LST pattern in a local area which is important since it can further help in either land use planning for developmental activities or make environmental policies to save it from excess thermal effects locally. Since people of Nepal are highly dependent on natural resources and agriculture, slight changes in temperature and rainfall pattern make people more vulnerable to climate change (KC, 2014). Finding the causal factors of variation in the pattern of LST change, needs a very detailed micro level analysis and probably, the reason of these 15 temperature patterns might be local biotic or abiotic factors. Nonetheless, the reasons behind different temperature patterns are out of the scope of this paper.

## 5. Conclusions

The method of cubic spline function and polynomial regression model, accounting for seasonal adjustment and autocorrelation effects in data, can be applied to find the temperature patterns a local level area. Although the seasonal patterns (intra annual) are comparatively consistent with respect to the nearby locations, the annual temperature patterns vary a lot. An evidence of 15 different patterns of temperature change, identified in this study, are more effective in explaining how the actual path (pattern) of temperature change looks like. This is the characteristics of temperature change that linear trends can never explain about. The methods can be useful not only in identifying the patterns of temperature change in a local area but it can also be generalized to a large scale area. It provides a base for climate change information at a local level and can be used by local stakeholders for managing and planning their cities and villages.

## References

Devkota, R.P. 2014. Climate change: trends and people's perception in nepal. Journal of Environmental Protection. 5: 255-265. DOI: 10.4236/jep.2014.54029

Dhimal, M., Ahrens, B., and Kuch, U. 2015. Climate change and spatiotemporal distributions of vector-borne diseases in Nepal- a systematic synthesis of literature. PLOS ONE. 10(6): 1/31-6/31. DOI: https://doi.org/10.1371/journal.pone.0129869

Dong, D., Huang, G., Qu, X., Tao, W., and Fan, G. 2014. Temperature trend-altitude relationship in China during 1983-2012. Theor Appl Climatol. 122(1): 285-294. DOI: 10.1007/s00704-014-1286-9.

Fu, P., and Rich, P.M. 2002. A geometric solar radiation model with applications in agriculture and forestry. Computers and Electronics in Agriculture. 37: 25-35.

Hughes, G.L., Rao, S.S., and Rao, T.S. 2006. Statistical analysis and time-series models for minimum/maximum temperatures in the Antarctic Peninsula. The Royal Society. 463: 241-259. DOI: 10/1098/rspa.2006.1766

IPCC. (2013). Climate Change 2013: The physical science basis. Contribution of working group I to the fifth assessment report of the Intergovernmental Panel on Climate Change. Cambridge United Kingdom and New York, USA. Retrieved from http://www.climatechange2013.org/images/report/WG1AR5_ALL_FINAL.pdf

Jaglom, W.S., McFarland, J.R., Colley, M.F., Mack, C.B., Venkatesh, B., Miller, R.L., Haydel, J., Schultz, P.A., Perkins, B., Casola, J.H., Martinich, J.A., Cross, P., Kolian, M.J., and Keyin, S. 2014. Assessment of projected temperature impacts from climate change on the U.S. electric power sector using the Integrated Planning Model. Energy Policy. 73: 524–539. DOI: 10.1016/j.enpol.2014.04.032

Johannessen, O.M., Bengtsson, L., Miles, M.W., Kuzmina, S.I., Semenov, V.A., Alekseev, G.V., Naguarnyi, A.P., Zakharov, V.F., Bobylev, L.P., Pettersson, L.H., Hasselmann, K., and Cattle, H.P. 2004. Arctic climate change: observe and modeled temperature and sea-ice variability. Tellus. 56: 328-341. DOI: 10.1111/j.1600-0870.2004.00060.x

Jones, P.D., New M., Parker, D.E., Martin, S., and Rijor, I.G. 1999. Surface air temperature and its changes over the past 150 years. Reviews of Geophysics. 37: 173-199. DOI: 10.1029/1999RG900002

Joshi, N.P., Maharjan, K.L., and Piya, L. 2011. Effect of climate variables on yield of major food-crops in Nepal -A time-series analysis. MPRA. Paper No. 35379, posted 15 December 2011. Retrieved from https://mpra.ub.uni-muenchen.de/35379/

KC, A., 2014. Climate change communication in Nepal. p. 21-36. In: Filho, W.L., Manolas, E., Azul A.M., Azeiteiro, U.M. and McGhie, H. (ed) Handbook of climate change communication. Springer, Switzerland.

KC, A., and Ghimire, A. 2015. High-Altitude Plants in Era of Climate Change: A Case of Nepal Himalayas. Chapter 6. p. 176-187. In: Ozturk M., Hakeem K., Faridah-Hanum I., Efe R. (eds). Climate Change Impacts on High-Altitude Ecosystems. Springer, Cham. DOI: 10.1007/978-3-319-12859-7_6

Lancaster, I.N. 2012. Relationships between altitutude and temperature in Malawai. South African Geographical Journal. 62(1): 89-97. DOI: 10.1080/03736245.1980.10559624

Lean, J.L., and Rind, D.H. 2009. How will Earth's surface temperature change in future decades? Geophysical Research Letter. p. 36. L5708. DOI: 10.1029/ 2009 GL o38932.

Li, Z.-L., Tang, B.-H., Wu, H., Ren, H., Yan, G., Wan, Z., Trigo, I.F., and SobrinoLi, J.A. 2013. Satellite-derived land surface temperature: Current status and perspectives. Remote Sensing of Environment. 131: 14–37.

Me-ead, C., and McNeil, N. 2016. Graphical display and statistical modeling of temperature changes in tropical and subtropical zones. Songklanakarin Journal of Science and Technolog. 36 (6): 715-721.

NASA. 2015. Global Climate Change: Vital Signs of the Planet. Retrieved from http://climate.nasa.gov/effects

NPHC. 2011.  2012. National Survey Report. Volume 1 (pp. 3, 40) Central Bureau of Statistics. Government of Nepal, Kathmandu.

ORNL DAAC. 2015. MODIS subset of NASA Earth Data. Retrieved from: http://daacmodis.ornl.gov/cgi-bin/MODIS/GLBVIZ_1_Glb/modis_subset _order _global_col5.pl.

Paniagua-Tineo, A., Salcedo-Sanz, S., Casanova-Mateo, C., Ortiz-Garcia, E.G., Cony, M.A., and Hernandez-Martin, E. 2011. Prediction of daily maximum temperature using a support vector regression algorithm. Renewable Energy. 36: 3054-3060. DOI: 10.1016/j.renene.2011.03.030

Portmann, R.W., Solomon, S., and Hegerl, G.C. 2009. Spatial and seasonal patterns in climate change, temperatures, and precipitation across the United States. Proceedings of National Academy of Sciences of United States of America (PNAS). 106 (18): 7324–7329.  DOI: 10.1073/pnas.0808533106

Pouteau, R., Rambal, S., Ratte, J.-P., Goge, F., Joffre, R., and Winkel, T. 2011. Downscaling MODIS-derived maps using GIS and boosted regression trees: The case of frost occurrence over the arid Andean highlands of Bolivia. Remote Sensing of Environment. 115: 117–129.  DOI: http://dx.doi.org/10.1016/j.rse.2010.08.011

R Core Team. 2015. R: A language and environment for statistical computing. R Foundation for Statistical Computing, Vienna, Austria. Retrieved from http://www.R-project.org/

Sano, M., Furuta, F., Kobayashi, O., and Sweda, T. 2005. Temperature variations since the mid-18th century for western Nepal, as reconstructed from tree-ring width and density of Abies spectabilis. Dendrochronologia. 23: 83–92.  DOI: 10.1016/j.dendro.2005.08.003

Schlenker, W., and Roberts, M.J. 2009. Nonlinear temperature effects indicate severe damages to U.S. crop yields under climate change. Proceedings of National Academy of Sciences of United States of America (PNAS). 106 (37): 15594–15598. DOI: 10.1073/pnas.0906865106

Shrestha, A.B., and Aryal, R. 2011. Climate change in Nepal and its impact on Himalayan glaciers Regional Environmental Change. Regional Environmental Change. 11(suppl.1): 65–77. DOI:10.1007/s10113-010-0174-9

Smith, J.B., Schneider, S.H., Oppenheimer, M., Yohe, G.W., Hare, W., Mastrandrea, M.D., Patwardhan, A., Burton, I., Corfee-Morlot, J., Magadza, C.H.D., Fussel H.-M., Pittock, A.B., Rahman, A., Suarez, A., and Ypersele, J.-P.V. 2009. Assessing dangerous climate change through an update of the Intergovernmental Panel on Climate Change (IPCC) "reasons for concern". Proceedings of National Academy of Sciences of United States of America (PNAS). 106(11): 4133–4137.

Stroppiana, D., Antoninetti, M., and Brivio P.A. 2014. Seasonality of MODIS LST over Southern Italy and correlation with land cover, topography and solar radiation. European Journal of Remote Sensing. 47(1): 133-152. DOI: https://doi.org/10.5721/EuJRS20144709

UNEP. 2001. Nepal: state of the environment 2001 (p. 12-13). Retrieved from http://www.rrcap.ait.asia/Publications/nepal%20soe.pdf

UN-Habitat. (2015). Cities and climate change initiative, abridged report: Kathmandu Valley, Nepal. United Nations Human Settlements Program, Nairobi, Kenya.

Wan, Z., Wang, P., and Li, X. 2004. Using MODIS Land Surface Temperature and Normalized. Difference Vegetation Index products for monitoring drought in the southern Great Plains, USA. International Journal of Remote Sensing. 25 (1): 61-72. DOI: 10.1080/0143116031000115328

Wanishsakpong, W., and McNeil, N. 2016. Modelling of daily maximum temperatures over australia from 1970 to 2012. Meteorological Applications. 23: 115-122. DOI: http://dx.doi.org/10.1002/met.1536

Wongsai, N., Wongsai, S., and Huete, A. R. 2017. Annual seasonality extraction using the cubic spline function and decadal trend in temporal daytime Modis lst data. Remote Sensing. 9, 1254. DOI: http://dx.doi.org/10.3390/rs9121254

Xu, Z., Jiang, Y., and Zhou, G. 2015. Response and adaptation of photosynthesis, respiration, and antioxidant systems to elevated $CO_2$ with environmental stress in plants. Frontiers in Plant Science. 6. article 701. DOI: 103389/fpls.2015.00701

Yue, W., Xu, J., Tan, W., and Xu, L. 2007. The relationship between land surface temperature and NDVI with remote sensing: application to Shanghai Landsat 7 ETM+ data. International Journal of Remote Sensing. 28 (15): 3205–3226.

Zhou, L., Dickinson, R.E., Dirmeyer, P., Dai, A., and Min, S-K. 2009. Spatiotemporal patterns of changes in maximum and minimum temperatures in multi-model simulations. Geophysical Research Letters. 36. L02702. DOI:10.1029/2008GL036141.

**Appendix III**

# Modeling of Temperature Patterns in Kathmandu Valley of Nepal from 2000 to 2016

Ira Sharma*

Prince of Songkla University, Pattani campus, Thailand. Email: irasg123@gmail.com

Phattrawan Tongkumchum

Prince of Songkla University, Pattani campus, Thailand. Email: phattrawan.t@psu.ac.th

Attachai Ueranantasun

Prince of Songkla University, Pattani campus, Thailand. Email: attachai.u@psu.ac.th

**Abstract**

The aim of this study was to determine a pattern of Land Surface Temperature (LST) in Kathmandu, Nepal from 2000 to 2016 using appropriate statistical methods. The data, recorded every eight day with 1 km$^2$ spatial resolutions, were obtained from Moderate Resolutions Imaging Spectro-radiometer. The study area had 9 regions of $21\times21$ km$^2$ area, each of which was further divided into 9 sub regions. The data for all sub regions were separately used for time series pattern analysis. First, the data were seasonally adjusted and auto correlation was detected by autoregressive method. Then, the data were filtered to eliminate correlation effects. Finally, polynomial regression model of second degree was applied to find the temperature patterns. The results showed that 27% of the area were found to have the temperature patterns of steep rising, while the patterns in another 27% had increasing then decreasing shape. Moreover, 25% of the area had decreasing then increasing pattern and the remaining 21% of the area showed no change appreciably. This method can be applied in other climatic factors that have influence on ecosystem.

**Keywords:** LST, auto-regression method, polynomial regression model

JEL classification: **Q54**

## Introduction

The changes in climate parameters due to global warming have been creating negative impacts on human society and the natural environment. The local, regional or global warming of air is connected to the destruction of ecosystem. It has impacts on different spheres of public life as well. In Asia, hot days and hot nights are predictedly increasing as compared to the cold days and the cold nights in the period from 2011 to 2099 (e.g. Mahmood and Babel, 2014). The corn yield, in USA, increases as temperature rises but only upto 29°C and after that, the production decreases (e.g. Schlenker and Roberts, 2009). A similar result was seen for rice and wheat production in Nepal (e.g. Malla, 2008). Climate change can be particularly hard-hitting for the developing countries, including Nepal, which rely on natural resources for the economy and livelihoods.

A difficult task is to detect the pattern of temperature change in an area using appropriate statistical method. Climate scientists have found temperature change by using different methods such as observation and computer simulation modeling (e.g. Johannessen *et al*., 2003), annual average method (Jones *et al*., 1999), empirical orthogonal functions (e.g. Semenov, 2007), factor analysis (e.g. Chooprateep and McNeil, 2015) and Pearson correlation analysis (e.g. Griffiths *et al.,* 2005). In addition, majority of the studies rely on the linear regression model to find the variation of temperature in different parts of the world (e.g. Lean and Rind, 2009; Chooprateep and McNeil, 2016; Wanishsakpong and McNeil, 2016; Hughes *et al*., 2006). However, the linear regression can show only the change between the beginning and end of study period. Therefore, in this study, the temperature patterns were obtained by using polynomial regression model after adjusting the seasonal effects and auto correlation of the

data to show the pattern of change varying within the study period. Additionally, the trend of temperature is analysed using linear regression model to see the net temperature change in 15 years period.

## Methodology

The study was carried out around Kathmandu valley of Nepal in an area of 3969 km$^2$. The area extends to a total of 8 districts: Kathmandu, Bhaktapur, Lalitpur, Sindhupalchok, Ramechhap, Makwanpur, Nuwakot and Dhading. The first three districts make up the Kathmandu valley, and other five surround the valley. The average maximum temperature of the Valley is more than 30°C in summer and the minimum is less than 1°C in winter. There is a heavy monsoon period in the mid of the year.

*The data*

Land Surface Temperature (LST) is a remote sensing data from Moderate Imaging Spectro-radiometer (MODIS) sensor fitted in Terra satellite of National Aeronautics and Space Administration (NASA). It can monitor the various environmental changes like temperature, rainfall, vegetation, draught, fire, flood (see NASA, 2015). First, the LST data of 1 km$^2$ pixel resolutions with an area of 21×21 km$^2$ for 9 different regions were ordered for a period of March 2000 to June 2016. The data can be retrieved from MODIS website (see ORNL DAAC, 2016). Nine different regions were selected at coordinates 27.761E/ 85.206N,27.761E/ 85.394N,27.761E/ 85.582N, 27.595E/ 85.207N, 27.595E/ 85.394N, 27.595E/ 85.581N, 27.429E/ 85.207N, 27.429E/ 85.394N and 27.429E/ 85.581N. Figure 1 shows that eight regions surrounding the centrally located region, the number 5.
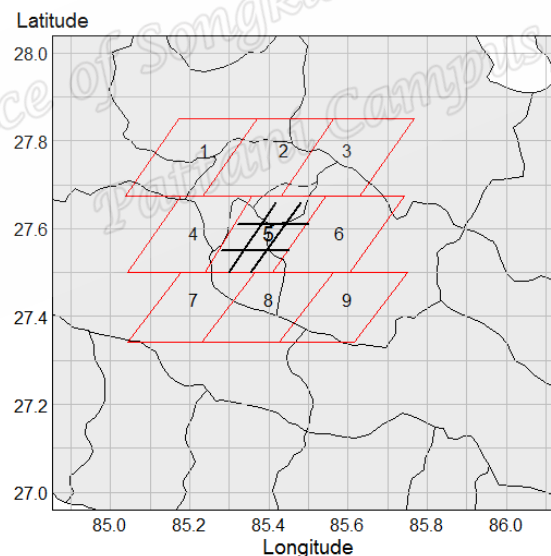


Figure 1 Study area around the valley, showing 9 regions and the sub regions

The coordinates for making polygons around each region were obtained from Modland Tile Calculator by forward and backward mapping procedure and the tool is available freely at its website (see Modland tile calculator, 2016). For each region, a time series of 742 successive observations at 8 days time intervals were available. The data were truncated to 690 by eliminating some from the beginning and the end period of the data set to adjust it for just the 15 years time frame. Then the data of each region were aggregated within a smaller sub regions, approximately 7×7 km$^2$ in area as shown for region 5 in Figure 2. These sub regions were named as North-East (NE), North (N), North-West (NW), West (W), Central (C), East (E), South-West (SW), South (S) and South-East (SE). There are total 81 sub regions in study area.

The coordinates for the plots of slopes within 81 sub regions were obtained from the same Modland Calculator. In each region, eight co-ordinates surrounded the central one in a pattern of 3×3 matrix. The process was repeated for all 9 regions.

*Methods for analysis*

The statistical methods and plots are created for each of the 81 sub regions separately. First of all, the data are seasonally adjusted with the use of spline function, that helps to stabilize the mean of the data at each sub region. The autocorrelation of these data is detected by an autoregressive process of the first order lag (AR1). The model takes the form,

$$y_t = \phi_1 y_{(t-1)} + z_t \qquad (3)$$

Here, $y_t$ is the seasonal adjusted temperatures at observation $t$, $\phi_1$ is the constant and $y_{(t-1)}$ is the first order lag phase ($t-1$) of seasonally adjusted data, $z_t$ the value not explained by the past values.

Finally, the correlation free data were obtained by moving auto correlation component by convolution method of filtration, from equation (3), and the form of equation is,

$$z_t = y_t - \phi_1 y_{(t-1)} \qquad (4)$$

Now, $z_t$ is the filtered temperature at observation $t$, and all other components are explained as above. Furthermore, simple linear regression model was fitted to the filtered data. The model takes the form,

$$z_t = \beta_0 + \beta_1 y_t + \varepsilon \qquad (5)$$

Here, $z_t$ is the filtered data, $\beta_0$ is the intercept and $\beta_1$ is the coefficient, while $y_t$ is seasonal adjusted temperature and $\varepsilon$ is the error term. Finally, the predicted temperature from this linear model was fitted to polynomial regression model of second degree (quadratic model). The form of model is,

$$x = \alpha_0 + \alpha_1 t + \alpha_2 t^2 + e \qquad (6)$$

Here, $x$ is the fitted temperature derived from the linear model, $\alpha_0$ is the intercept and $\alpha_1, \alpha_2$ are the coefficients, $t$ is the observation day of each sub region and $e$ is the error term.

All data analysis and graphical displays were carried out using R Statistical Programming (see R Core Team 2015).

**Results**

The data, seasonally adjusted and auto correlation filtered, were fitted with linear regression model. Figure 2 shows a total 10 panels for Region 5. Nine of them show the linear trends of the temperature at nine sub-regions. The plots for all the regions indicated that, 46% of the sub region had decreasing trend, 53% had increasing and one sub region showed no temperature change during the study period. Moreover, none of them had significant p-value. During 15 years period, the net linear rise of vegetation ranged from 0.009 to 0.430 and the fall from -1.047 to -0.010, along with overall auto correlations (a1) below 0.30, in the study area.
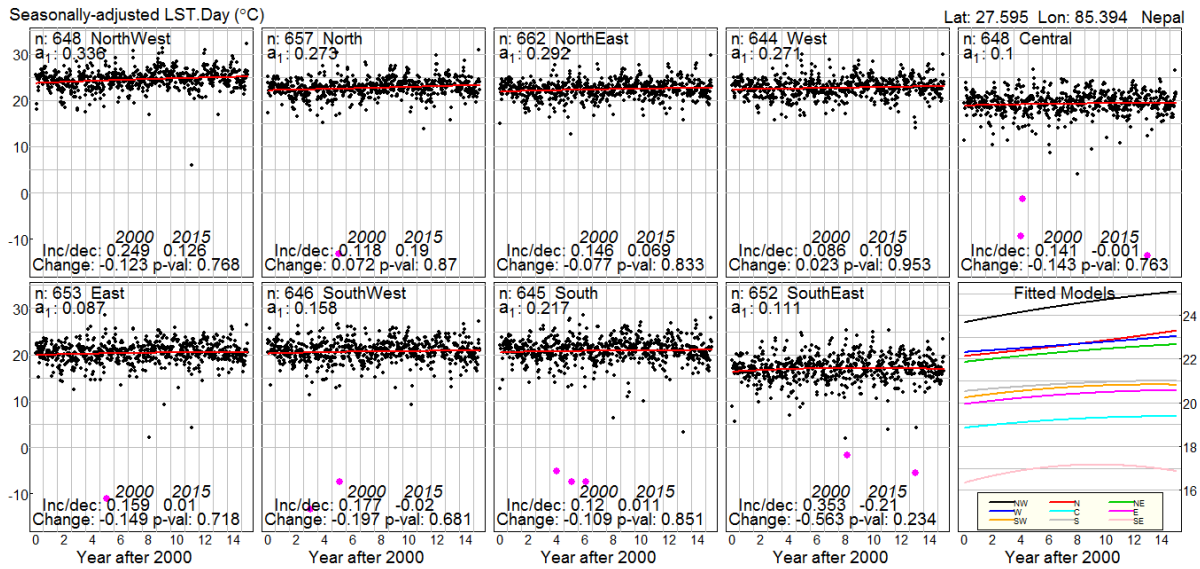
3

Figure 2. Linear trends of nine sub regions of region 5 and the respective quadratic slopes
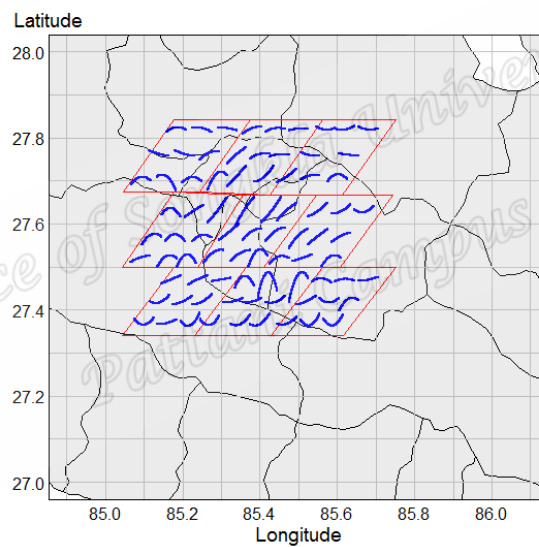


Figure 3 Temperature patterns in nine regions

The fitted values were obtained from liner model and the polynomial model was fitted to them. The quadratic slopes of the temperature were obtained for each sub region. The last panel in Figure 2 shows the quadratic slopes of all those nine sub regions, of region 5, in a single panel. These slopes, plotted separately for 81 sub regions in Figure 3, showed various patterns which were categorized into 4 different groups as per their shapes- 'steep rising' (27%), 'increasing then decreasing' (27%), 'decreasing then increasing' (25%) and finally the 'no change' (21%) group.

## Discussions

This study analyses the linear trend of vegetation in 81 sub regions and that does not show statistically significant results. Therefore the quadratic slopes were used, that could serve the purpose to show the patterned changes of temperature. The study detects four different patterns, steep rising, increase then decrease, decrease then increasing and the final group having no change in 15 years period. The linear model has been used by most of the previous research works to find temperature change (e.g. Hughes *et al*., 2006; Griffiths *et al*., 2005; Choprateep and McNeil, 2015) in a specified period of time. They

have shown, just the net change from initial to end time of study period. No pattern could be seen in the period between the two time points. It can be explained that the net temperature change between beginning and end of the study time cannot describe temperature patterns on how it has been changing during the specified period.

This study has applied a combination of linear regression followed by polynomial regression models, which is an effective technique for modeling the temperature. This method also adjusts for spatial correlation and seasonal variations of the data. Therefore, the results are more accurate as compared to the other pervious methods.

## Conclusions

The combination of autoregressive process, linear regression and polynomial regression model can be successfully applied to find time series patterns and the trends of temperature. The time series patterns show that there are a lot of variations of temperature change, even in adjacent sub regions, during 15 years period. The methodological approach used in this study can be applied to similar studies at local, regional and global scale. Also, it is applicable to model the other factors, for example vegetation, precipitation and wind in future and the method can be applicable to find the analysis of temperature pattern of any other areas, both regionally and globally.

## Acknowledgments

## References

Chooprateep, S. and McNeil, N. (2015). Surface air temperature changes from 1909 to 2008 in Southeast Asia assessed by factor analysis. *Theoretical and Applied Climatology*. Vol. 123 (1). Pp: 361-368.

Griffiths, G.M., Chambers, L.E., Haylock, M.R., Manton, M.J., Nicholls, N., Baek, H.J., Choi, Y., Della-Marta, P.M., Gosai, A., Iga, N., Lata, R., Laurent, V., Maitrepierre, L., Maamigawa, H., Ouprasitwong, N., Solofa, D., Tahani, L., Thuy, D.T., Tibig, L., Trewin, B., Vediapan, K. and Zhai, P. (2005). Change in mean temperature as a predictor of extreme temperature change in the Asia-Pacific region. *J. Climatol*. Vol. 25. Pp: 1301-1330

Hughes, G.L., Rao S.S., and Rao, T.S. (2006). Statistical analysis and time-series models for minimum/ maximum temperatures in the Antarctic Peninsula. *The Royal Society*. Vol. 463. Pp: 241-259. DOI: 10/1098/rspa.2006.1766.

Johannessen, O.M., Bengtsson, L., Miles, M.W., Kuzmina, S.I., Semenov, V.A., Alekseev, G.V., et al. (2004). Arctic climate change: observe and modeled temperature and sea-ice variability. *Tellus*. Vol. 56. Pp:328-341

Jones, P.D., New, M., Parker, D.E., Martin, S. and Rijor, I.G. (1999). Surface air temperature and its changes over the past 150 years. *Reviews of Geophysics*. Vol. 37. Pp: 173-199.

Lean, J.L. and Rind, D.H. (2009). How will Earth's surface temperature change in future decades?. *Geophysical Research Letters*. Vol. 36. L5708. DOI: 10.1029/ 2009 GL o38932.

Mahmood, R. and Babel, S.M. (2014). Future changes in extreme temperature events using the statistical downscaling model (SDSM) in the trans-boundary region of the Jhelum river basin. *Weather and Climate Extremes*. Vol.5-6(1), Pp: 56-66

Malla, G. (2008). Climate change and its impact on nepalese agriculture.*The Journal of Agriculture and Environment.* Vol.9, Jun.2008.Pp: 62-71

Modland tile calculator. (2016). Available from http://landweb.nascom.nasa.gov/cgi-bin/developer/tilemap .cgi. Accessed on 5 September 2016.

NASA. (2015). Global Climate Change Vital Signs of the Planet. Available from: http://climate.nasa.gov/effects. Accessed on 5 December 31, 2015.

ORNL DAAC. (2016). MODIS subset of NASA Earth Data. Available from http://daacmodis.ornl.gov/cgi-bin/MODIS/GLBVIZ_1_Glb/modis_subset_order_ global_col5.pl. Accessed 5 October 2016.

R Core Team. (2015). R: A language and environment for statistical computing. R Foundation for Statistical Computing, Vienna, Austria. URL http://www.R-project.org/.

Schlenker, W. and Roberts, M. J. ( 2009). Nonlinear temperature effects indicate severe damages to U.S. crop yields under climate change. *Proceedings of National Academy of Sciences of United States of America (PNAS)*. vol. 106 no. 37. Pp.:15594–15598, doi: 10.1073/pnas.0906865106

Semenov, V.A. (2007). Structure of temperature variability in the high latitudes of northern hemisphere. *Atmos. Oceanic Phys*. Vol. 43. Pp: 744-753.

Wanishsakpong, W. and McNeil, N. (2016). Modelling of daily maximum temperature over Australia from 1970-2012. *Meteorological applications*. Vol. 23(1). Pp: 115-122.

# ISI REGIONAL STATISTICS CONFERENCE

International Statistical Institute
**Regional Statistics Conference**
Bali, 20 - 24 March 2017

**BANK INDONESIA**

## Certificate of Paper Presentation

This is to certify that the contributed paper entitled

Modelling of Temperature Pattern in Kathmandu Valley of Nepal from 2000 to 2016

by

Ira Sharma*; Phattrawan Tongkumchum; Attachai Ueranantasum

was presented in the Contributed Paper Session of the ISI Regional Statistics Conference 2017 held in Bali, Indonesia, from 20 - 24 March 2017

**Appendix IV**

# High Performance Scientific Computing

## Modeling, Simulation and Optimization
## of Complex Processes

March 19–23, 2018

Hanoi, Vietnam

# Abstracts
# &
# Participants

Institute of Mathematics

Vietnam Academy of Science and Technology

# Modeling of NDVI and LST to Identify and Compare the Changing Trends in Nepal by Using GEE

I. Sharma[1,2], P. Tongkumchum[1], and A. Ueranantasun[1]

**Abstract:** Normalized difference vegetation index (NDVI) and Land Surface Temperature (LST) data, in a sample plot each from east, center and west of Nepal, from 2000 to 2015, were analyzed to identify and compare the trends of vegetation and temperature changes during the period. The data were obtained from Moderate Resolutions Imaging Spectro-radiometer (MODIS). NDVI charactiszes a resolution of 250250 m2 and a 16-day composite period while LST has 8 days frequency with resolution of 11 km2. The analysis was separate for NDVI and LST. The data were seasonally adjusted and then divided into three groups of five year period each, separate for every region. The generalized estimating equations (GEE) were fitted to each period data. For all three regions, the results showed, there was a trend of significantly rising vegetation in eastern and western sub urban parts while the central urban city had a significant decline in trend. Whereas the temperature showed statistically significant and uniform fluctuating pattern of change in all three regions. However, the results revealed no relationship of trend of changing temperature with that of vegetation.

7th International Conference on
**HIGH PERFORMANCE SCIENTIFIC COMPUTING**
March 19-23, 2018, Hanoi, Vietnam

## CONFIRMATION

We hereby confirm that

......Isa Sharma......................................

did present a talk at our conference.

Hanoi, March 23, 2018

Prof. Dr. Hoang Xuan Phu
Co-chair of the Organizing Committee

**Appendix V**

**Curriculum Vitae**

**Name**                    Mrs. Ira Sharma

**Student ID**              58203330003

**Educational Attainment**

| Degree | Name of Institution | Year of Graduation |
|---|---|---|
| M A (Sociology) | Purbanchal University | 2011 |
| M Sc (Botany) | Tribhuwan University | 1998 |

**Scholarship Awards during Enrolment**

1. The Scholarship Awards for PhD Studies by Higher Education Research Promotion and Thailand's Education Hub for Southern Region of ASEAN Countries (TEH-AC, grant number 018/2015), 2015.

2. Research scholarship from Graduate School, Prince of Songkla University, Thailand, 2017.

3. Scholarship for paper presentation at ISI RSC conference at Bali, Indonesia, March 2017

4. Scholarship for paper presentation at $7^{th}$ International conference on High performance Scientific Computing at Hanoi, Vietnam, March 2018.

**Work – Position and Address**

Lecturer

Nepal Institute of Health Sciences College, Purbanchal University, Kathmandu, Nepal

**List of Publication and Proceeding**

*Publications*

1. Sharma, I., Ueranantasun, A., Tongkumchum, P. 2018. Modeling of satellite data to identify the seasonal patterns and trends of vegetation index in Kathmandu Valley, Nepal from 2000 to 2015. Jurnal Teknologi. 80(4), 125-133.

2. Sharma, I., Tongkumchum, P., Ueranantasun, A. 2018. Modeling of LST to determine temperature patterns and detect their association with altitude in Kathmandu Valley of Nepal. Chiang Mai University Journal of Natural Sciences. 17 (4). (Accepted to publish in Oct-Dec 2018).

3. Sharma, I., Tongkumchum, P, Ueranantasun, A., Chuangchang, P., 2018. Identifying the Land Surface Temperature (LST) change patterns in 3 ecozones of Nepal.

4. Sharma, I., Ueranantasun, A., Tongkumchum, P. 2018. Seasonal patterns and annual trends of vegetation from east to west of Nepal using NDVI.

*Proceedings*

1. Sharma, I., Tongkumchum, P., Ueranantasun, A. 2017. Modeling of temperature patterns in Kathmandu Valley of Nepal from 2000 to 2015. Proceedings of 2nd ISI Regional Statistics Conference. 20-24 March 2017. Indonesia (Session CPS34).

2. Sharma, I., Ueranantasun, A., Tongkumchum, P. 2018. Modeling of NDVI and LST to identify and compare the changing trends in Nepal by using GEE. 7th International Conference on High Performance Scientific Computing, Hanoi, Vietnam.